

**Mouse models targeted for the tissue inhibitor of  
metalloproteinases-3 (TIMP3) - molecular and functional  
dissection of Sorsby fundus dystrophy (SFD)**

**Dissertation zur Erlangung des Doktorgrades der Naturwissenschaften (Dr. rer. nat.)  
der Naturwissenschaftlichen Fakultät III – Biologie und Vorklinische Medizin der  
Universität Regensburg**

Vorgelegt von  
**Marton Fogarasi**  
aus Rumänien

**Regensburg  
April, 2009**

**Promotionsgesuch eingereicht am: 22.04.2009**

**Tag der mündlichen Prüfung:**

**Die vorliegende Arbeit wurde von Prof. Dr. Bernhard Weber angeleitet.**

**Prüfungsausschuss:**

<b>Vorsitzender:</b>	<b>Prof. Dr. Herbert Tschochner</b>
<b>Erstgutachter:</b>	<b>Prof. Dr. Rainer Deutzmann</b>
<b>Zweitgutachter:</b>	<b>Prof. Dr. Bernhard Weber</b>
<b>Prüfer aus der Fakultät:</b>	<b>Prof. Dr. Ernst Tamm</b>
<b>Vertreter des Drittprüfers:</b>	<b>Prof. Dr. Stephan Schneuwly</b>

### **Eidesstattliche Erklärung**

(zu § 6 Abs. 1, Nr. 3 der Promotionsordnung der Naturwissenschaftlichen Fakultäten der Universität Regensburg)

Ich erkläre hiermit an Eides statt, daß ich die vorliegende Arbeit ohne unzulässige Hilfe Dritter und ohne Benutzung anderer als der angegebenen Hilfsmittel angefertigt habe; die aus anderen Quellen direkt oder indirekt übernommenen Daten und Konzepte sind unter Angabe des Literaturzitats gekennzeichnet.

Weitere Personen waren an der inhaltlich-materiellen Herstellung der vorliegenden Arbeit nicht beteiligt. Insbesondere habe ich hierfür nicht die entgeltliche Hilfe eines Promotionsberaters oder anderer Personen in Anspruch genommen. Niemand hat von mir weder unmittelbar noch mittelbar geldwerte Leistungen für Arbeiten erhalten, die im Zusammenhang mit dem Inhalt der vorgelegten Dissertation stehen.

Die Arbeit wurde bisher weder im In- noch im Ausland in gleicher oder ähnlicher Form einer anderen Prüfungsbehörde vorgelegt.

Regensburg, 22.04.2009

## Table of contents

<b>1. Introduction.....</b>	<b>1</b>
1.1 Sorsby fundus dystrophy .....	1
1.2 Structure and function of the retina .....	1
1.3 The extracellular matrix (ECM) .....	3
1.4 Mouse models of TIMP3 mutations .....	6
1.4.1 TIMP3 knock-out mouse .....	6
1.4.2 TIMP3 Ser156Cys knock-in mouse.....	7
1.5 Structure of tissue inhibitors of metalloproteinases (TIMPs).....	7
1.6 Biological functions of TIMP3 .....	8
1.6.1 Inhibition of MMPs by TIMP3 .....	8
1.6.2 Regulation of the activity of ADAMs by TIMP3 .....	10
1.6.3 TIMP3 and ADAMTS inhibition.....	14
1.6.4 Antiangiogenic properties of TIMP3 .....	17
1.6.5 Proapoptotic activity of TIMP3 .....	18
1.6.6 TIMP3 as tumour suppressor gene .....	19
1.7 Aims of the present study .....	19
<b>2. Materials and Methods.....</b>	<b>21</b>
2.1 Molecular biology methods .....	21
2.1.1 Mammalian cell culture and cryopreservation of cells.....	21
2.1.2 Culture and conservation of <i>E. coli</i> strains .....	21
2.1.3 Preparation and transformation of <i>E. coli</i> competent cells.....	22
2.1.3.1 Preparation of bacterial competent cells.....	22
2.1.3.2 Transformation of competent cells with plasmid DNA.....	22
2.1.4 RNA isolation from primary cell culture.....	22
2.1.5 Plasmid DNA isolation from <i>E. coli</i> .....	22
2.1.6 Gel electrophoresis and DNA purification .....	23
2.1.6.1 Analytical agarose gel electrophoresis .....	23
2.1.6.2 Preparative agarose gel electrophoresis.....	23
2.1.7 <i>In vitro</i> modification of DNA .....	24
2.1.7.1 Site directed mutagenesis.....	24
2.1.7.2 Dephosphorylation of linearized plasmid DNA .....	24
2.1.7.3 Filling in DNA sticky end.....	24

2.1.7.4	Polymerase chain reaction (PCR)	25
2.1.7.5	First-strand cDNA synthesis	25
2.1.7.6	Double stranded DNA cleavage with restriction endonucleases	26
2.1.7.7	Ligation of DNA fragments	26
2.1.7.8	Double stranded DNA sequencing	26
2.1.7.9	Phenol/chloroform extraction and ethanol precipitation	27
2.1.8	Production of recombinant proteins in <i>E. coli</i>	28
2.1.8.1	Protein expression in inclusion bodies	28
2.1.8.2	Recombinant protein refolding	29
2.1.9	Recombinant protein expression in mammalian cells	29
2.1.9.1	Transiently transfection	30
2.1.9.2	Stable transfection	30
2.2	Protein biochemistry methods	30
2.2.1	Protein purification	30
2.2.1.1	Immobilized metal affinity chromatography (IMAC)	31
2.2.1.2	Glutathione-S-transferase (GST) chromatography	31
2.2.2	SDS-Polyacrylamide gel electrophoresis (SDS-PAGE)	31
2.2.3	Zymography	32
2.2.4	Reverse zymography	33
2.2.5	Measurement of protein concentration	34
2.2.5.1	Estimation of protein concentration at 280 nm absorption	34
2.2.5.2	Estimation of protein concentration by Lowry assay	34
2.2.6	ECM protein preparation	35
2.2.7	Preparation of cell extracts	35
2.2.8	Concentration of protein solution	35
2.2.9	Pull-down assay	36
2.3	Immunochemistry methods	36
2.3.1	Immunoprecipitation of proteins	36
2.3.2	Enzyme-Linked Immunosorbent Assay (ELISA)	36
2.3.2.1	Determination of the apparent dissociation constant by ELISA	37
2.3.2.2	ELISA applied to cells	38
2.3.2.3	Competitive ELISA	39
2.3.3	Western blotting	40
2.3.4	Immunocytochemistry	40

2.4	Biophysical methods.....	41
2.4.1	Fluorescence resonance energy transfer (FRET).....	41
2.4.1.1	Fluorometric TACE assay .....	41
2.4.1.2	Fluorometric MMP13 assay.....	42
2.5	Cell biology methods.....	42
2.5.1	Isolation of primary chondrocytes from mouse ribs.....	42
2.5.2	Preparation of liver extract .....	42
<b>3.</b>	<b>Results.....</b>	<b>43</b>
3.1	Production and structural characterization of soluble recombinant proteins.....	43
3.1.1	Construction of a bacterial expression vector for the production of TIMP-1, -2, -3, -4, MMP13 and TACE-CD.....	43
3.1.2	Purification and refolding of recombinant proteins expressed in the bacterial system.....	46
3.1.3	Construction of a bacterial expression vector for the production and purification of antibody epitope peptides fused to GST. ....	48
3.1.4	Generation of a mammalian expression vector for production of the extracellular domain of human DDR2 and its expression in HEK-293 cells .....	49
3.2	Functional analysis of recombinant proteins expressed in <i>E. coli</i> .....	51
3.2.1	Bioactivity assessment of recombinant TIMPs by reverse zymography.....	51
3.2.2	Fluorometric titration of MMP13 for the functional assay of full-length TIMP3.....	52
3.2.3	Analysis of antibody binding to epitopes and their specific recognition.....	54
3.3	Functional implications of TIMP3 on TACE catalytic activity.....	55
3.4	Cleavage activity of ADAMTS4/ADAMTS5 and MMPs inhibition by TIMP3.....	60
3.5	Competitive inhibition of VEGF binding to VEGFR2 by TIMP3 .....	67
3.6	Analysis of TIMP3 binding to collagens .....	68
3.7	Structural implications of S156C mutation on TIMP3 molecule. ....	71
3.8	Quantification of the S156C-TIMP3 mutant protein in knock-in fibroblasts.....	73
3.9	TIMP3 turnover in the ECM.....	74
<b>4.</b>	<b>Discussion .....</b>	<b>76</b>
4.1	TIMP3 involvement in the modulation of sheddase activity of TACE.....	76
4.2	Regulation of ADAMTS4/ADAMTS5 and MMPs proteolytic activity by TIMP3.....	79
4.3	TIMP3 and angiogenesis .....	81

4.4	TIMP3 interaction with ECM components.....	82
4.5	S156C-TIMP3 mutant oligomerization and aggregation.....	83
<b>5.</b>	<b>Summary.....</b>	<b>87</b>
<b>6.</b>	<b>Appendix.....</b>	<b>89</b>
<b>7.</b>	<b>References.....</b>	<b>92</b>

## 1. Introduction

### 1.1 Sorsby fundus dystrophy

Sorsby fundus dystrophy (SFD) is a rare autosomal dominant disorder affecting the central retina, the region responsible for high resolution and colour vision. The disease generally manifests in the fourth decade of life, with rapid loss of central vision followed by progressive loss of peripheral vision, ultimately leading to blindness (Sorsby *et al.*, 1949). The main histopathological features are deposits of lipofuscin-like material (known as drusen) and thickening of Bruch's membrane. As the disorder progresses, there is subretinal neovascularization, peripheral atrophy of the retinal pigment epithelium, and later atrophy of the choriocapillaris. SFD has phenotypic resemblances with age related macular degeneration (AMD), a complex retinal disease with a multifactorial genesis. AMD is the most common cause of late-onset blindness in the elderly of developed countries (Klein *et al.*, 1992).

In affected individuals a heterozygous point mutation in the tissue inhibitor of metalloproteinases-3 (TIMP3) gene has been identified (Weber *et al.*, 1994). So far, several point mutations in TIMP3 have been reported, all localized in the C-terminal domain of the protein. Of these, the majority result in unpaired cysteine residues in the mature protein, namely S156C (Felbor *et al.*, 1995), G166C (Felbor *et al.*, 1997), G167C (Jacobson *et al.*, 1995), Y168C (Weber *et al.*, 1994), S170C (Barbazetto *et al.*, 2005), Y172C (Jacobson *et al.*, 2002) or S181C (Weber *et al.*, 1994). Another existing mutation introduces a stop codon (E139X), deleting a segment from the C-terminal of TIMP3 (Clarke *et al.*, 2001). A splice site mutation at the intron 4/exon 5 junction of TIMP3 has been reported in two Japanese families (Tabata *et al.*, 1998). More recently, a non-cysteine mutation in the TIMP3 gene was identified which replaces His at position 158 with an Arg residue (Lin *et al.*, 2006).

### 1.2 Structure and function of the retina

The human eye is a highly complex photosensitive organ of neuronal origin, having several important layers in its structure which facilitate high resolution vision (Fig. 1). In the outer layer of the eye wall the sclera and cornea are found, which have protective roles for the inner part of the eye. The cornea, together with the crystalline lens, focuses the light which enters the eye onto the photoreceptor cells in the retina. The intermediate layer of the eye is represented by the choroid which includes the the



iris, lens, ciliary body, and the pupil. The ciliary body is attached to the lens for protection and changes the shape of the lens to modify the focus of the eye. The iris generates the colour of the eye and allows light to pass to the retina. The circular muscle in the iris controls the size of the pupil and thus regulates the intensity of light that reaches the retina. The lens together with the cornea allows the eye to focus on objects at various distances and generates a sharp image on the retina.

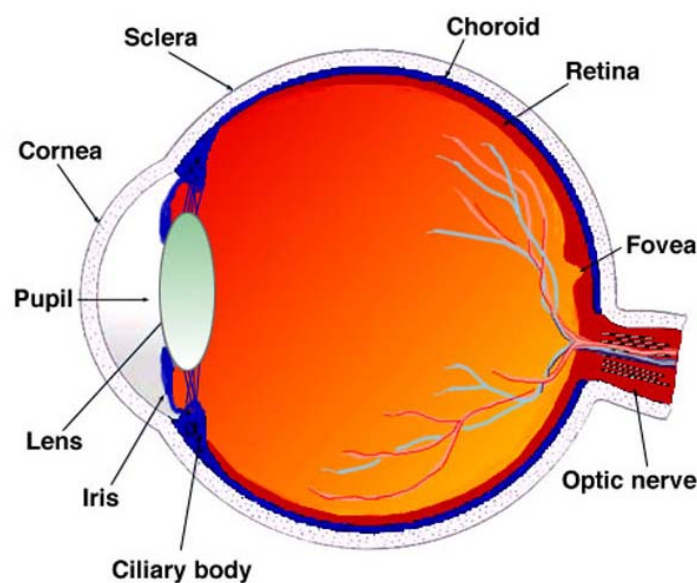


**Figure 1.** Vertical section of a human eye (Taken from <http://webvision.med.utah.edu/anatomy.html>)

The inner layer of the eye is the retina and is composed of many types of cell which form several retinal layers (Fig.2). The photoreceptors comprise two types of cells: rods and cones, with major functional differences between them. Cones provide the eye with colour sensitivity, and function well in bright light; while rods are more sensitive and are responsible for dark-adapted vision. The outer plexiform layer is the region where synapses are formed between photoreceptors and bipolar and horizontal cell dendrites. The inner plexiform layer is also an area of synapses where the bipolar and amacrine cells are linked to the ganglion cells. The retinal pigment epithelium (RPE) forms the outer blood-retinal barrier and plays a central role in retinal physiology by carrying out phagocytosis of the outer segment of photoreceptor cells, storage and synthesis of trans-

retinal (or vitamin A) and transporting metabolites, thus supporting the function of the photoreceptors (Rizzolo, 1997)

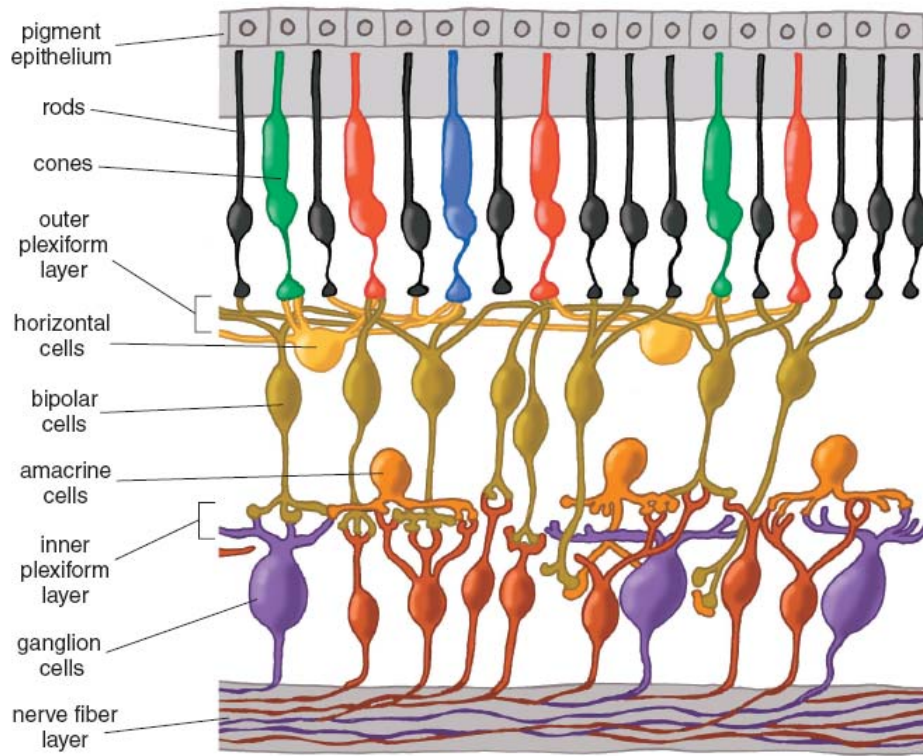


**Figure 2.** Schematic representation of the cell layers found in the structure of the retina (Taken from Kolb, 2003)

### 1.3 The extracellular matrix (ECM)

The ECM is a highly complex structure that serves as a scaffold to stabilise the physical structure of tissues and regulate the behaviour of cells by influencing apoptosis, migration, proliferation, development, shape and function (Alberts *et al.*, 1994). The ECM is secreted locally by specialized types of cells such as fibroblasts, chondroblasts, and osteoblasts. The macromolecules found in matrix can be divided in two main classes: fibrous proteins such as collagen, elastin, fibronectin and laminin, and proteoglycans with glycosaminoglycans (GAGs) which are covalently linked to core. Glycosaminoglycans are built from repeating disaccharide units consisting of one sulfated sugar (N-acetylglucosamine or N-acetylgalactosamine) and a second sugar related to uronic acid (glucuronic or iduronic). Four groups of glycosaminoglycans are found in the ECM: (i) hyaluronan, (ii) chondroitin and dermatan sulfate, (iii) heparan

sulfate, and (iv) keratan sulfate (Alberts *et al.*, 1994), which are distinguished by the type and linkage of the sugar and the number and the position of the sulphur atom. Because polysaccharide chains are highly negatively charged due to sulfate or carboxyl groups they attract cations and are able to retain large amounts of water. This enables the ECM to withstand compressive forces and at the same time provides mechanical support for tissue.

Hyaluronan, unlike the other three groups of GAGs, does not contain a sulfur atom in its structure and is not linked covalently to any core protein (Toole, 2000). Functionally, it is involved in the facilitation of cell migration during tissue morphogenesis and repair (Oliferenko *et al.*, 2000; Bourguignon *et al.*, 2000; Evanko *et al.*, 1999). It is produced in response to injury where it mediates wound healing and is important in joint motility as a lubricant. Tissue specific functions of hyaluronan are given by its interaction with other matrix components such as proteins (either glycosylated or non glycosylated) from the matrix as well as membrane anchored cell surface proteins.

Proteoglycans have major roles in intercellular biochemical signalling such as binding of fibroblast growth factors (FGFs) to heparan sulfate chains causing oligomerization of the growth factors and leading to the activation of cell surface tyrosine kinase receptors (Iozzo, 1998). Proteoglycans can also bind other types of secreted proteins including proteases and their inhibitors, in this way modulating their activity. In the case of inflammation, heparan sulfate proteoglycans sequester secreted chemokines and stimulate white blood cells to migrate into inflamed tissue from the bloodstream. The heparan sulfate proteoglycan percalan is found in the structure of the basal lamina of the kidney glomerulus where it participates in filtering molecules passing into the urine from the bloodstream. Some proteoglycans are integral components of the plasma membrane whereas others are bound to the surface of the lipid bilayer by a glycosylphosphatidylinositol (GPI) anchor and act as coreceptors (Bernfield *et al.*, 1999). The plasma membrane proteoglycan syndecan belongs to this category and binds several types of proteins, including FGFs, integrins and fibronectins.

The collagens are the most abundant matrix proteins in mammals (Prockop & Kivirikko, 1995). There are about 20 different types of collagen known. The primary structure of a typical collagen is a triple helix in which 3 alpha helical chains are wound around one another to form a superhelix. Collagens are very rich in proline and glycine residues which have an important role in the assembly of this triple helix structure. Glycine is found at every third position of the alpha chain and allows the three alpha

helical chains to pack tightly to form the collagen superhelix. This provides tensile strength. Proline and lysine in the collagen are hydroxylated, contributing to the stabilization of the triple helix by forming interchain hydrogen bonds. These interactions in the triple helix give a rope like structure called fibrillar collagens. In the extracellular space some collagens can assemble into higher order polymers called collagen fibrils which can further self-organize into even higher order structures known as collagen fibers. This category of collagens includes collagen types I, II, III, V, and XI. Collagen type IX and XII are fibril associated collagens, making the link between the fibrils and other matrix components. Collagen type IV forms a meshwork and is found in the structure of the basal lamina. Collagen type VII is organized in structures called anchoring fibrils which link the basal lamina to the underlying connective tissue. Type IV and VII collagen are also called network-forming collagens. Collagen type XVII is anchored at the cell surface by a transmembrane domain and is found in hemidesmosomes. Collagen type XVIII is localized in the basal lamina of blood vessels. Cleavage at its C-terminal domain leads to the production of endostatin, a peptide with antiangiogenic properties (Zatterstrom *et al.*, 2000).

Elastic fibers are important components of the extracellular matrix of tissues such as skin, blood vessel and lung and provide the required elasticity for these organs (Debellea & Tamburro, 1999). The principal component of elastic fiber is elastin which is composed of stretches of hydrophobic segments (which give the elastic properties) alternating with alanine and lysine rich  $\alpha$ -helical segments involved in the formation of links between molecules. In the structure of elastic fibers microfibrils composed of a number of different proteins can be found. Fibrillin, a well characterized glycoprotein, binds to elastin and has a protective role for the integrity of elastic fiber.

Other classes of ECM proteins are involved in attachment and organization of cells. One of the best characterized proteins from this category is fibronectin, which is a large glycoprotein composed of disulfide linked dimers (Schwarzbauer & Sechler, 1999). It can be found in both soluble and fibrillar forms due to alternate splicing of the gene. Soluble fibronectin circulates in the blood stream where it is involved in blood clotting, wound healing and phagocytosis. Fibrillar fibronectin is a component of the ECM and is associated with cell surface molecules and involved in guiding cell migration in vertebrate embryos.

Laminin, another important component of the ECM, is a component of basal lamina where it has diverse functions (Cognato & Yurchenco, 2000). Structurally, laminin is

composed of three long polypeptide chains ( $\alpha,\beta,\gamma$ ) that are disulfide-bonded into an asymmetric structure. Laminin in the basement membrane can bind to several proteins. One domain interacts with percalan, another with nidogen and another can bind to cell surface receptors. Basal lamina, besides its filtering role in the kidney glomerula, is involved in cell metabolism, polarity, migration, proliferation and differentiation.

## **1.4 Mouse models of TIMP3 mutations**

Mouse models provide important tools to study and dissect the function of a gene both in health and disease. Although yeast, worms, and flies are suitable models to study various biological processes, a major advantage of the mouse is its similarities with humans at the genetic (approximately, 80-90% homology) and the physiological level. Therefore murine models can be used to study human diseases, providing useful information about the function of a gene/gene product or the mechanism of a disease. Towards this end, an important advance was the generation of transgenic mice by insertion of a foreign gene in the mouse germline. An alternative approach was to generate knock-out mice by homologous recombination (Thomas *et al.*, 1987). Generation of knock-in animals allows the alteration of a certain(s) amino acid(s) at a precise position in a specific gene. The advantage of a gene targeting strategy is that the mouse gene is modified in its natural location representing a very good *in vivo* model. However, there are limitations of the knock-out technology since in some cases (10-15%) the inactivation of a gene leads to lethality of the embryo thus making it impossible to study the function of the respective gene. To overcome this situation so-called conditional knock-out mice were developed (Gu *et al.*, 1994; Gu *et al.*, 1993, Rajewsky *et al.*, 1996). Conditional gene targeting can be achieved by crossing the mutant mouse line with Cre transgenic mice in which the Cre recombinase is under strict cell type specific and/or inducible promoter control.

### **1.4.1 TIMP3 knock-out mouse**

This mouse model was generated by our group (Soboleva *et al.*, 2003, Janssen *et al.*, 2008) and independently by a US laboratory (Leco *et al.*, 2001). These mice show several pathological features such as development of spontaneous air space enlargement in the lungs, probably due to enhanced MMP-mediated ECM degradation (Leco *et al.*, 2001), accelerated apoptosis of epithelial cells in the mammary gland (Fata *et al.*, 2001),

dilated cardiomyopathy (Fedak *et al.*, 2004) and chronic hepatic inflammation (Mohammed *et al.*, 2004).

#### **1.4.2 TIMP3 Ser156Cys knock-in mouse**

A targeted knock-in mouse model for SFD was generated in house and characterized by Weber *et al.*, 2002. This mouse line carries a Ser156Cys mutation in the endogenous Timp3 of the mouse. This homologous mutation was associated with SFD in a large pedigree (Felbor *et al.*, 1995). Phenotypically, the knock-in mouse shows several abnormalities in Bruch's membrane and the RPE. At the biochemical level, typical high molecular weight complexes of S156C-TIMP3 mutant protein can be observed under non-reducing conditions (Weber *et al.*, 2002; Yeow *et al.*, 2002).

### **1.5 Structure of the tissue inhibitors of metalloproteinases (TIMPs)**

The activity of proteolytic enzymes in the extracellular space must be controlled in a homeostatic way to avoid uncontrolled turnover of ECM components. Cells are endowed with several mechanisms which allow them to keep the anabolism and catabolism of the ECM in equilibrium. One of these mechanisms is that proteases are biosynthesized in an inactive form, called a proform or zymogen, which needs to be activated, usually by cleavage of the propeptide from the zymogen. Specific control of proteinase activity is achieved by a family of proteins known as tissue inhibitors of metalloproteinases (TIMPs).

The TIMPs are a family of secreted proteins comprising four members (TIMP1, -2, -3, -4), which are endogenous inhibitors of a variety of extracellular proteases. They form tight stoichiometric noncovalent 1:1 complexes with proteases, which are resistant to various proteolytic treatments. The TIMPs share about 40 % identity at the primary amino acid sequence structure. A common feature of the TIMPs is that they contain 12 evolutionary conserved cysteine residues which contribute to the formation of 6 disulfide bonds. TIMPs have a rigid structure which is held together by these 6 intramolecular disulfide bonds and fold into two distinct independent domains, often referred to as the N-terminal and C-terminal domain (Murphy and Willenbrock, 1995). Mature mouse TIMP1 is a secreted 181 amino acid glycoprotein with a molecular mass of 21 kDa (Docherty *et al.*, 1985). Initially, this inhibitor was found in cultured human fibroblasts (Bauer *et al.*, 1975), human serum (Woolley *et al.*, 1975), cartilage and aorta (Keuttner *et al.*, 1976).

TIMP2 is composed of 192 amino acids and is a soluble non-glycosylated protein with a molecular mass of 22 kDa (Stetler-Stevenson *et al.*, 1989; 1990). TIMP2 was first identified in rabbit brain capillary endothelial cells treated with 12-O-tetradecanoylphorbol-13-acetate (Herron *et al.*, 1986).

TIMP3 was first identified in the ECM of virus transformed chicken embryo fibroblasts (Blenis *et al.*, 1983) and is the only family member tightly associated with the ECM (Leco *et al.*, 1994). TIMP3 is a 24 kDa glycoprotein with 12 conserved cysteine residues which form 6 disulfide bonds. The N-terminal domain is responsible for the interaction with a number of proteases and the C-terminal is known to bind to the ECM (Langton *et al.*, 1998). However, it has been shown recently that binding of TIMP3 to the ECM is mediated by both the N-terminal and the C-terminal of the inhibitor (Lee, *et al.*, 2007).

The last member of the family, TIMP4, was identified by cloning (Greene *et al.*, 1996) and has a molecular weight of 23 kDa with 195 amino acids.

## **1.6 Biological functions of TIMP3**

Over the last two decades several biological and pathological functions of TIMP3 have been demonstrated. These functions can be classified in two groups of activity. First, TIMP3 has an inhibitory function towards a variety of proteolytic enzymes in the ECM, attributed to the N-terminal domain, and the second, nonenzymatical inhibitory activity for which the C-terminal seems to be responsible (Langton *et al.*, 1998).

### **1.6.1 Inhibition of MMPs by TIMP3**

Matrix metalloproteinases (MMPs) are a family of calcium and zinc dependent endopeptidases which are responsible for ECM protein turnover and play a key role in matrix remodeling. The substrates of these proteases are diverse and include various types of collagen and noncollagenous components of the ECM, in this way different activation factors important for processes involved in ECM remodeling, such as cell adhesion, cell-cell interaction, and cell migration (Table 1) are released. The MMPs are expressed as inactive proforms, consisting of a signal sequence (which directs them into the extracellular environment), a propeptide that needs to be removed for full biological activity, a zinc dependent catalytic domain responsible for substrate cleavage, a hinge region and a hemopexin like domain.

A subclass of MMPs are represented by the so-called membrane-type MMPs (MT-MMPs) (Sato *et al.*, 1994; Cao *et al.*, 1995) which, unlike the classical MMPs, contain either a stretch of 20 hydrophobic amino acids, which forms a transmembrane domain, and a small cytoplasmic domain (in the case of MMP14, MMP15, MMP16, and MMP24) or a glycosylphosphatidyl inositol linkage (for MMP17 and MMP25), which anchors these proteinases to the cell surface. Currently, there are approximately 26 MMPs known, all of which can be inhibited by TIMP3 but also by other TIMP family members, although with different binding affinities (Murphy and Willenbrock, 1995). Therefore, all four TIMPs possess overlapping inhibitory function towards the MMPs. This is supported by individual TIMP knock out mice where unaffected MMP activities further demonstrate the redundant function of these inhibitors.

**Table 1.** A list of known matrix metalloproteinases (MMPs) and their corresponding biological functions.

<b>MMP</b>	<b>Alternative names</b>	<b>Substrates</b>
MMP1	Collagenase, Fibroblast Collagenase, Interstitial Collagenase	Collagen type I, II, III, VII, VIII, X, aggrecan, gelatin MMP2, MMP9
MMP2	72 kDa Gelatinase, Gelatinase A, Type IV collagenase, Neutrophil gelatinase	Collagen type I, II, III, IV, VII, X, XI, aggrecan, elastin, fibronectin, gelatin, laminin, MMP9, MMP13
MMP3	Procollagenase, Stromelysin- 1, Transin-1	Collagen type II, III, IV, IX, X, XI, aggrecan, elastin, fibronectin, gelatin, laminin, MMP8, MMP13
MMP7	Matrilysin, Matrin, Uterine metalloproteinase	Collagen type IV, X, aggrecan, elastin, fibronectin, gelatin, laminin, MMP1, MMP2, MMP9
MMP8	Collagenase-2, Neutrophil collagenase, PMNL collagenase	Collagen type II, III, V, VII, VIII, X, aggrecan, elastin, fibronectin, gelatin, laminin
MMP9	92 kDa Gelatinase, Type IV	Collagen type IV, V, VII, X, XIV, aggrecan,



	collagenase, Gelatinase B	elastin, fibronectin, gelatin
MMP10	Stromelysin-2, Transin-2	Collagen type III, IV, V, aggrecan, elastin, fibronectin, gelatin, laminin, MMP1, MMP8
MMP11	Stromelysin-2	Aggrecan, fibronectin, laminin
MMP12	Macrophage metalloelastase	Collagen type IV, elastin, fibronectin, gelatin, laminin
MMP13	Collagenase-3	Collagen type I, II, III, IV, aggrecan, gelatin
MMP14	MT1-MMP	Collagen type I, II, III, aggrecan, elastin, fibronectin, gelatin, laminin, MMP2, MMP13
MMP15	MT2-MMP	fibronectin, gelatin, laminin, MMP2
MMP16	MT3-MMP	Collagen type III, gelatin, fibronectin, MMP2
MMP17	MT4-MMP	Fibrin, gelatin
MMP18	Xenopus Collagenase-4, xCol4	
MMP19	RASI-1	Collagen type IV, aggrecan, gelatin, fibronectin, laminin, COMP
MMP20	Enamelysin	Aggrecan, amelogenin, COMP
MMP23	Cysteine array MMP	
MMP24	MT5-MMP	
MMP25	MT6-MMP, leukolysin	Collagen type IV, gelatin, fibronectin, laminin
MMP26	Matrilysin-2, Endometase	gelatin, fibronectin
MMP28	Epylisin	

### 1.6.2 Regulation of the activity of ADAMs by TIMP3

A disintegrin and metalloproteinases (ADAMs) comprise a large family of membrane bound proteases consisting of 34 members (Mochizuki and Okada, 2007). Structurally, they are composed of a signal sequence, a pro-domain, a metalloproteinase or metalloproteinase-like domain, a disintegrin-like domain, a cysteine-rich domain, EGF-like repeats, a transmembrane domain, and a cytoplasmic tail. Proteolytically active ADAMs are mainly involved in the cleavage of the extracellular domain of the

membrane anchored proteins, a process called shedding, although they may also have additional functions such as cell-cell fusion, cell adhesion and cell signalling through the intracellular domain (Table 2). Unlike the broad selectivity of the TIMPs for all MMPs, the ADAMs are inhibited mainly by TIMP3. To date, TIMP3 has been shown to inhibit several ADAMs including ADAM10 (Amour *et al.*, 2000), ADAM12 (Loechel *et al.*, 2000), ADAM28 (Mochizuki *et al.*, 2004), ADAM33 (Zou *et al.*, 2004). However, there are several reports which show that other TIMP family members are able to block ADAM activity, although often with lower efficiency, e.g. ADAM10 (Amour *et al.*, 2000), ADAM28 (Mochizuki *et al.*, 2004), ADAM33 (Zou *et al.*, 2004). In this context, a unique inhibitory function of TIMP3 is to block the shedding activity of ADAM17 (also known as TNF- $\alpha$  converting enzyme, TACE) (Amour *et al.*, 1998). TACE is involved in the cleavage of membrane anchored TNF- $\alpha$  to its soluble form (Black *et al.*, 1997) and has an important role in shedding of many other membrane bound proteins (Peschon *et al.*, 1998). Among the other ligands, TIMP3 can block TACE mediated ectodomain shedding of syndecan-1 and syndecan-4 (Fitzgerald *et al.*, 2000); L-selectin (Borland *et al.*, 1999); and the interleukin-6 receptor (Hargreaves *et al.*, 1998). Also, it has been shown that TACE is able to cleave several membrane anchored proteins including IL1-RII, IL-15Ra, VCAM-1 (Garton *et al.*, 2003), GPIIb/IIIa, M-CSFR (Rovida *et al.*, 2001), fractalkine (CX3CL1) (Garton *et al.*, 2001), c-kit (Cruz *et al.*, 2004), collagen type XVII (Franzke *et al.*, 2002), p55 TNFR1, p75 TNFR2, TGF $\alpha$  (Fan *et al.* 1999), HB-EGF (Sunnarborg *et al.*, 2002), amphiregulin, epiregulin, MUC1 (Thathiah *et al.*, 2003), c-Met (Nath *et al.*, 2001; Wajih *et al.*, 2002), CD30 (Hansen *et al.*, 2000), CD40 (Contin *et al.* 2003), HER4/erbB4 (Rio *et al.* 2000), p75 neurotrophin receptor (p75<sup>NTR</sup>) (Weskamp *et al.*, 2004), TRANCE (Lum *et al.*, 1999), NRG (Neuregulin) (Montero *et al.*, 2000) and APP (amyloid protein precursor). The importance of TIMP3 inhibition towards TACE has been demonstrated in the liver of TIMP3 deficient mice (Mohammed *et al.*, 2004). This study shows an increased amount of soluble TNF- $\alpha$  as a consequence of upregulated TACE activity leading to a failure of liver regeneration.

**Table 2.** Summary of ADAM family members and their functions, if known

<b>ADAM</b>	<b>Alternative names</b>	<b>Proteolytic activity</b>	<b>Function and substrate</b>
ADAM1	PH-30 $\alpha$ , Fertillin- $\alpha$	-	Sperm-egg binding and fusion
ADAM2	PH-30 $\beta$ , Fertilin- $\beta$	-	Sperm-egg binding and fusion
ADAM3	Cyritestin, tMDC, CYRN	-	
ADAM4	tMDC V	-	
ADAM5	tMDC II	-	
ADAM6	tMDC IV	-	
ADAM7	EAP I, GP-83	-	
ADAM8	MS2 (CD156)	+	Neutrophil infiltration, shedding of CD23
ADAM9	MDC9, MCMP, Meltrin- $\gamma$	+	Shedding of HB-EGF, TNF-p75 receptor, cleavage of APP, digestion of fibronectin and gelatin
ADAM10	MDAM, Kuzbanian	+	Release of TNF- $\alpha$ , digestion of collagen IV, gelatin and myelin basic protein, cleavage of delta, APP, L1, and CD44, shedding of HB EGF
ADAM11	MDC	-	
ADAM12	Meltrin- $\alpha$ , MCMP, MLTN, MLTNA	+	Muscle formation, digestion of IGFBP-3

			and 5, shedding of HB-EGF, digestion of collagen IV, gelatin and fibronectin
ADAM13	xMDC13a, x ADAM13a	-	Movement of neural crest
ADAM14	ADM-1	-	
ADAM15	Metargidin, MDC15, AD56, CR II-7	+	Expression in arteriosclerosis, digestion of collagen IV and gelatin
ADAM16	xMDC16	-	
ADAM17	TACE, cSVP	+	Shedding of TNF- $\alpha$ , TGF- $\beta$ , TNF-p75 receptor, ErbB4, TRANCE and HB-EGF, presence of RRKR sequence, cleavage of APP, Notch, L-selectin and CD44
ADAM18	tMDC III	-	
ADAM19	Meltrin- $\beta$ , FKSG34	+	Formation of neuron, digestion of neuregulin
ADAM20		+	Formation of sperm
ADAM21	ADAM31	+	
ADAM22	MDC2	-	
ADAM23	MDC3	-	
ADAM24	Testinase-1	-	Sperm-egg binding

			and fusion
ADAM25	Testinase-2	-	
ADAM26	Testinase-3	-	
ADAM27	ADAM18, tMDCIII	-	
ADAM28	e-MDC II, MDC-Lm, MDC-Ls	+	Digestion of myelin basic protein and IGFBP-3
ADAM29	svph 1	-	
ADAM30	svph 4	+	
ADAM32	AJ131563	-	
ADAM33		+	Mutation in bronchial asthma patients, cleavage of APP, KL-1 and insulin B chain
ADAM34	Testinase-4	-	

(+) and (-) indicates that the ADAM protein does or does not exhibit proteolytic activity, respectively;

### 1.6.3 TIMP3 and ADAMTS inhibition

ADAMTSs (a disintegrin and metalloproteinase with thrombospondin motifs) form a class of secreted proteinases comprising 19 members (Porter *et al.*, 2005) (Table 3). Some members of this family of metalloenzymes are bound to the ECM whereas others are secreted as soluble molecules. The domain structure of ADAMTS proteins from the N- to the C-terminal is as follows: signal peptide (for extracellular export), prodomain which confers the latency of the enzyme, a metalloproteinase domain, a disintegrin-like domain, a central thrombospondin (TS) type I-like repeat (TS1 and TS2), a cysteine-rich domain with ten conserved cysteine residues, a spacer region and

various numbers of C-terminal TS repeats (Apte SS, 2004). Functionally, ADAMTS proteins are involved in a variety of biological processes. ADAMTS-1 and ADAMTS-8 have antiangiogenic properties (Vázquez *et al.*, 1999); ADAMTS-1, -4, -5, -8, -9 and -15 are able to cleave the major cartilage proteoglycan aggrecan; ADAMTS-2, -3 and -14 are procollagen N-proteinases and process procollagens to collagen by removal of their N-terminal propeptide. ADAMTS-1 and ADAMTS-4 are able to cleave versican (Sandy *et al.*, 2001; Westling *et al.*, 2004) and brevican (Nakamura *et al.*, 2000; Matthews *et al.*, 2000). ADAMTS proteolytic activities are regulated at both the transcriptional and the posttranslational level. At the protein level, aggrecanolytic activity of the two aggrecanases ADAMTS-4 and ADAMTS-5 are potently inhibited by TIMP-3 (Kashiwagi *et al.*, 2001), although it has been shown that the other family members can also inhibit ADAMTS4 but with less efficiency (Hashimoto *et al.*, 2001). In addition, TIMP3 is able to inhibit the procollagen N-proteinase activity of ADAMTS-2 (Wang *et al.*, 2006). Pathologically, some of the ADAMTS family members, e.g. ADAMTS4 and ADAMTS5, are involved in osteoarthritis (Malfait *et al.*, 2002). The major characteristic of this disease is loss of the articular cartilage which is mainly composed of aggrecan and collagen type II accounting for 90% of dry weight of cartilage. In the excessive catabolism of aggrecan and collagen type II the MMPs are also involved (Downs *et al.*, 2001; Otterness *et al.*, 1999).

**Table 3.** A list of known ADAMTS family members and their functions

ADAMTS	Alternative names	Proteolytic activity	Function and substrate
ADAMTS 1	C3-C5, METH1, KIAA1346	+	Binding to heparin, presence of RRKR sequence, digestion of aggrecan and versican
ADAMTS 2	Procollagen N-proteinase, hPCPNI, PCINP	+	Processing of collagen I and II N - propeptides

ADAMTS 3	KIAA 0366	+	Processing of collagen N-propeptides
ADAMTS 4	KIAA0688, aggrecanase-1, ADMP-1	+	Digestion of aggrecan, brevican and versican
ADAMTS 5	ADAMTS11, aggrecanase-2, ADMP-2	+	Digestion of aggrecan
ADAMTS 6			
ADAMTS 7			
ADAMTS 8	METH-2	+	Digestion of aggrecan, inhibition of angiogenesis
ADAMTS 9	KIAA1312	+	Digestion of aggrecan
ADAMTS 10			
ADAMTS 12			
ADAMTS 13	vWFCP, C9orf8	+	Cleavage of von Willebrand factor
ADAMTS 14		+	Processing of collagen N-propeptides
ADAMTS 15		+	Digestion of aggrecan
ADAMTS 16			
ADAMTS 17	FLJ32769, LOC123271		
ADAMTS 18	ADAMTS21, HGNC:16662		
ADAMTS 19			

ADAMTS 20			
-----------	--	--	--

(+) indicates that the ADAMTS presents enzymatic activity

#### 1.6.4 Antiangiogenic properties of TIMP3

Formation of the vascular network is a prerequisite for growth and maintenance of tissue homeostasis. Formation and remodelling of new blood vessels occurs by three distinct processes: vasculogenesis, angiogenesis and arteriogenesis (Buschmann and Schaper, 1999).

Vasculogenesis is a process requiring the differentiation of angioblast (the precursors of endothelial cells) into blood islands, which then fuse to form a primitive cardiovascular system during embryonic development. Angiogenesis is defined as the formation of new capillary blood vessels by sprouting of endothelial cells from pre-existing blood vessels. The growth of new blood vessels is a complex network of coordinated interactions between several important processes and includes production of proteolytic enzymes which degrade the ECM prior to migration of endothelial cells followed by endothelial cell differentiation into new vessels and maturation of the vascular wall by recruiting mesenchymal cells (Bussolino *et al.*, 1997). Finally, arteriogenesis is the rapid proliferation of pre-existing collateral vessels that occurs in ischemic tissue (Buschmann and Schaper, 1999).

Vascular endothelial growth factor (VEGF) is an essential regulator of physiological angiogenesis during embryogenesis (Uhlmann, 2006) and is also involved in pathological angiogenesis like tumour growth (Ferrara, 1995; Ferrara, 2002), retinal disorders (Gariano and Gardner, 2004) and other diseases (Ferrara, 1995). The VEGF protein family consists of four isoforms: VEGF<sub>121</sub>, VEGF<sub>165</sub>, VEGF<sub>189</sub> and VEGF<sub>206</sub>, which arise from alternative exon splicing and bind to 3 different types of tyrosine kinase receptors: VEGF receptor 1 (Flt-1), VEGF receptor 2 (also known as kinase domain receptor (KDR) or Flk1) and VEGF receptor 3 (Ferrara *et al.*, 2003). The first two receptors are expressed on the cell surface of most blood endothelial cells whereas VEGFR-3 is mainly expressed on endothelial cells associated with the lymphatic system (Ferrara *et al.*, 2003). VEGF binds to the extracellular domain of the respective receptor and initiates dimerization leading to the activation of an intracellular kinase



domain by phosphorylation and initiating a signalling cascade that finally induces angiogenesis (Ferrara *et al.*, 2003).

Initially, it has been shown that TIMP3 protein is able to inhibit angiogenesis (Anand-Apte *et al.*, 1997) and later that it can inhibit VEGF induced inhibition of angiogenesis by blocking VEGF binding to VEGF receptor-2 (Qi *et al.*, 2003).

### **1.6.5 Proapoptotic activity of TIMP3**

Apoptosis often occurs in tandem with programmed cell death, but there are a few distinguishing features. Programmed cell death is characterized mainly by changes within the cell at the molecular level resulting from a preexisting death program (Saikumar *et al.*, 1999). Apoptosis refers to the morphological features such as cell shrinking, chromatin condensation, plasma membrane blebbing or budding and finally cell fragmentation into membrane-enclosed structures called “apoptotic bodies” containing cytosol, the condensed chromatin and organelles.

Programmed cell death has an important role during physiological processes of multicellular organisms especially during embryogenesis and morphogenesis and also plays an important role in the development and maintenance of biological systems. These aspects of apoptosis are emphasized by its involvement in many normal but also pathological processes. Physiological cell death is a normal process which occurs constantly, but it must be balanced with cellular proliferation to maintain the proper homeostasis of a pluricellular organism. Distinct from apoptosis, unphysiological cell death –termed necrosis- may occur in response to chemical and physical injuries and is characterized by cell swelling which leads to membrane disruption. Thus, the cell content is released to the extracellular space and elicits an inflammatory response. Dysfunction of the apoptotic program can be involved in several diseases such as cancer, autoimmune disorder, neurodegenerative diseases (Fadeel *et al.*, 1999).

TIMP3 induction of cell death has been shown in rat vascular smooth muscle cell (Baker *et al.*, 1998). Overexpression of TIMP3 in melanoma cell lines (Ahonen *et al.*, 1998), HeLa and HT1080 (Baker *et al.*, 1999) promotes apoptosis. Cell death due to TIMP3 was demonstrated not only in cancer cells but also in primary porcine chondrocytes (Gendron *et al.*, 2003). The proapoptotic activity of TIMP3 was mapped to its N-terminus (Bond *et al.*, 2000) and seems to depend on its MMP inhibitory activity.

### 1.6.6 TIMP3 as a tumour suppressor gene

DNA modifications (e.g. DNA methylation) that do not involve changes in the underlying DNA sequence of the organism (epigenetics) are the most common covalent modifications in the human genome. Their importance has been demonstrated in X chromosome inactivation, progress of carcinogenesis and for the developmental control of gene expression. In this regard, DNA methylation is directly connected to gene silencing through chromatin-remodelling complexes (Robertson & Wolffe, 2000).

TIMP3 as a tumour suppressor gene is involved in tumour progression by hypermethylation of its promoter which, in turn, correlates with TIMP3 gene inactivation (loss of protein expression). It has been shown that TIMP3 is involved in a variety of tumour invasion/metastatic processes, e.g. in kidney (Bachman *et al.*, 1999), pancreatic endocrine tumours (Wild *et al.*, 2003), gastric cancer (Kang *et al.*, 2000), and glioblastomas (Nakamura *et al.*, 2005). A possible mechanism of TIMP3 as a tumour suppressor gene is suggested by the correlation of TIMP3 expression with the invasiveness of glioblastoma. This type of tumour metastasis is associated with the cleavage of the extracellular matrix hyaluronan-binding protein brevican (or brain-enriched hyaluronan binding (BEHAB)) whereas in the non-invasive tumour the protein is not cleaved or is not expressed (Zhang *et al.*, 1998; Nutt *et al.*, 2001). The enzyme responsible for the cleavage of the brevican was identified to be ADAMTS4 (Matthews *et al.*, 2000) and therefore inactivation of TIMP3 might lead to the upregulation of ADAMTS4 mediated cleavage of brevican in glioblastomas.

### 1.7 Aims of the present study

The main goal of the present study was to elucidate TIMP3 function and its possible pathomechanism in Sorsby fundus dystrophy by analyzing two available mouse models: TIMP3 knock-out and S156C-TIMP3 knock-in. In the dissection of molecular mechanisms underlying the SFD condition an important question was whether the free cysteine mutation in TIMP3 could lead to a gain-of-function or alternatively a loss-of-function. In this context, it is important to identify the primary molecular event that initiates SFD pathogenesis. Towards this goal, the known biological functions of TIMP3 were analysed both *in vivo* by using the mouse models and *in vitro* with recombinant proteins. The inhibitory activity of the S156C mutant TIMP3 versus wildtype (WT) TIMP3 towards ADAMTS4, ADAMTS5, TACE and

MMPs was analysed in parallel with the remaining TIMP family members to assess the redundancy in the functions of these proteins.

Another objective of the project was to identify new binding partners in an effort to gain further insight into disease mechanism. In this context, the binding of TIMP3 to several types of collagens was investigated. One of the characteristics of SFD is that the mutant protein accumulates in the eyes of the affected patients. Therefore, quantification of the S156C mutant TIMP3 in the ECM was determined together with its rate of turnover.

## **2. Materials and Methods**

### **2.1 Molecular biology methods**

#### **2.1.1 Mammalian cell culture and cryopreservation of cells**

Mammalian cell lines were cultivated in different media depending on the cell type. HEK-293 EBNA (Human Embryonic Kidney 293, Epstein-Barr virus nuclear antigen-1) were maintained in DMEM high glucose with 10 % FBS (Foetal bovine serum), Penicillin 100 Units/ml / Streptomycin 100 µg/ml and 500 µg/ml G418 sulfate (Geneticin). COS7 and the fibroblasts derived from the TIMP3 knock-out and the S156C-TIMP3 knock-in mice were grown in DMEM high glucose with 10 % FBS and Penicillin/Streptomycin. Chondrocytes were grown in DMEM/F12, 10% FBS and Penicillin/Streptomycin. All cells were grown at 37°C in 5% CO<sub>2</sub> atmosphere. For propagation of the cells a confluent 10 cm dish was washed with sterile PBS and then incubated with 2 ml of trypsin solution (0.05% in PBS) at 37°C for a few minutes depending on cell adherence. After cell detachment, the suspension was added to 8 ml of culture medium to inactivate the trypsin and centrifuged for 3 min at 1500 rpm. The cell pellet was resuspended in 2 ml of medium and cells plated at the density required by the experiment. For long term storage, the cell pellet was resuspended in the growing medium supplemented with 10% DMSO and the tube was placed in a cryo freezing container in the -80°C freezer which allows freezing of the cells with -1°C/min rate of cooling.

#### **2.1.2 Culture and conservation of *E. coli* strains**

A single colony from freshly transformed *E. coli* was inoculated in 4 ml LB medium (Bacto Tryptone 10 g/l, Bacto Yeast Extract 5 g/l, NaCl 5 g/l, pH 7.5) with the corresponding selective antibiotic determined by the plasmid and shaken overnight at 37 °C at 200 rpm. Alternatively, 50 ml of LB medium was inoculated with one colony. After overnight growth, 1 L of LB medium was inoculated with this stationary culture for protein expression.

For *E. coli* cell preservation, a freshly transformed colony was picked and a 5 ml preculture was inoculated and grown overnight at 37°C. From the stationary *E. coli* culture an aliquot was taken and mixed with glycerol to a final concentration of 20% and stored at -80°C.

### **2.1.3 Preparation and transformation of *E. coli* competent cells**

#### **2.1.3.1 Preparation of bacterial competent cells**

One single colony was inoculated in 5 ml LB medium and grown overnight at 37 °C. Next day, 500 ml of LB medium was inoculated with the overnight culture and grown until OD<sub>600</sub> reached 0.8. The cells were harvested by centrifugation at 4000 rpm for 15 min at 4°C and subsequently washed with 30 mM potassium acetate, 50 mM MnCl<sub>2</sub>, 100 mM CaCl<sub>2</sub> and 15% glycerol, pH 7.0 and incubated on ice for 15 min. After centrifugation, the cells were resuspended in 8 ml of 10 mM MOPS, 75 mM CaCl<sub>2</sub>, 10 mM KCl, 15 % glycerol, pH 7.0, aliquoted and stored at -80°C.

#### **2.1.3.2 Transformation of competent cells with plasmid DNA**

*E. coli* competent cells (200 µl) were incubated with 10 µl of ligation mixture (or 1 µl of plasmid DNA) on ice for 20 min. The cells were heated at 42°C for 45 seconds and then 500 µl of SOC medium was added and the cells incubated for 20 minutes at 37°C. Finally, 100 µl of the transformed cells were plated on a LB agar plate with the appropriate antibiotic and incubated overnight at 37°C.

### **2.1.4 RNA isolation from primary cell culture**

Total RNA was isolated from primary fibroblasts and chondrocytes using the Qiagen RNeasy kit according to the manufacturer's instructions. Briefly, confluent cells grown in a monolayer were washed with sterile PBS and detached using trypsin. The cell pellet was resuspended in the provided lysis buffer and disrupted by freeze/thaw steps. The extract was applied to a spin column and after several washing steps total RNA was eluted with 50 µl RNase free water and stored at -80°C.

### **2.1.5 Plasmid DNA isolation from *E. coli***

Analytical scale. To analyse transformed clones for the presence of a specific plasmid, to confirm the mutation after site directed mutagenesis or for DNA sequencing, the analytical preparation of the plasmid DNA was performed. Plasmid DNA was isolated from 5 ml of overnight bacterial culture using a kit from Macherey-Nagel. Typically, DNA was eluted in 50 µl of buffer.

Preparative scale. In order to obtain higher amounts of DNA, necessary for mammalian cells transfection, plasmid DNA was isolated from 100 ml overnight

bacterial culture using the midiprep kit from Macherey-Nagel. DNA was resuspended in 100  $\mu$ l of ddH<sub>2</sub>O and the concentration measured with a NanoDrop ND-1000 Spectrophotometer.

## **2.1.6 Gel electrophoresis and DNA purification**

Separation of double stranded DNA was performed by using horizontal agarose gel electrophoresis.

### **2.1.6.1 Analytical agarose gel electrophoresis**

Analytical agarose gel electrophoresis was carried out to analyse PCR fragments or the presence of insert after restriction digest. For analytical gel electrophoresis, 100 ml of 1 to 2 % (w/v) agarose gel (depending on the size of the fragments) was prepared in TBE (89 mM Tris/HCl, 89 mM borate acid, 2 mM EDTA, pH 8.3) buffer with ethidium bromide. Normally, 5  $\mu$ l of DNA fragment mixed with 1  $\mu$ l of 5x PAA loading buffer (95% formamide, 5 mM NaOH, 0.1% Bromphenol blue, 0.1% xylene cyanole) was applied to each lane. DNA was visualised under UV light after electrophoresis.

### **2.1.6.2 Preparative agarose gel electrophoresis**

Cloning of PCR fragments or subcloning of DNA fragments after restriction digest was performed by preparative agarose gel electrophoresis. 100 ml of 1 to 2 % (w/v) agarose gel in TBE buffer with ethidium bromide was prepared. The electrophoresis was performed at 120 V for approximately 25 min. DNA fragments were visualized under UV light and agarose gel containing the correct size DNA fragment was excised with a clean scalpel. In the next step, DNA was extracted from the gel using a kit from Macherey-Nagel following the manufacturer's instruction. Finally, the DNA was eluted with 20  $\mu$ l of the supplied buffer. 5 $\mu$ l of the eluted DNA was loaded on an analytical gel to check for the recovery and purity of DNA.

## **2.1.7 *In vitro* modification of DNA**

### **2.1.7.1 Site directed mutagenesis**

Site directed mutagenesis was carried out to introduce point mutations or insertions/deletions in a given gene. For this purpose, a primer pair was designed that contained the mutated codon or the insertion/deletion. Templates to be modified by site directed mutagenesis were present in pGEM vector and subsequently subcloned in the desired vector.

The mutagenesis reaction was performed in a final volume of 25  $\mu$ l with the following composition: 15.8  $\mu$ l H<sub>2</sub>O, 2.5  $\mu$ l 10x Pfu buffer 0.6  $\mu$ l forward primer (10  $\mu$ M), 0.6  $\mu$ l reverse primer (10  $\mu$ M), 2  $\mu$ l dNTPs (1.25 mM of dATP, dCTP, dGTP and dTTP), 2.5  $\mu$ l plasmid (200 ng of template) and 1  $\mu$ l of Pfu ultra high fidelity polymerase. All components were pipetted on ice for a hot start PCR reaction. The PCR program used was 95°C for 30 sec, annealing 55°C for 60 sec, extension at 68°C for 5 min. After the PCR reaction, the methylated DNA (template) was digested by incubating the mixture with 1  $\mu$ l DpnI plus 2.5  $\mu$ l of 10x NEB4 buffer for 3 hours at 37°C. 10  $\mu$ l of the digested product was transformed into *E. coli* XL 1 blue competent cells and another 5  $\mu$ l was used for analytical gel electrophoresis. Next day the plasmid DNA was prepared from a few picked colonies, then sequenced (and/or restriction digest) to detect the mutation or insertion/deletion.

### **2.1.7.2 Dephosphorylation of linearized plasmid DNA**

In order to subclone a gene using a single restriction enzyme, the digested vector was dephosphorylated to avoid the religation of the empty vector backbone. Therefore, after a preparative digestion of the vector, the mixture was incubated with 1  $\mu$ l of Antarctic phosphatase at 37°C for 1 hour to remove 5' phosphate groups from the DNA strand. The enzyme was finally inactivated by heating at 65°C for 5 min.

### **2.1.7.3 Filling in DNA sticky end**

To fill the 5' overhangs of a DNA fragment after restriction digest to generate a blunt end, the large fragment of Klenow DNA polymerase I was used. In a final volume of 20  $\mu$ l the following components were added: 500 ng of restriction digested DNA fragment, 2  $\mu$ l 10x NEB2 buffer, dNTPs to a final concentration of 33  $\mu$ M, 0.2  $\mu$ l large fragment of Klenow DNA polymerase I (10 u) and 7  $\mu$ l H<sub>2</sub>O. The reaction mixture was

incubated at 25°C for 15 min and then the enzyme was heat inactivated at 75°C for 20 min. Finally, 2 µl of 10x ligation buffer and 2 µl T4 DNA ligation was added and incubated overnight at 16°C.

#### **2.1.7.4 Polymerase chain reaction (PCR)**

The polymerase chain reaction (PCR; Saiki *et al.*, 1988) was employed for the specific amplification of a gene of interest, site directed mutagenesis or DNA sequencing. In principle, in a regular PCR a primer pair is used one of which anneals at the 3' end and the other which anneals at the 5' end with at least 18 bases hybridising specifically to the template. If required, the primers contain at the 5'-end and at 3' -end restriction sites for cloning in a vector. To achieve the amplification of the desired gene, thermostable Pfu polymerase (Lundberg *et al.*, 1991) and/or Taq polymerase was used. The Pfu DNA polymerase is a proofreading enzyme containing a 3'-to-5' exonuclease activity so that incorrectly incorporated nucleotides are excised.

Standard PCR reactions were performed in a final volume of 25 µl containing the following components: 20-500 ng of DNA template, 10 pmol of each primers, 0.2 µl of Pfu and/or Taq DNA polymerase (in-house made), dNTPs and 1x PCR buffer (50 mM KCl, 10 mM Tris/HCl, pH 8.3, 1 mM MgCl<sub>2</sub>) with hot start reaction. The PCR amplification of a gene was performed in three steps: first the template DNA was denatured by heating it at 94°C for 3-4 min, followed by annealing of the primers to the DNA at 52°C to 64°C depending on their melting temperature and the third step, elongation of the DNA at 72°C for 1 min per kilobase. Generally, for amplification of a gene 25 cycles were performed.

#### **2.1.7.5 First-strand cDNA synthesis**

In order to clone a gene or to quantify it by different methods it is necessary to reverse transcribe the RNA to obtain the template cDNA. The elongation reaction was performed in a final volume of 20 µl using Superscript II reverse transcriptase (RT) (Invitrogen, Karlsruhe, Germany). 1 µg of total RNA together with 1µl oligo dT (500 µg/ml), 1 µl dNTPs (10 mM of dATP, dGTP, dCTP, dTTP), RNase free water and heated to 72°C for 3 min followed by quick chill on ice. Next, 4 µl of 5x first strand buffer (250 mM Tris/HCl pH 8.3, 30 mM MgCl<sub>2</sub>, 375 mM KCl), 2 µl 0.1 M DDT was added to the reaction buffer and incubated for 2 min at 42°C. In the end, 0.5 µl of



Superscript II was pipetted into the reaction and further incubated for 50 min at 42°C. Finally, the enzyme was heat inactivated at 72°C for 15 min.

#### **2.1.7.6 Double stranded DNA cleavage with restriction endonucleases**

For the restriction analysis of plasmid DNA and preparation of DNA fragments, restriction digestion was made with the corresponding endonucleases. The reaction takes place in a buffer which was supplied by the suppliers. In the case of digestion with two different enzymes the buffer was chosen such that both enzymes have the highest activity.

Analytical restriction digestion was carried out in a final volume of 10 µl using 5U of the endonuclease, 1 µg of DNA for 60 min at the temperature required for the enzyme. For preparative restriction digest, 1 to 10 µg of plasmid DNA was incubated with 20U of endonuclease in a final volume of 30 µl. In the case of cloning of PCR fragments, the DNA was digested in the same way as for preparative DNA cleavage. For further manipulation, digested DNA was separated on a preparative agarose gel or phenol/chloroform extracted.

#### **2.1.7.7 Ligation of DNA fragments**

To clone a DNA fragment in a defined vector, the restriction endonuclease cleaved DNA fragment was linked covalently via phosphodiester bonds using T4 DNA ligase. A typical ligation reaction was performed in a final volume of 10 µl containing: 1 µl 10x ligation buffer, 1 µl T4 DNA ligase (400 u), vector backbone : insert fragment in a ratio of 1:3 and H<sub>2</sub>O up to 10 µl. The mixture was incubated overnight at 16°C followed by transformation of the ligation product into competent bacteria. As a control, another ligation reaction was performed containing only the linearized vector.

#### **2.1.7.8 Double stranded DNA sequencing**

DNA sequencing was carried out on a 3130x/Genetic Analyzer using the BigDye Terminator Cycle Sequencing Ready Reaction Kit. This is based on a modified Taq DNA polymerase (AmpliTaq; Tabor & Richardson, 1995) that is able to incorporate a chain-terminating dideoxynucleotide (ddATP, ddCTP, ddGTP, ddTTP) into DNA labelled with different dichlororhodamine dyes (Rosenblum *et al.*, 1997). In the PCR reaction the nascent chain is interrupted and results in PCR fragments of different sizes, ending with a terminator base labelled with the corresponding

fluorophor. During capillary-electrophoresis the PCR fragments are separated on a special polymer (Performance Optimized Polymer 6, POP-6) according to size. The florescent signal is detected with a CCD (Charge-Coupled Device) camera and recorded as a digital signal.

A standard cycle sequencing reaction is performed in a final volume of 10  $\mu$ l and has the following components: 0.3  $\mu$ l of BigDye ready reaction mix, 1  $\mu$ l of one primer (either forward or reverse), ddH<sub>2</sub>O and the template DNA. This can be plasmid DNA (often further purified by phenol/chloroform extraction before adding it to the reaction), a PCR fragment obtained from colony PCR or amplified from plasmid DNA. In the latter case, prior to starting the amplification reaction, the PCR fragments were treated with shrimp alkaline phosphatase (dephosphorylates remaining dNTPs) and exonuclease I (degrades single-stranded DNA/PCR primers). The incorporation of the fluorescently labelled dNTPs takes place in 29 cycles according to the PCR sequencing program: 96°C, 30 s; 56°C, 15 s; 60°C, 2 min. The resulting PCR product is precipitated by adding 1  $\mu$ l 3 M Na acetate pH 4.6, 2  $\mu$ l 125 mM EDTA pH 8.0 and 50  $\mu$ l ethanol (p.a.) mixed vigorously and incubated 15 min at room temperature. After pelleting the DNA by centrifugation, it is washed with 70  $\mu$ l of 70% ethanol and dried at room temperature. Finally, the DNA pellet is resuspended in 10  $\mu$ l HiDi –formamide, followed by loading into the sequencer.

#### **2.1.7.9 Phenol/chloroform extraction and ethanol precipitation**

To obtain high quality DNA preparations, phenol/chloroform extractions were performed to remove contaminating *E. coli* proteins.

##### Phenol/chloroform extraction

After preparation of plasmid DNA (see section 2.1.5), samples were extracted with phenol/chloroform by adding 10  $\mu$ l of 3 M sodium acetate pH 4.8 and 100  $\mu$ l phenol/chloroform/isoamylalcohol (with the ratio of 25:24:1) and mixed well. The samples were centrifuged for 5 min at 14000 rpm, 4°C to separate the aqueous (upper) and organic (lower) phases. The upper phase was transferred to a new tube containing chloroform/isoamylalcohol (24:1) and reextracted.

### Ethanol precipitation

Remaining trace amounts of phenol from the extraction were removed by ethanol precipitation. For this, the aqueous phase was mixed with 250  $\mu$ l of cold ethanol (p.a.) and incubated for at least 1 hour at  $-20^{\circ}\text{C}$ . After centrifugation (30 min, 14000 rpm,  $4^{\circ}\text{C}$ ) the supernatant was discarded and the pellet was washed with 250  $\mu$ l 70% ethanol. After further centrifugation for 10 min, the supernatant was removed and the pellet dried at room temperature. Finally, the precipitated DNA was resuspended in 100  $\mu$ l of sterile water and stored at  $-20^{\circ}\text{C}$ .

## **2.1.8 Production of recombinant proteins in *E. coli***

### **2.1.8.1 Protein expression in inclusion bodies**

For the production of recombinant proteins or fusion proteins in *E. coli* as inclusion bodies the vectors pET21 or pGEX4T3 were used. 50 ml of LB medium/ampicillin was inoculated with a freshly transformed colony of BL21 (DE3) strain and incubated overnight at  $37^{\circ}\text{C}$ , 200 rpm. Next day, the stationary grown culture was added to 1 L of fresh LB medium and the cells were grown until an  $\text{OD}_{600}$  of  $\sim 1$ . Protein expression was induced by adding IPTG to a final concentration of 1 mM and protein production continued overnight at  $30^{\circ}\text{C}$ . For the isolation of the inclusion bodies, the induced culture was centrifuged 15 min at  $4^{\circ}\text{C}$  and the cell pellet resuspended in 10 ml of 50 mM Tris/HCl pH 8.0, 100 mM NaCl and 1 mM EDTA. To this mixture lysozyme and  $\text{MgCl}_2$  was added to a final concentration of 1.5 mg/ml and 5 mM, respectively and incubated for 30 min on ice. To lyse the cells, sonification was performed 3 times for 3 min each time with a 3 min interval. Since the viscosity of the solution was high, Dnase I (20U) was added to the suspension and incubated for 30 min at room temperature. The suspension was then centrifuged at 12000 rpm for 15 min. The isolated inclusion bodies were denatured by resuspending the pellet in 25 ml of 50 mM Tris/HCl pH 8.0, 6 M guanidine hydrochloride, 10 mM  $\beta$ -mercaptoethanol and mixing it overnight at room temperature. Next day, the suspension was centrifuged 15 min at 12000 rpm to remove insoluble material. Denatured recombinant proteins were handled in two different ways: TIMP1, TIMP2, TIMP4, N-TIMP3, C-TIMP3 were used in this form for refolding whereas full length WT-TIMP3, S156C-TIMP3, MMP13 and the TACE catalytic domain were directly applied to a Ni-NTA column for purification.

For the expression of proteins fused to GST, 10 ml of preculture was inoculated with one freshly transformed colony and incubated overnight by shaking at 200 rpm, 37°C. Next day, 500 ml of LB/Amp was added to the overnight culture and further incubated until OD<sub>600</sub> reached ~1. Protein production was induced overnight by adding IPTG to a final concentration of 0.1 mM. The cells were pelleted at 5000 rpm for 15 min, resuspended in 5 ml cold PBS supplemented with lysozyme 1 mg/ml and incubated on ice for 1 hour. The suspension was sonicated for 1 minute on ice, then for a further 4 minutes to disrupt the cells. The suspension was centrifuged for 15 min at 12000 rpm and the soluble fraction was saved for further purification.

In parallel, to prepare whole cell extract for the visualization of the proteins, 1 ml of the bacterial culture was centrifuged and the cell pellet was resuspended in 100 µl of SDS loading buffer. After centrifugation of the lysate, 25µl of the soluble fraction was applied to an SDS-PAGE gel together with samples from each purification step to check for the presence and purity of the protein.

#### **2.1.8.2 Recombinant protein refolding**

After denaturation, proteins were refolded in 100 ml of refolding buffer. 1 ml of denatured protein solution was added dropwise to 100 ml of refolding buffer with the following composition: 100 mM Tris/HCl pH 8.5, 1 M arginine, 100 mM NaCl, 5 mM reduced glutathione, 0.5 mM oxidized glutathione and stirred for 2 days at 4°C. In the case of TIMP1, TIMP2, TIMP4, N-TIMP3 and C-TIMP3 the refolded protein solution was dialyzed against 50 mM NaH<sub>2</sub>PO<sub>4</sub>, 300 mM NaCl, pH 8.0 (dilution factor 100) before Ni-NTA chromatography. For full length WT-TIMP3 and S156C-TIMP3 (obtained after Ni-NTA purification), the recombinant refolded proteins were kept and used in the bioactivity assays in this buffer.

#### **2.1.9 Recombinant protein expression in mammalian cells**

Unlike bacterial expression systems – where the overexpressed mammalian protein most often is found unfolded in inclusion bodies and needs to be refolded – expression of proteins in mammalian cells has the advantage of natural environment allowing proper protein folding.

### **2.1.9.1 Transient transfections**

Various cell lines (HEK-293 EBNA, COS-7) were grown to approximately 80% confluency and transfected using calcium phosphate method (Chen *et al.*, 1987). Typically, for one 10 cm dish, 10 µg of plasmid DNA was pipetted in 370 µl (final volume) of water and, 123 µl of 1 M CaCl<sub>2</sub> and 495 µl 2x BBS (50 mM BES [N,N-Bis(2-hydroxyethyl)-2-aminoethanesulfonic acid], 280 mM NaCl, 1.4 mM Na<sub>2</sub>HPO<sub>4</sub>, pH 6.95) by vortexing and incubated at room temperature for 30 min. The calcium-phosphate/DNA precipitate was added dropwise to the cells such that the whole plate was covered. Next day, the medium was changed as the solution used for transfection is toxic to the cells. Recombinant proteins were harvested after one to three days.

### **2.1.9.2 Stable transfections**

To obtain higher amounts of protein, stable transfectants were generated. Plasmid DNA prepared by using a commercially available kit was further purified by phenol-chloroform extraction and ethanol precipitation. The cells were transfected using the calcium-phosphate method as described for transient transfections. The medium was changed next day for regular medium and the cells were incubated for one more day for recovery. 36 hours posttransfection a selection medium was applied containing 250 µg/ml hygromycin B. The medium was changed every day for approximately 3 weeks until colonies resistant to hygromycin B started to appear. The colonies were trypsinized and plated on a new cell culture dish. The cells were maintained in DMEM with 50 µg/ml hygromycin. On a control plate containing non-transfected cells, the cells died within 10 days of the start of selection.

## **2.2 Biochemical methods**

### **2.2.1 Protein purification**

Enzyme-inhibitor kinetic analysis requires that the recombinant proteins are homogenous and in a highly pure state. Purification of recombinant proteins can be achieved by attaching an affinity tag to the protein of interest and performing the corresponding chromatography.

### **2.2.1.1 Immobilized metal affinity chromatography (IMAC)**

This method is based on the principle of interaction of an oligohistidine tag with a bidentate or tridentate chelating agent. For isolation of recombinant his-tagged proteins, a column was used with 5 ml bed volume (Ni-NTA agarose) and a peristaltic pump. First, the column was regenerated with 50 mM EDTA, 300 mM NaCl (regeneration buffer) followed by washing the column with water. After recharging the column with 50 mM NiSO<sub>4</sub> and washing with water, the column was again loaded with IMAC buffer (50 mM Na H<sub>2</sub>PO<sub>4</sub>, 300 mM NaCl pH 8.0). Next, recombinant protein was applied to the column and washed with IMAC buffer. Elution of protein bound to the column was achieved using a 40 ml linear concentration gradient from 0 to 250 mM of imidazole in IMAC buffer at a flow rate of 1 ml/min, and 2 ml fractions were collected. After elution, the column was washed with regeneration buffer to remove all proteins which might have remained after competitive elution to allow the column to be reused for purification of other proteins. The collected fractions of eluted recombinant protein were analysed on a SDS-PAGE gel to check for purity. The fractions with the highest purity and yeild of protein were pooled and concentrated with an Amicon concentrator. Alternatively, proteins were used directly for refolding after purification. Recombinant proteins were stored in aliquots at -20°C.

### **2.2.1.2 Glutathione-S-transferase (GST) chromatography**

The soluble fraction from disrupted cells expressing GST fusion proteins was used for purification via glutathione beads. Prior to the purification, 250 µl of glutathione beads were washed 3 times with 1 ml cold PBS. After that, the soluble fraction was added to the washed beads and incubated by rotation at 4°C for 1 hour. The beads were collected by centrifugation (5 min, 500 rpm) followed by washing 3 times with 1 ml cold PBS. The GST fusion protein was eluted with 250 µl of 35 mM of reduced glutathione prepared in 50 mM Tris/HCl pH 8.8. From the collected fractions, the recombinant fusion proteins were checked on a SDS-PAGE for purity and/or degradation.

### **2.2.2 SDS-Polyacrylamide gel electrophoresis (SDS-PAGE)**

Proteins were separated according to their molecular mass by discontinuous SDS-Polyacrylamide gel electrophoresis (SDS-PAGE) (Laemmli, 1970). The percentage of acrylamide in the gel for separation of protein depends on the size of the

protein. The higher the molecular mass the lower is the percentage of the gel used and vice-versa. For separation of TIMPs, a 15% SDS gel was regularly used. To prepare SDS gels with different percentages the following components were mixed:

stock solution	Lower Gel Percentage (vol in mls)											Upper gel
	5%	6%	7%	8%	9%	10%	11%	12%	13%	14%	15%	
1 M Tris 8.8	3.75	3.75	3.75	3.75	3.75	3.75	3.75	3.75	3.75	3.75	3.75	0.62 ml pH 6.8
10% SDS	0.1	0.1	0.1	0.1	0.1	0.1	0.1	0.1	0.1	0.1	0.1	0.05
40% Acrylamide	1.25	1.50	1.75	2.00	2.25	2.50	2.75	3.00	3.25	3.50	3.75	0.5
H <sub>2</sub> O	4.95	4.70	4.45	4.20	3.95	3.70	3.45	3.20	2.95	2.70	2.45	3.8
TEMED(μl)	30	30	30	30	30	30	30	30	30	30	30	30
APS 10%(μl)	30	30	30	30	30	30	30	30	30	30	30	30

After assembling the plates and mixing the SDS gel components the gel was poured between two glass plates and then covered with 1 ml of water. Polymerization was allowed for 20 min and thereafter the upper gel was added with inclusion of a comb. In the meantime, 25-35 μl of protein sample with the corresponding loading buffer was denatured by heating to 95°C for 5 min and then loaded on the gel. Electrophoresis was performed at 120 V and run until the bromphenol blue reached the bottom of the gel. The gel was either used for transfer of the proteins to a membrane for western blotting or stained with Coomassie brilliant blue for 20 min followed by destaining.

### 2.2.3 Zymography

Zymography is a method for analysing the gelatinolytic activity of MMP2 (gelatinase A) and MMP9 (gelatinase B). In principle, the method is similar to SDS-PAGE except for incorporation of the enzymes substrate – gelatin – in the gel. A 10% SDS gel was prepared with the addition of 10 mg/ml gelatin. To do this, 40 mg of gelatine was dissolved in 3 ml water and 3.75 ml 1 M Tris/HCl pH 8.8 by heating in a microwave for up to 1 min. After cooling the gelatine solution to approximately 50°C, the rest of the components were added: 2.5 ml acrylamide, 100 μl 10% SDS, 30 μl of 10% APS (ammonium persulfate) and 30 μl TEMED (N,N,N',N'-

Tetramethylethylenediamine). After polymerization, the upper part was made as for normal SDS-PAGE. To prepare samples for testing MMP activity, 30  $\mu$ l of a solution containing the enzymes was mixed with SDS loading buffer without reducing agent ( $\beta$ -mercaptoethanol or DDT) and incubated for 10 min at room temperature. Thereafter, the samples were loaded on the gel and electrophoresed at 120 V, 25 mA on ice until the bromphenol blue reached the bottom of the gel. Then, after electrophoresis the gel was incubated 3 times for 30 min in 50 mM Tris/HCl pH 7.5, 5 mM  $\text{CaCl}_2$  and 2.5 % triton X-100. Triton will replace the SDS from the gel thus promoting the renaturation of the MMPs. In the next step, the gel was incubated in 50 mM Tris/HCl pH 7.5, 5 mM  $\text{CaCl}_2$  overnight at 37°C to allow the cleavage of the gelatin by MMPs. Finally, the gel was stained with Coomassie brilliant blue for 10 min, followed by destaining with a solution containing 20 % methanol and 10 % acetic acid. At the corresponding molecular mass for migration of the MMPs the gelatin is cleaved and appears as a clear band on a blue background.

#### **2.2.4 Reverse zymography**

With this procedure, the inhibitory activity of TIMPs towards MMPs can be determined. Typically, for reverse zymogram, a 12.5% gel was prepared; 40 mg of gelatin was dissolved in 2 ml water and 3.75 ml 1 M Tris/HCl pH 8.8 by heating it in a microwave. After cooling 1 ml of conditioned medium from HT1080 cell line (a fibrosarcoma cell which secretes MMPs) was added with the remaining SDS gel components: 3.1 ml acrylamide, 100  $\mu$ l 10% SDS and 30  $\mu$ l of 10% APS/TEMED. SDS loading buffer was added to the samples without reducing agent and incubated for 10 min at room temperature. The gel was loaded with the respective TIMP protein and electrophoresed on ice at 120 V, 25 mA for 1.5 hour followed by staining with Coomassie brilliant blue for 10 min. Finally, the SDS gel was destained until the bands were visible.



## 2.2.5 Measurement of protein concentration

### 2.2.5.1 Estimation of protein concentration at 280 nm absorption

In order to measure the concentration of a purified protein in solution for kinetic measurements, Lambert-Beer law was employed:

$$A = \varepsilon \cdot c \cdot d$$

where A = absorbance at 280 nm;  $\varepsilon$  = molar extinction coefficient; d = pathlength in cm; c = molar concentration. Calculation of the extinction coefficient was made using software available on the internet (<http://www.biomol.net/tools-protein-extinction-coefficient.php>). The extinction coefficient is given by the sum of the absorption of the aromatic residues (tryptophan and tyrosine) in the polypeptide chain of a protein (Gill & von Hippel, 1989).

In the present study the extinction coefficients of the following proteins were used:

Protein	$\varepsilon_{280} [M^{-1} cm^{-1}]$
TIMP1	27555
TIMP2	33180
TIMP3	46590
TIMP4	40630
N-TIMP3	19285
C-TIMP3	27305
MMP13	83958
TACE catalytic domain	32235

### 2.2.5.2 Estimation of protein concentration by Lowry assay

The Lowry assay (Lowry, 1951) is a colorimetric method that provides an estimation of the total protein concentration in a cell extract or a mixture of proteins (unpurified proteins). It was performed using the BioRad DC kit according to the manufacturer's recommendations. Briefly, for a sample of 20  $\mu$ l, 100  $\mu$ l of solution A' (composed of 200  $\mu$ l reagent A plus 4  $\mu$ l reagent S) was added and mixed with 800  $\mu$ l reagent B followed by incubation for 15 min at room temperature. In the meantime, a serial dilution of BSA was prepared in the concentration range of: 0.2 mg/ml, 0.4

mg/ml, 0.8 mg/ml, 1.6 mg/ml, 3.2 mg/ml. The absorbance of the colorimetric reaction was measured at 750 nm. The absorbance values thus obtained were plotted against the corresponding concentration creating the calibration curve.

### **2.2.6 ECM protein preparation**

In the cell culture system TIMP3 is localized bound to the ECM of the cell. To remove the proteins from this compartment, the cells were trypsinized and the plates were washed 2 times with PBS followed by scraping the ECM proteins with 70 to 100  $\mu$ l of SDS loading buffer or 1% PBS Triton X100 and then stored at  $-20^{\circ}\text{C}$ .

### **2.2.7 Preparation of cell extracts**

Cell lysate was made by resuspending the cells from a 10 cm dish in 250  $\mu$ l cold PBS and then adding 250  $\mu$ l of 2% Triton X-100 in PBS. The mixture was incubated for 30-60 min on ice with occasional agitation. After this incubation time the cell extract was centrifuged 10 min at 13000 rpm to remove the insoluble material, while the supernatant was kept for further analysis and stored at  $-20^{\circ}\text{C}$ .

### **2.2.8 Concentration of protein solution**

Secreted proteins from cell culture supernatant or proteins after purification are often at low concentrations in large volumes. For analysis (e.g. detection in Western blotting, ELISA, SDS-PAGE) it is necessary to concentrate these protein solutions to bring the protein concentration to a more optimal level for the assay. The protein solution was placed in an Amicon concentrator (reservoir volume 4 ml) with a molecular cut-off of at least 10 000 Da less than the size of the protein and then centrifuged at 3500 g until the protein solution reached typically 200-250  $\mu$ l. In some instances, the buffer was exchanged by adding 8 ml of the final desired buffer and spun again to 200-250  $\mu$ l final volume. Concentrated protein was transferred to an eppendorf tube and then centrifuged at 13000 rpm for 1 min to remove any aggregated protein which may have occurred during concentration. The supernatant was saved and the protein concentration was measured either by the Lowry method or by absorption at 280 nm, aliquoted and stored at  $-20^{\circ}\text{C}$ .

### **2.2.9 Pull-down assay**

One method to investigate the interaction of two proteins in solution is the so-called pull-down assay. The assay is based on the presence of a tag fused to one of the interacting partners that can be pulled down by specific affinity beads. In this particular experiment Ni-NTA (Nickelnitrilotriacetate) beads were used to pull down the complex formed between His-tagged TIMP3 and TTR (transthyretin). 300 nM of purified and refolded TIMP3 with a hexahistidine tag was mixed with concentrated conditioned medium from HEK-293 cells transfected with pCEP4-TTR with a 1D4 tag and rotated overnight at 4°C. Next day, 100 µl of washed Ni-NTA beads were added to the protein solution and further incubated for 2 hours at 4°C. The beads with the protein complex bound via hexahistidine tag were washed 3 times and the complex was eluted with 50 mM NaH<sub>2</sub>PO<sub>4</sub>, 300 mM NaCl, 250 mM imidazole, pH 8.0. The eluted protein fraction was divided into two equal aliquots and analysed by western blotting for the presence of TTR and for TIMP3.

## **2.3 Immunochemistry methods**

### **2.3.1 Immunoprecipitation of proteins**

By immunoprecipitation an antigen can be specifically bound to an antibody and enriched or purified from a complex protein mixture. The protein to be immunoprecipitated was prepared from cell extract or ECM and incubated with the corresponding antibody (typically around 10 µg) by rotation for 2-4 hours or overnight at 4°C. Protein A beads were washed 2 times with 500 µl 0.1% PBS Triton X-100 and centrifuged 2 min at 1000 rpm. The washed beads (20-40 µl) were added to the antibody-antigen complex and rotated for an additional 2 hours. The antibody-antigen complex bound to protein A beads was recovered by centrifugation for 5 min at 1000 rpm and then washed two times with 0.1% Triton X-100 in PBS. The antigen was eluted from the beads in 50 µl SDS loading buffer. Typically, 20 to 25 µl of the elution product was analyzed by SDS-PAGE and western blotting and the rest was stored at -20°C.

### **2.3.2 Enzyme-Linked Immunosorbent Assay (ELISA)**

The binding activity of an antibody towards its antigen can be analyzed by ELISA. In principle, the antigen is immobilized on the surface of a microtiter plate by

adsorption. After the application of antibody the complex can be detected by using a secondary antibody (specific for mouse or rabbit IgG) conjugated with horse radish peroxidase (or another reporter enzyme). The intensity of the chromogenic reaction is directly proportional to the amount of antibody bound to the immobilized antigen.

For ELISA, 96-well microtiter plates were coated with 50  $\mu\text{l}$  of antigen (GST fusion proteins or collagens) and incubated overnight at 4°C. Next day the antigen solution was discarded and the wells blocked with 200  $\mu\text{l}$  of 3% w/v BSA in PBST 0.1 per well for 1 hour at room temperature. After washing the wells with PBST 0.1, 50  $\mu\text{l}$  of PBST 0.1 was added to each well except for the second and the last rows. The first row represents the control which accounts for the background given by unspecific binding of the secondary antibody. In the second row 100  $\mu\text{l}$  of antibody (or protein) solution was pipetted and from this volume 50  $\mu\text{l}$  was taken and serial dilutions of 1:1 were made. The plate was then incubated for 1 hour at room temperature. After three washing steps with PBST 0.1, the secondary antibody conjugated with horse radish peroxidase was added and the plate incubated for 1 hour room temperature. The wells were washed with PBST 0.1 before the enzyme substrate (tetramethyl benzidine) was added. This produces a blue colour. For end point measurement the enzymatic reaction was stopped by adding 1 N HCl and the intensity of the chromogenic reaction was measured at 450 nm. The absorption values thus obtained were plotted against the concentration of the antibody.

### 2.3.2.1 Determination of the apparent dissociation constant by ELISA

For evaluation of the data obtained in a binding assay between a protein and its ligand, a simple thermodynamic reaction is used:



The dissociation constant is defined by the following equation:

$$K_D = \frac{[P] \cdot [L]}{[P \cdot L]} \quad (2)$$

Where: [P] is the concentration of free protein; [L] is the concentration of uncomplexed ligand and [P · L] is the concentration of the protein-ligand complex.

Making a few assumptions that:

$$[P]_t = [P] + [P \cdot L] \quad (3)$$

and

$$[L]_t = [L] + [P \cdot L] \quad (4)$$

Where:  $[P]_t$  is the total amount of protein;  $[L]_t$  is the total amount of ligand.

Rearranging equations (3) and (4) gives:

$$[P] = [P]_t - [P \cdot L] \quad (5)$$

and

$$[L] = [L]_t - [P \cdot L] \quad (6)$$

In the initial dissociation equation (2) the concentrations of the protein and ligand are replaced with the equation (5) and (6) resulting in:

$$K_D = \frac{([P]_t - [P \cdot L]) \cdot ([L]_t - [P \cdot L])}{[P \cdot L]} \quad (7)$$

Assuming that  $[P]_t \gg [P \cdot L]$  and resolving the equation for  $[P \cdot L]$  gives:

$$[P \cdot L] = \frac{[P]_t \cdot [L]_t}{[P]_t + K_D} \quad (8)$$

The measured absorbance values at 450 nm are plotted against the corresponding protein concentrations (representing  $[P]_t$  which was used in the assay). The points obtained in the graph are fitted by non-linear least squares regression according to equation (8) with  $K_D$  and  $[P]_t$  as parameters (Voss & Skerra, 1997).

### 2.3.2.2 ELISA applied to cells

In order to study the inhibitory activity of TIMP3 towards ADAMTS4/ADAMTS5 a modified ELISA was developed. In this assay the primary chondrocytes were plated on a microtiter plate. After growing, the cells were incubated with the first antibody (neoepitope) and the secondary antibody conjugated with HRP. The intensity of the chromogenic reaction correlates with the activity of enzymes inhibited by TIMP3.

Isolated chondrocytes were plated on an ELISA plate at a density of  $1.5 \times 10^4$  cells per wells and grown for 7 days changing the medium every second day. Then the cells were incubated in serum free medium for 2 days before starting detection of the enzymes and their cleavage product. In the case of treatment with recombinant TIMP proteins at day 5 the cells were incubated with 100 ng/ml of inhibitors in medium with serum for two days and then two additional days in serum free medium, exchanging the medium every day with fresh inhibitors. At the end of the growing phase, the cells were washed 2 times with PBS and fixed with 4% paraformaldehyde in PBS for 30 min at

room temperature. The cells were washed again with PBS (3 times) and then incubated with 50  $\mu$ l of 0.05U of chondroitinase ABC (prepared in 50 mM Tris/HCl, 60 mM sodium acetate, 0.01% BSA, pH 8.0) for 2 hours at 37°C. Digestion with chondroitinase was necessary to remove the chondroitin sulfate from the aggrecan in order to unmask the antibody recognition epitope (this treatment was for detection of ADAMTS neo, MMP neo and aggrecan). After blocking with 3% BSA (in PBS containing 0.3% Triton X-100) cells were incubated with the first antibody overnight at 4°C. Next day, the wells were washed 3 times with PBS and then incubated with the corresponding secondary antibody coupled with horse radish peroxidase for 1 hour at room temperature. The wells were washed again and incubated with 100  $\mu$ l of tetramethylbenzidine. The enzymatic reaction produced a blue colour which was stopped by adding 100  $\mu$ l of 1 N HCl giving a yellow colour of which intensity was measured at 450 nm, using a FLUOstar OPTIMA (BMG Labtech) plate reader. As a control a well was processed the same way but omitting the first antibody. The control value was subtracted from the sample absorption intensity before plotting the data.

### **2.3.2.3 Competitive ELISA**

This assay is similar to a regular ELISA except that a competitor is preincubated with the ligand. Briefly, increasing concentrations of TIMP3 (27.5 nM to 1760 nM) were added to a constant amount of VEGFR2 (20 nM) in a final volume of 50  $\mu$ l in PBS and complexes were allowed to form overnight at room temperature. The wells of a microtiter plate were coated with 50  $\mu$ l of 0.2  $\mu$ g/ml VEGF solution and incubated overnight at 4°C. Next day, the wells were washed with PBS and blocked with 3% BSA (w/v in PBS) for 1 hour at RT. The complex formed between TIMP3 and VEGFR2 was added to the immobilized VEGF for 2 hours. After washing the wells with PBS, polyclonal anti-VEGFR2 antibody (dilution 1:500) was applied for 1 hour. In the next step, VEGFR2 bound to its ligand VEGF, was detected by addition of secondary antibody coupled to peroxidase. After 1 hour the substrate of the enzyme - tetramethyl benzidine - was added. The enzymatic reaction was stopped by adding 100  $\mu$ l 1 N HCl. The intensity of the yellow reaction product was measured at 450 nm. In the control well the complex between TIMP3 and VEGFR2 was omitted to quantify the unspecific background (given by the first and the secondary antibodies). The absolute absorbance values were calculated by subtracting the background from the sample values and were plotted against the concentration of TIMP3.

### 2.3.3 Western blotting

In western blotting an antibody is used to detect a specific protein in a mixture separated by SDS-PAGE. First, the protein mixture is separated on a SDS Polyacrylamide gel by electrophoresis then it is electro-transferred to a hydrophobic membrane and immuno-detected with the corresponding antibody.

Proteins were separated by SDS-PAGE as described in section 2.2.2. After electrophoresis finished, the gel was soaked in Towbin buffer (25 mM Tris/HCl pH 8.3, 190 mM glycine, 10% methanol). In the meantime, the hydrophobic membrane (Immobilon PVDF, Millipore) was activated in 10 ml of methanol for 5 min and then incubated in Towbin buffer. At the same time two whatman filter papers were soaked in Towbin buffer. For the electro-transfer, the prewetted whatman paper was laid on the electro-transfer apparatus followed by the hydrophobic membrane and the SDS gel and one whatman filter paper. Electro-transfer took place at 120 mA, 10 V for 1 hour. Next the membrane with the transferred protein was blocked with 3% milk or BSA prepared in PBS for 1 hour at room temperature or overnight at 4°C. The first monoclonal or polyclonal antibody was added at a previously determined dilution for 1 hour. The blot was washed three times with 20 ml PBST 0.05, 10 min each time. The secondary antibody (anti rabbit or anti mouse) conjugated with horse radish peroxidase was added and incubated for 1 hour and then washed again three times with PBST 0.05. Antibody bound to antigen was detected by incubating the membrane for 1-2 min with 2 ml of ECL reagent composed of: 1 ml SuperSignal West Pico Luminol/enhancer solution and 1 ml SuperSignal West Pico Stable Peroxide solution (Pierce). X-ray film was exposed to the blot, depending on the signal intensity, for 30 seconds up to 30 min to detect the signal on the blot.

### 2.3.4 Immunocytochemistry

In order to localize/colocalize a protein/two proteins or detect a specific marker on primary isolated cells (to identify the marker for a specific cell type) or to determine the transfection efficiency, cells are stained with the appropriate primary antibody followed by a secondary antibody conjugated with a fluorophor which can be detected by using a fluorescence microscope.

Cells were grown on cover slips then washed two times with PBS and fixed with 4% PFA for 30 min at room temperature. After washing, the cells were blocked with 10 % goat serum in PBS containing 0.3% Triton X-100 (Triton X-100 helps to permeabilize

the cells so that the antibody has access to intracellular proteins), for one hour at room temperature. The cover slips were incubated with the first antibody (at various dilutions) in 2.5 % goat serum and 0.1% Triton X-100 for 1 hour at room temperature or overnight at 4°C. The cover slips were washed 3 times with PBS and then incubated with the secondary antibody conjugated with a fluorophor at a dilution of 1:1000 or 1:5000 for 1 hour. From this stage all other steps were carried out in the dark due to the light-sensitivity of the fluorophor. The cells were washed three times and incubated with DAPI to stain the nucleus of the cells. Cover slips were mounted onto slides in confocal matrix oil. Specific staining was visualized using a fluorescence microscope.

## **2.4 Biophysical methods**

### **2.4.1 Fluorescence resonance energy transfer (FRET)**

In principle, fluorescence resonance energy transfer (FRET) is the transfer of energy from a fluorescent donor excited at a specific wavelength to an acceptor over distances as large as 70 Å (Stryer, 1978). In these experiments (TACE and MMPs assay), the fluorophor group (7-methoxycoumarin-4-yl) acetyl is separated from the quencher group (N-3-(2,4-dinitrophenyl)-L-2,3-diaminopropionyl) by a short peptide containing the cleavable site for TACE or MMP; quenching occurs by resonance energy transfer (Knight *et al.*, 1992).

#### **2.4.1.1 Fluorometric TACE assay**

TACE extraction from the liver of gene targeted mice was performed essentially as described by Mohammed *et al.*, 2004. Briefly, 200 µg of total liver extract was incubated with 1 µM of TACE substrate (MCA-PLAQAV-Dpa-RSSSR-NH<sub>2</sub>) in TACE assay buffer (50 mM Tris/HCl pH 7.5, 150 mM NaCl, 10 mM CaCl<sub>2</sub>, 0.05% Brij 35). Fluorescence was measured after 1 h incubation at 27°C with a FLUOstar OPTIMA (BMG Labtech) set at 330 nm excitation and 390 nm emission. For TACE inhibition by recombinant proteins, the recombinant catalytic domain of TACE (100 nM) or native TACE (50µg) was incubated with increasing concentrations of TIMPs (3 nM to 220 nM for recombinant TACE catalytic domain and 25 nM to 1000 nM for native TACE) and the complex allowed to form for 3 h at room temperature. 1 µM fluorogenic substrate (final concentration) was added to the complex in a 100 µl reaction volume. The fluorescence was measured after 2 h incubation at 27°C.



### **2.4.1.2 Fluorometric MMP13 assay**

Recombinant mouse MMP13 was expressed in inclusion bodies, purified and refolded. Prior to performing the fluorometric inhibitory assay, MMP13 was activated by incubation with 1 mM of APMA (4-Aminophenylmercuric acetate) at 37°C for 2 h. For the concentration dependent inhibition of MMP13, 0.6 nM of activated enzyme was mixed with an increasing concentration of recombinant TIMP3 (0 to 3.8 nM). The complex formation between MMP13 and TIMP3 was allowed to form for 2 hours at room temperature, before 1  $\mu$ M of MMP13 fluorogenic substrate (MCA-Pro-Cha-Gly-Nva-His-Ala-Dpa-NH<sub>2</sub> [Cha=L-cyclohexylalanine; Dpa=3-(2,4-dinitrophenyl)-L-2,3-diaminopropionyl; Nva=L-norvaline], Calbiochem) was added to the reaction and further incubated for 2 hours at 27°C. Fluorescence was measured with the excitation wavelength set at 330 nm and the emission wavelength at 390 nm.

## **2.5 Cell biology methods**

### **2.5.1 Isolation of primary chondrocytes from mouse ribs**

Tissue was removed from mouse ribs and incubated in 2 mg/ml collagenase in DMEM with 10% FBS for 10 min at 37°C, then for 20 min at room temperature to remove the remaining tissue. The medium was changed for a fresh solution of 2 mg/ml collagenase and incubated overnight in a 37°C incubator. Next day the cell suspension was filtered through a mesh (pore size 50  $\mu$ m) and the cells pelleted for 5 min at 1500 g. The cells were resuspended in fresh DMEM with 10% FBS and plated on a 6 cm dish. Chondrocytes were grown for 2-4 days and then split into 2x 10 cm dishes. One dish was used for conservation of the cells and the other for plating in ELISA wells.

### **2.5.2 Preparation of liver extract**

Livers from mice were removed, shock frozen in liquid nitrogen and stored at -80°C. One complete liver was homogenized in 3 ml of extraction buffer (50 mM Tris/HCl, 150 mM NaCl, 0.1% SDS, 1% sodium deoxycholate, 1% Nonidet P40, 1% Triton X-100, pH 7.4). The solution thus obtained was centrifuged for 15 min, 13000 rpm at 4°C and the supernatant was aliquoted and stored at -80°C.

### 3. Results

#### 3.1 Production and structural characterization of soluble recombinant proteins

Investigation of TIMP3 biological function and analysis of the pathomechanism of SFD required the production of recombinant proteins. Moreover, TIMP3 is an enzyme inhibitor and study of inhibitory kinetics requires high purity and reasonable amounts of protein. Therefore, TIMP3 and the other necessary recombinant proteins were cloned in a bacterial vector, expressed, purified and refolded.

##### 3.1.1 Construction of a bacterial expression vector for the production of TIMP-1, -2, -3, -4, MMP13 and TACE-CD

Although bacterial expression of the recombinant proteins has the disadvantage that the proteins are non-functional and deposited in inclusion bodies, it also has the advantage that proteins are produced in large amounts and, after refolding, yields are still good. On the other hand, it is possible to express proteins in bacteria in a soluble form by directing them to the periplasmic space of gram negative bacteria where the proper oxido-reducing conditions are present which favour the formation of disulfide bonds – necessary for the protein to be biologically active and perform its function. However, high numbers of cys residues in a recombinant protein usually leads to a drastic drop in the amount expressed in the periplasm, presumably from overloading the secretory pathway and folding machinery of the bacteria. Therefore, in the present study I chose to express all the recombinant proteins in the cytosol.

The T7 expression system (Studier *et al.*, 1990) was used for prokaryotic expression of recombinant proteins in the commercially available vector pET21 (Novagen). TIMP cDNAs were cloned in-frame with a hexahistidine tag at the C-terminus to facilitate protein purification. The expressed proteins formed inclusion bodies and after solubilisation and refolding the proteins were purified by IMAC and further characterized for functionality.

The templates used for cloning of the TIMPs and other recombinant proteins were made from cDNA. First strand synthesis was carried out from RNA isolated from WT chondrocytes or fibroblasts. The cDNAs were amplified using the following primer combinations: TACE\_CD\_pET\_F/ TACE\_CD\_pET\_R (TACE catalytic domain, Arg215 to Val477), MMP13\_F/ MMP13\_R (MMP13, Tyr24 to Cys449),

TIMP1\_N\_F/TIMP1\_C\_R (full length TIMP1, Cys1 to Arg181);  
 TIMP2\_N\_F/TIMP2\_C\_R (full length TIMP2, Cys1 to Pro194);  
 TIMP3\_N\_F/TIMP3\_C\_R (full length TIMP3, Cys1 to Pro188);  
 TIMP3\_N\_F/TIMP3\_N\_R (N-terminal TIMP3, amino acid Cys1 to Asn121);  
 TIMP3\_C\_F/TIMP3\_C\_R (C-terminal TIMP3, amino acids Cys122 to Pro188);  
 TIMP4\_N\_F/TIMP4\_C\_R (full length TIMP4, Cys1 to Arg195). S156C-TIMP3 was amplified with the same primers as for WT, and the point mutation was introduced by site directed mutagenesis using the primers: F\_S156C/B\_S156C prior to cloning into pET vector. Fragments were amplified with a mixture of Taq and Pfu polymerases (8:1) (Pfu polymerase has a proof reading activity and Taq polymerase leaves single A overhangs and thus is useful for cloning into pGEM vector) using a touch-down PCR protocol. The amplified PCR fragments were ligated in the pET21 vector using NdeI and XhoI restriction sites (Fig. 3).

```

1 (Timp3_N_F) GCT
ATGACTCCCTGGCTTGGGCTTGTGCTCCTGAGCTGTTGGAGCCTTGGGCACCTGGGGC
-----|-----|-----|-----|-----|-----|-----|
TACTGAGGGACCGAACCCGAACAGCACAGGACTCGACAACCTCGGAACCCGTGACCCCG
MetThrProTrpLeuGlyLeuValValLeuLeuSerCysTrpSerLeuGlyHisTrpGly
1 10 20

NdeI
AGCCCATATGTGCACATGCTCTCCCAGCC 120
GCGGAAGCGTGACATGCTCTCCCAGCCATCCCCAGGATGCCTTCTGCAACTCCGACATC
-----|-----|-----|-----|-----|-----|-----|
CGCCTTCGCACGTGTACGAGAGGGTTCGGTAGGGTTCCTACGGAAGACGTTGAGGCTGTAG
AlaGluAlaCysThrCysSerProSerHisProGlnAspAlaPheCysAsnSerAspIle
30 40

121 180
GTGATCCGGGCCAAAGTGGTGGGAAAGAAGCTGGTGAAGGAGGGGCCCTTTGGCACTCTG
-----|-----|-----|-----|-----|-----|-----|
CACTAGGCCCGGTTTACCACCCTTTCTTCGACCACTTCTCCCCGGGAAACCGTGAGAC
ValIleArgAlaLysValValGlyLysLysLeuValLysGluGlyProPheGlyThrLeu
50 60

181 240
GTCTACACTATTAAGCAGATGAAGATGTACCGAGGCTTCAGTAAGATGCCCCACGTGCAG
-----|-----|-----|-----|-----|-----|-----|
CAGATGTGATAATTCGTCTACTTCTACATGGCTCCGAAGTCATTCTACGGGTGCACGTC
ValTyrThrIleLysGlnMetLysMetTyrArgGlyPheSerLysMetProHisValGln
70 80

241 300
TACATTACACGGAAGCCTCTGAAAGTCTTTGTGGCCTCAAGCTAGAAGTCAACAAATAC
-----|-----|-----|-----|-----|-----|-----|
ATGTAAGTGTGCCTTCGGAGACTTTCAGAAACACCGGAGTTCGATCTTCAGTTGTTTATG
TyrIleHisThrGluAlaSerGluSerLeuCysGlyLeuLysLeuGluValAsnLysTyr
90 100

301 360
CAGTACCTGCTGACAGGGCGCGTGTATGAAGGCAAGATGTACACAGGACTGTGCAACTTT

```

```

-----|-----|-----|-----|-----|-----|
GTCATGGACGACTGTCCC GCGCACATACTTCCGTTCTACATGTGTCTGACACGTTGAAA
GlnTyrLeuLeuThrGlyArgValTyrGluGlyLysMetTyrThrGlyLeuCysAsnPhe
                                         110                               120

361                                         420
GTGGAGAGGTGGGACCACCTCACACTGTCCAGCGCAAGGGCCTCAATTACCGCTACCAC
-----|-----|-----|-----|-----|-----|
CACCTCTCCACCTGGTGGAGTGTGACAGGGTTCGCGTTCCCGGAGTTAATGGCGATGGTG
                                         CGATGGTG
ValGluArgTrpAspHisLeuThrLeuSerGlnArgLysGlyLeuAsnTyrArgTyrHis
                                         130                               140

NdeI
GCTAGCCATATGTGCAAGATCAAGTCCTGC (Timp3_C_F)                               480
CTGGGTTGCAATTGCAAGATCAAGTCCTGCTACTACTTGCCTTGTTTTGTGACCTCCAAG
-----|-----|-----|-----|-----|-----|
GACCCAACGTTAACGTTCTAGTTCAGGACGATGATGAACGGAACAAAACACTGGAGGTTTC
GACCCAACGTTAGAGCTCCGATCG (Timp3_N_R)

XhoI
LeuGlyCysAsnCysLysIleLysSerCysTyrTyrLeuProCysPheValThrSerLys
                                         150                               160

481                                         540
AATGAGTGTCTCTGGACCGACATGCTCTCCAATTTTGGGTACCCTGGCTATCAGTCCAAA
-----|-----|-----|-----|-----|-----|
TTACTCACAGAGACCTGGCTGTACGAGAGGTTAAAACCCATGGGACCGATAGTCAGGTTT
AsnGluCysLeuTrpThrAspMetLeuSerAsnPheGlyTyrProGlyTyrGlnSerLys
                                         170                               180

541                                         600
CACTACGCCTGCATCCGGCAGAAGGGTGGCTACTGCAGCTGGTACCGAGGATGGGCTCCC
-----|-----|-----|-----|-----|-----|
GTGATGCGGACGTAGGCCGTCTTCCCACCGATGACGTCGACCATGGCTCCTACCCGAGGG
HisTyrAlaCysIleArgGlnLysGlyTyrCysSerTrpTyrArgGlyTrpAlaPro
                                         190                               200

601                                         636
CCAGACAAGAGCATCAGCAACGCCACAGATCCCTGA
-----|-----|-----|-----|
GGTCTGTTCTCGTAGTCGTTGCGGTGTCTAGGGACT
                                         GTCGTTGCGGTGTCTAGGGGAGCTCCGATCG (Timp3_C_R)
                                         XhoI
ProAspLysSerIleSerAsnAlaThrAspProEnd
                                         211

```

**Figure 3.** Primary structure of murine TIMP3. The nucleotide sequence of TIMP3 and the corresponding amino acid translation (Apte *et al.*, 1994a and 1994b; Sun *et al.*, 1995). The polypeptide chain is composed of 211 amino acids and the quaternary structure contains 188 amino acids. The remaining 23 residues are the signal sequence (represented in the figure by the underlined amino acid sequence) which direct the inhibitor molecule to the extracellular matrix to perform its biological function. For the construction of the bacterial expression vector containing TIMP3 (full length TIMP3 and its individual domains) primers sequences are given and the restriction sites used in the cloning procedure are in bold. The oligonucleotides used for amplification are indicated with their corresponding annealing sites.

After transformation of the ligation products into the *E. coli* strain XL1 blue several clones were picked from the colonies which had grown. To check for the presence of the insert, colony PCR was performed by adding a bacterial colony to a PCR reaction as template. In parallel, to further analyse the obtained clones, plasmid DNA was prepared and digested with restriction enzymes. Two colonies containing the right insert size (based on restriction digestion and the colony PCR) were chosen from each ligation for sequencing with the pET\_F/pET\_R primers. The forward sequencing primer anneals to the vector sequence in the region of the T7 promoter, whereas the reverse primer is localized to the T7 terminator sequence.

### **3.1.2 Purification and refolding of recombinant proteins expressed in the bacterial system**

The BL21 (DE3) *E. coli* strain was used for protein expression because this *E. coli* strain has the gene for T7 RNA polymerase inserted in its genome under the control of the lac promoter/operator. Protein synthesis is induced by IPTG which binds to the lac repressor causing a conformational modification which prevents binding to the lac operator. This leads to transcription of T7 RNA polymerase and in turn this polymerase recognises the T7 promoter on the vector and transcribes the inserted cDNA, leading to recombinant protein synthesis.

Production of bacterial recombinant TIMP proteins was performed in 1 liter of LB medium. Protein synthesis was induced by adding isopropyl- $\beta$ -D-thiogalactopyranosid (IPTG) to a final concentration of 1mM when the OD<sub>550</sub> of the bacterial culture reached 1, and expression of proteins was allowed overnight at 30°C. After centrifugation and lysis, inclusion bodies were denatured in 6 M guanidine-hydrochloride and recombinant proteins purified by immobilized metal affinity chromatography (IMAC). To obtain biologically active protein, the denatured TIMPs were refolded in a buffer with a high concentration of arginine and oxido-reducing agents. After the whole procedure was completed, bacterial recombinant proteins were analysed by SDS-PAGE for the presence of refolded TIMPs and also for purity (Fig. 4). Coomassie stained gels show that there are no major non-TIMP3 protein contaminants in the preparation. Refolded recombinant WT-TIMP3 and S156C-TIMP3 appear as a doublet, one band at approximately 22 kDa and the other at 23 kDa. The slower migrating band might correspond to incorrectly folded protein. The N- and the C-terminal domains of TIMP3 were expressed in bacteria and analysed by SDS-PAGE. These two TIMP3 fragments

were homogeneous on the gel and under non-reducing conditions both fragments ran at a lower apparent molecular mass, suggesting that the protein has a compact structure due to correctly formed disulfide bonds (data not shown). Full length TIMP1, TIMP2 and TIMP4 were also expressed in *E. coli*. Refolded forms of these proteins appeared on an SDS gel as a major band of the correct molecular weight, but a minor fraction of the protein also appeared as a higher molecular weight form with the apparent size of a dimer. The yield of refolded protein varies between 1 and 10 % of the initial amount of the inclusion bodies.

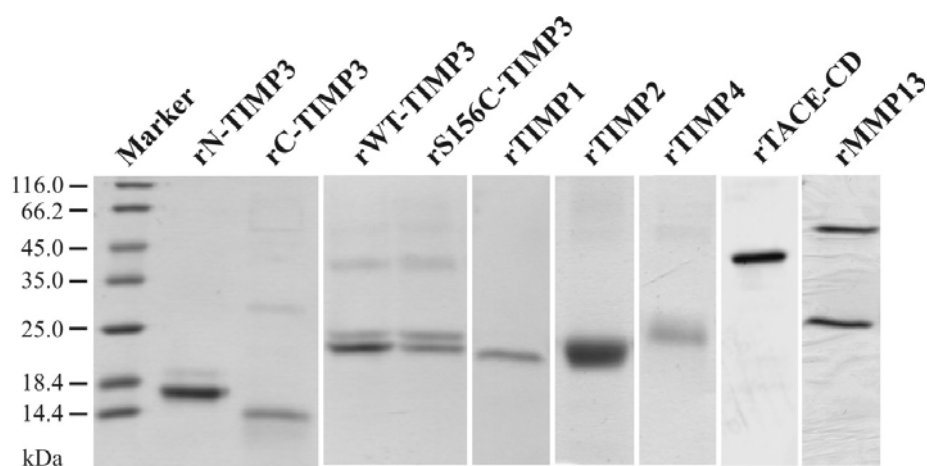


**Figure 4.** Characterization of bacterially expressed recombinant proteins by SDS-PAGE. Recombinant proteins with a hexahistidine tag fused to the C-terminal were expressed in inclusion bodies, purified via IMAC and refolded. Prior to loading to the gel, refolded proteins were incubated with  $\beta$ -mercaptoethanol as reducing agent and separated on a 15 % SDS gel, followed by staining with coomassie brilliant blue.

The recombinant catalytic domains of TACE and MMP13 were expressed in a similar manner to full length TIMP3. After purification, proteins were refolded for 2 days then dialysed against PBS. Analysis of these recombinant proteins by SDS-PAGE (Fig. 4) revealed that TACE-CD ran as a single band at a molecular weight corresponding to the catalytic domain, without major impurities. On a coomassie stained gel MMP13 showed two bands (Fig. 4) with equal intensities: one band which corresponds to full length MMP13 with a molecular weight of 55 kDa and a smaller fragment at 25 kDa. The lower band represents the C-terminal domain of the enzyme (Knäuper *et al.*, 1996) which presumably results from autocatalytic cleavage.

### 3.1.3 Construction of a bacterial expression vector for the production and purification of antibody epitope peptides fused to GST

For testing the binding and specificity of commercially purchased antibodies to their epitopes, sequences corresponding to the peptide epitopes were amplified and cloned into the pGEX-4T3 bacterial expression vector so that the peptide sequence is fused to the cDNA of GST. The ADAMTS4 antibody used recognises an epitope in the peptide Ala596 to Gln626 and this sequence was amplified using the primer pair ADAMTS4\_E\_F/ADAMTS4\_E\_R. The epitope recognised by the aggrecan antibody was amplified using Agc\_E\_F/Agc\_E\_R. The antibody to the Aggrecan neoepitope (generated by the cleavage of aggrecan by ADAMTS4/5) is raised against the human sequence Gly344 to Glu373. This sequence, and the corresponding sequence from the mouse was amplified using the Pept\_Gm\_F/Pept\_Gm\_R and Pept\_Gh\_F/Pept\_Gh\_R primer pairs respectively. The mouse and the human neoepitopes were cloned separately because there is one amino acid difference between the mouse and human neoepitope sequences: the human sequence is NITEGE while the mouse sequence is NVTEGE. This allows the specificity of the neoepitope antibody in recognising both neoepitope sequences to be tested. Finally Pept\_GA\_F/Pept\_GA\_R were used to amplify a peptide containing the ADAMTS4/ADAMTS5 cleavage site which is used as a negative control for the neoepitope antibody.

All epitope fragments were amplified using a mixture of Pfu/Taq polymerase from template cDNA isolated from WT chondrocytes. After restriction digest of the PCR products with BamHI and NotI they were ligated directly into pGEX-4T3 vector and transformed into *E.coli*. From each transformation 8 colonies were picked and the size of the inserts analysed by colony PCR. The identity of the DNA sequences was verified by sequencing. The correct constructs were transformed into *E. coli* strain BL21 and the proteins expressed in a 50 ml culture. Production of the peptides fused to GST was induced with 0.1 mM IPTG when the optical density of the bacterial culture reached the value of 1 at 550 nm. GST fusion proteins are expressed in a soluble form in the cytosol of the bacteria, therefore after disruption of the cells the soluble fraction was applied to glutathione beads. After several washing steps the GST tagged peptides were eluted with reduced glutathione. Recombinant protein analysis by coomassie stained SDS-PAGE (Fig. 5), revealed that all proteins ran as a single band corresponding to the molecular mass of GST fused to the peptides, with the exception of the aggrecan epitope which appeared as 4 bands. The largest protein has a molecular mass

corresponding to the full length protein so it can be assumed that the lower bands are proteolytic degradation products of the full length fusion protein. The yield of the proteins was variable, the highest was for ADAMTS4 epitope whereas the lowest was for the peptide which contains the cleavage site for ADAMTS4/ADAMTS5 (this fragment is designated as uncleaved aggrecan).

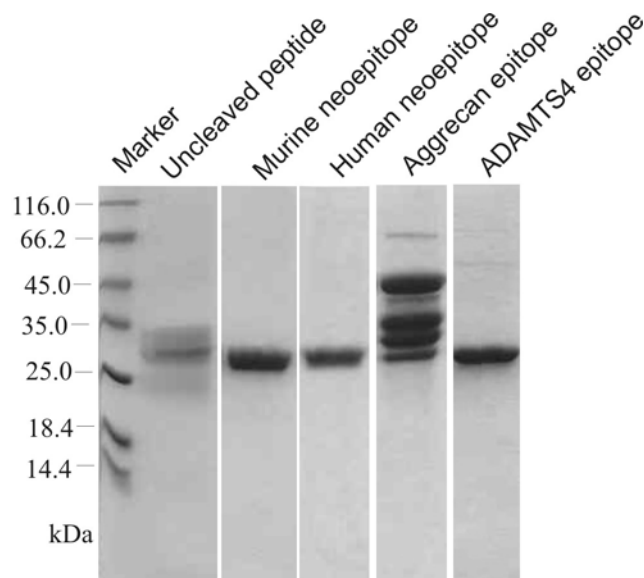


**Figure 5.** SDS-PAGE analysis of the expressed peptides fused to GST. Peptides corresponding to the antibody epitopes were cloned as fusion proteins with GST, expressed in bacterial strain BL21 and purified from the soluble fraction of the disrupted bacteria via glutathione beads. Before running the gel, the samples were reduced by adding  $\beta$ -mercaptoethanol.

### 3.1.4 Generation of a mammalian expression vector for production of the extracellular domain of human DDR2 and its expression in HEK-293 cells

DDR2 (Discoidin-domain receptor 2) is a member of a subfamily of receptor tyrosine kinases. Binding of fibrillar collagens to DDR2 results in tyrosine kinase activation (Vogel W. 1999). The extracellular domain of this receptor was used as a positive control in tests of binding of TIMP3 to collagens. DDR2 is an 855 amino acid transmembrane protein and in order to express it in a soluble form to perform ELISA experiments it was necessary to clone the extracellular domain of this receptor without the transmembrane and cytoplasmic regions. The full length construct was cloned into the pCEP4 vector with the 1D4 tag attached to its C-terminus. The extracellular domain



of DDR2 consists of the first 400 amino acids and for cloning of this region the full length construct was digested with BamHI restriction enzyme which cleaves at three sites; at the boundary of the extracellular domain and the transmembrane region, immediately before the 1D4 tag and in the middle of the cytoplasmic domain. Digestion with BamH I leaves sticky ends which were filled by using Klenow polymerase to generate blunt ends in the plasmid containing the extracellular domain of DDR2 before religation. The recombinant plasmid containing the extracellular domain of DDR2 (ECD-DDR2) in pCEP4 1D4 vector was verified by restriction digest before transfection into HEK-293 cells for overexpression. Protein production was allowed for two days in serum free medium to facilitate concentration of the conditioned medium. 20 ml of the cell culture supernatant was concentrated to 1.5 ml and an aliquot was analysed by western blotting for the presence of the overexpressed protein, using an anti-1D4 tag antibody (Fig. 6A). To further analyse the recombinant ECD-DDR expressed in mammalian cells an ELISA experiment was employed. As Fig. 6B shows the extracellular domain of DDR2 was able to bind to collagen type V in a concentration dependent manner, whereas it did not interact with BSA (negative control).

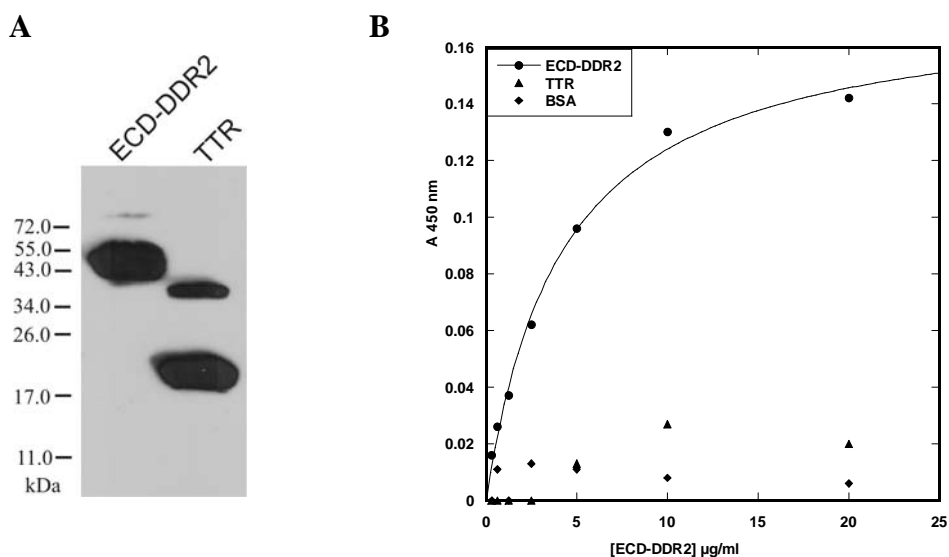


**Figure 6.** Western blotting analysis of overexpressed ECD-DDR2 and TTR in HEK-293 cells. (A) Subconfluent cells were transfected with 10  $\mu\text{g}$  of plasmid DNA by the calcium phosphate method. The transfected cells were grown in serum free medium for two days and the conditioned medium was harvested. After concentration of the conditioned medium, the samples were loaded on a gel and then blotted onto a hydrophobic membrane. Both proteins were detected with anti 1D4 antibody. (B) ELISA for analysis of ECD-DDR2 binding specificity. The wells of a microtiter plate were coated with collagen type V (10  $\mu\text{g/ml}$ ) or BSA. After blocking, the concentrated conditioned medium from HEK-293 cells

transfected either with ECD-DDR2 or TTR were applied in a dilution series. Recombinant protein was detected with HRP conjugated anti-1D4 tag antibody and the colourimetric reaction measured at 450 nm. The concentration of the recombinant proteins was plotted against the corresponding absorption values. The points in the graph are fitted according to equation (8).

TTR (transthyretin) was used as a negative control for the collagen binding assay. TTR is a serum tetrameric protein of four identical subunits with a molecular mass of 14 kDa per monomer and is a carrier of thyroxine and retinol-binding protein (Sousa *et al.*, 2001). This protein was cloned also in pCEP4 with the 1D4 tag fused to the C-terminal and overexpressed in HEK-293. Western blot analysis (Fig. 6A) shows that the TTR is expressed and secreted in the conditioned medium of the transfected cells. 1D4 antibody detected two bands, one corresponding to the monomeric form of the protein and the other for the dimeric structure. In the collagen binding assay recombinant TTR did not bind to collagen type V (Fig. 6B)

## **3.2 Functional analysis of recombinant proteins expressed in *E. coli***

### **3.2.1 Bioactivity assessment of recombinant TIMPs by reverse zymography**

Recombinant mammalian proteins expressed at high levels in *E. coli* are most often found in inclusion bodies. This has the disadvantage that in this form the proteins are not biologically functional as they are deposited as denatured, unfolded polypeptide. To achieve bioactivity these proteins must be refolded *in vitro* and the refolded recombinant proteins should be analysed for their functionality before they can be used in assays. The most commonly used method for investigating the inhibitory activity of TIMPs towards MMPs is reverse zymography. This method is based on electrophoretic separation of TIMPs in a SDS-PAGE gel which incorporates MMPs and their substrate - gelatin. Where TIMPs are present in the gel MMP activity is inhibited and gelatin is not cleaved, whereas in the rest of the gel the gelatin is digested by MMPs activity. Therefore, on the gel a dark band (given by the inhibited MMPs-mediated gelatin degradation) on a light blue background indicates the presence of active TIMP. Reverse zymographic analysis of TIMP1, TIMP2 and TIMP4 showed that these three refolded recombinant proteins are able to inhibit the gelatinolytic activity of MMPs

(Fig. 7). It is also observed on the gel that the dimeric forms of TIMP2 and TIMP4 are also capable of inhibiting MMPs activity. The two individual domains of TIMP3 – the N-terminal domain and the C-terminal domain – were also checked for inhibitory action against MMPs. As expected, the N-terminal domain of TIMP3 inhibited the gelatinolytic activity of MMPs, consistent with the observation that the N-terminal region of TIMP3 is responsible for the metalloproteinases inhibition, whereas the C-terminal domain of TIMP3 was not able to block MMPs activity (Fig. 7). Full length WT-TIMP3 and the S156C-TIMP3 mutant could not be analysed by reverse zymography because under non-reducing conditions the recombinant protein did not enter the gel. TIMP3 also would not run into normal SDS-PAGE under non-reducing conditions, probably due to the high concentration of arginine in the refolding buffer.

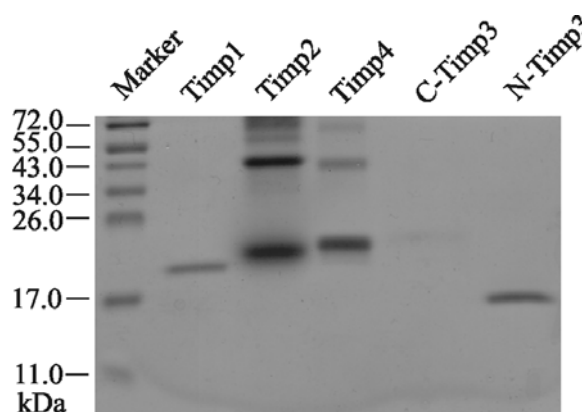


**Figure 7.** Reverse zymogram analysis of TIMP activity. Refolded recombinant TIMPs were separated under non-reducing conditions on a 15 % SDS gel containing gelatin and conditioned medium from HT1080 fibrosarcoma cell line as a source of MMPs. The gel was incubated in a buffer with Triton X-100 to replace the SDS from the gel and afterwards incubated overnight at 37°C for the digestion of the gelatin by MMPs. Finally, the gel was stained with coomassie blue.

### 3.2.2 Fluorometric titration of MMP13 for the functional assay of full-length TIMP3

Due to the fact that it was not possible to assess the activity of bacterially expressed full-length WT-TIMP3 and S156C-TIMP3 by reverse zymography, these recombinant proteins were assayed for bioactivity by fluorescence titration against MMP13 (Collagenase 3). MMP13 is a 55 kDa secreted matrix metalloenzyme which preferentially hydrolyzes collagen type II with high efficiency, and has lower cleavage activity against collagen type I and III (Knäuper *et al.*, 1996).

Prior to performing the inhibitory assay, MMP13 was activated by incubation with 1 mM APMA (4-Aminophenylmercuric acetate) at 37°C for 2 h. To test TIMP3 inhibitory activity, a concentration dependence curve was made by incubating a constant amount of activated enzyme with increasing concentrations of WT-TIMP3 and S156C-TIMP3 in an assay using a quenched MMP13 fluorogenic substrate specific for collagenase 3. Fluorescence was plotted against the concentration of TIMP3 used for the inhibitory assay, with a decrease in fluorescence showing inhibition of MMP13 activity. The results show that both WT-TIMP3 and mutant TIMP3 are able to reduce the cleavage activity of MMP13 in a concentration dependant manner (Fig. 8). These data indicate that bacterially expressed full-length WT-TIMP3 and S156C-TIMP3 are able to inhibit the catalytic activity of MMP13 after *in vitro* refolding, and shows that these two recombinant proteins are active and mainly correctly folded.

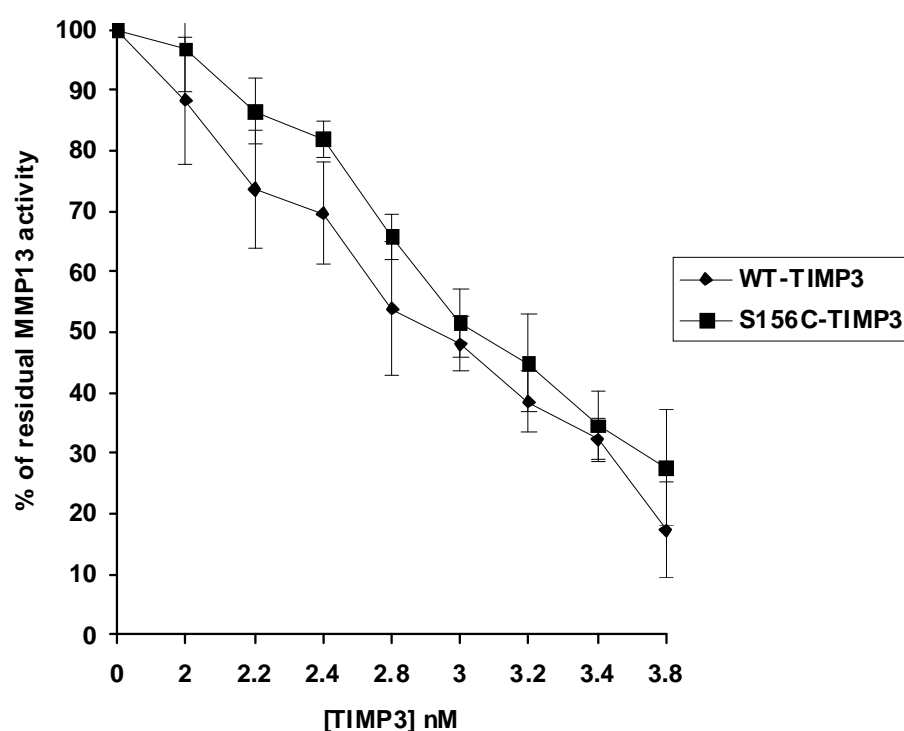


**Figure 8.** Fluorometric titration of MMP13. Mouse recombinant collagenase 3 was expressed in bacteria in inclusion bodies, purified and refolded. The enzyme was activated by incubation in 1 mM APMA for 2 h at 37°C. A constant amount of activated MMP13 was incubated with recombinant TIMP3 for 2 h at room temperature. 2 hours after adding the fluorogenic quenched substrate to the reaction mixture, fluorescence was measured at 330 nm excitation and 390 nm emission. The fluorescence given by the uncomplexed MMP13 was plotted against the concentration of TIMP3. The error bars represent  $\pm$ SD of three independent experiments.

### 3.2.3 Analysis of antibody binding to epitopes and their specific recognition

Commercial antibodies were tested by ELISA for binding to recombinant expressed epitopes fused to GST and specific recognition of their corresponding epitopes. An ELISA was used because all experiments involving these antibodies were done using this assay. ADAMTS neopeptide antibody bound specifically to the recombinant fused protein. Both the human and the mouse epitope were recognised, but not the uncleaved peptide containing the recognition site (Fig. 9A). The specificity of the antibody was further tested in an ELISA using different cell lines. For this propose, three cell lines were chosen as positive and negative controls. Isolated primary chondrocytes which express aggrecan and ADAMTS4/5 are positive controls for the antibody specificity. Fibroblasts and RAW 264.7 are the negative controls as they do not express the chondrocyte markers (see fig. 16 and Thomas Langmann, personal communication). These cell lines were grown in ELISA plate wells and probed with antibodies which bind to aggrecan, ADAMTS4, ADAMTS neo and MMP neo epitopes. As Fig. 9B shows the antibodies specifically recognise their protein-antigens in the ELISA. Therefore, this ELISA experiment shows that the antibody interacts specifically with its neopeptide and can be used as a positive control in the ADAMTS4/ADAMTS5 mediated cleavage of aggrecan.

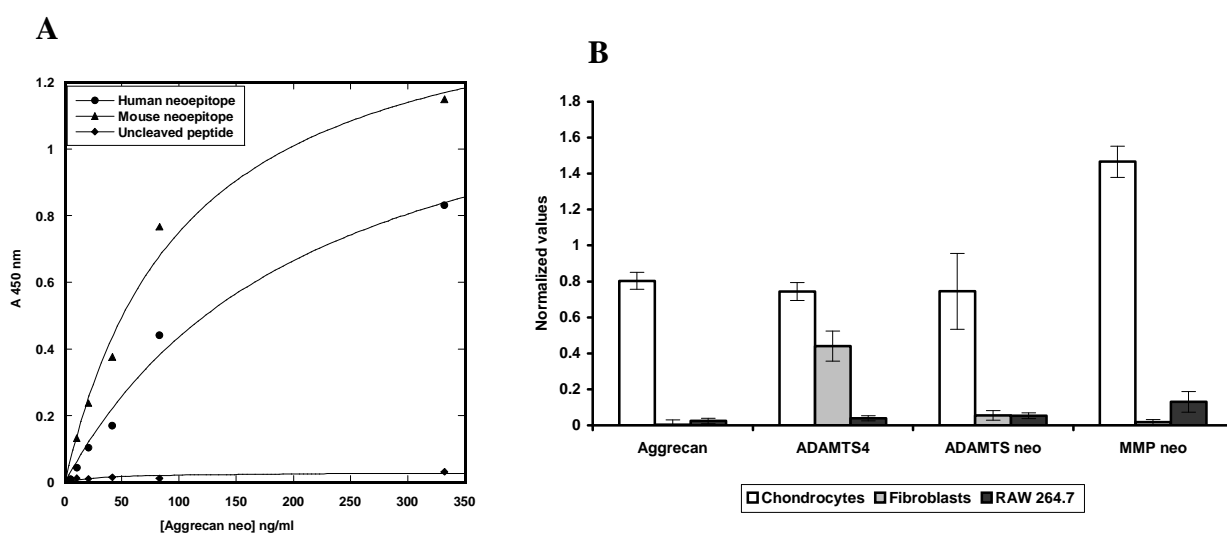


**Figure 9.** Analysis of antibody specificity and selectivity in ELISA. (A) ELISA determination of binding between the neopeptide antibody and its epitopes. An ELISA plate was coated with purified peptides

fused to GST, blocked and serial dilutions of the anti-ADAMTS neo antibody was applied. Antibody bound to the peptide was detected with anti rabbit antibody conjugated to horse radish peroxidase and the absorbance values at 450 nm were plotted against the antibody concentration. A curve was fitted to the points using the equation (8). (B)  $1.5 \times 10^4$  cells were plated on a microtiter plate and grown for 5 days. The primary antibodies were applied to the different cell lines followed by the secondary antibody. After adding the enzyme's substrate, the absorbance of the chromogenic reaction was measured at 450 nm. The plots represent three point readings with  $\pm$ SD as error bars.

### 3.3 Functional implications of TIMP3 on TACE catalytic activity

TIMP3 is unique among the TIMPs in that it is able to inhibit TACE (TNF- $\alpha$  converting enzyme) mediated shedding of membrane bound TNF- $\alpha$ . To determine whether inhibition of TACE activity is influenced by the S156C-TIMP3 point mutation, total protein from liver extracts was isolated by homogenation of whole liver of mice heterozygous (KI het) or homozygous (KI hom) for the S156C-TIMP3 knock-in as well as from wild type (WT) and TIMP3 knock out (KO) mice. Liver was chosen because it has been reported that TACE activity in the TIMP3 knock-out mouse is upregulated in this organ (Mohammed *et al.*, 2004). If the S156C mutation in TIMP3 molecule has an effect on TACE inhibition then it should be measurable in liver. TACE activity was assessed using a fluorogenic substrate (TACE substrate II) specific for this enzyme, in which the cleavage activity of TACE is measured by increased fluorescence of the cleaved peptide. This fluorogenic substrate consists of a short peptide containing a TACE-specific cleavage sequence separating the fluorescent group from dinitrophenyl group that acts as an internal quencher.

As shown in the Fig. 10 both native TACE from the liver extracts and recombinant TACE catalytic domain cleaved the fluorogenic substrate and displayed saturation kinetics for hydrolysis of the fluorogenic peptide.

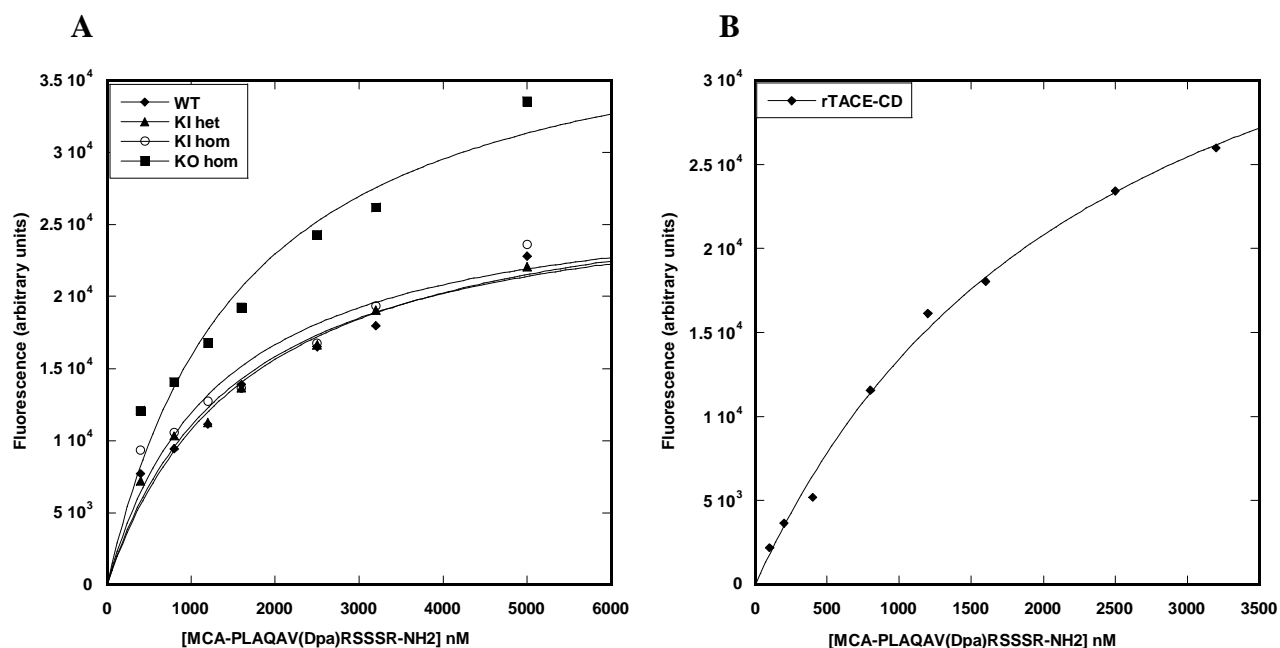


**Figure 10.** Substrate hydrolysis by native TACE from liver extracts and recombinant TACE catalytic domain. (A) 200  $\mu$ g of liver extract from animals of different genotypes were mixed with increasing concentration of fluorogenic TACE substrate II (100 nM to 5000 nM) and incubated for 1 hour at 27°C before measurement of fluorescence at 330 nm excitation and 390 nm emission. (B) 100 nM of rTACE catalytic domain was incubated with fluorogenic substrate (100 nM to 3200 nM) for 1 hour at 27°C and the fluorescence was measured as above. The fluorescence values obtained were plotted against the corresponding concentrations of the substrate. A curve was fitted to the points using the equation (8).

The activity of the enzyme in the liver extract of mice heterozygous (KI het) or homozygous (KI hom) for the S156C-TIMP3 knock-in shows that there is no change in the rate of fluorogenic substrate hydrolysis compared to their WT counterparts (Fig. 11). As expected, the loss of TIMP3 protein (KO hom) leads to the upregulation of TACE activity and it is in good agreement with other published data (Mohammed *et al.*, 2004).

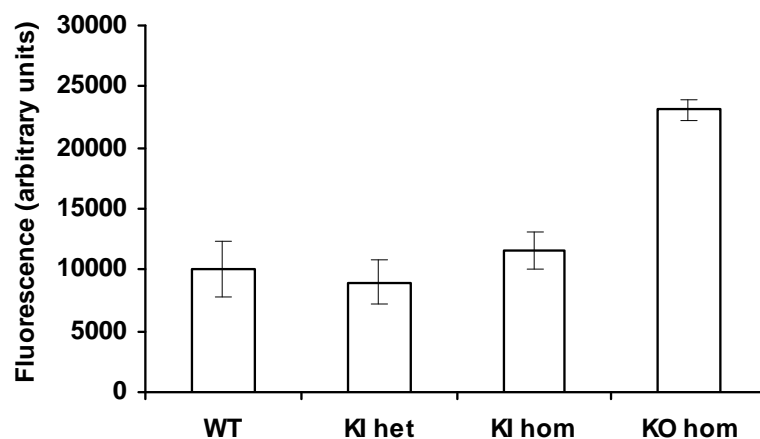


**Figure 11.** Analysis of TACE activity in liver extracts. 200  $\mu$ g of total liver protein extract was incubated with 1  $\mu$ M of TACE fluorogenic substrate for 1 hour at room temperature before the fluorescence was measured at 27°C using 330 nm excitation and 390 nm emission. The plots represent the means of three independent measurements. The error bars represent  $\pm$ SD.

In order to assess the specificity of the measurements and to attribute the inhibition of TACE to TIMP3, we incubated the liver extract with recombinant WT-TIMP3, S156C-TIMP3, TIMP1, TIMP2 and TIMP4 in a concentration dependent manner. Cleavage of the fluorogenic substrate was inhibited by WT-TIMP3 and S156C-TIMP3, whereas TIMP1, TIMP2 and TIMP4 had no effect on cleavage of the substrate in the range of concentrations used (Fig. 12).

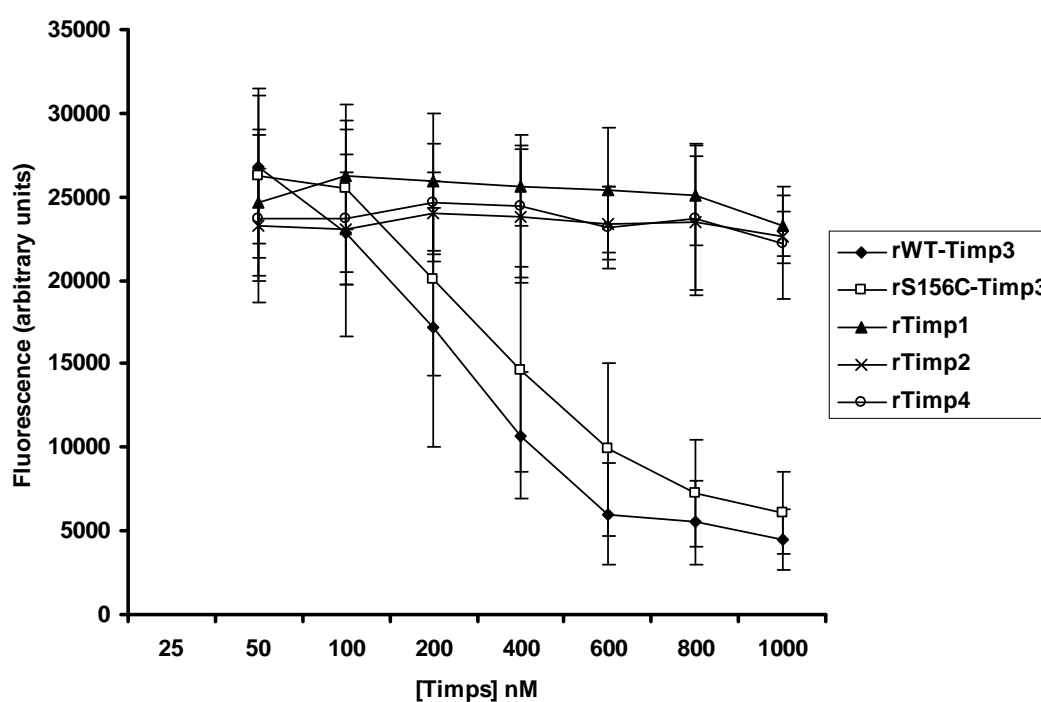




**Figure 12.** Inhibition of native TACE from WT liver extract by rTIMPs. Recombinant TIMPs were added to 50 $\mu$ g of total protein extract from WT mouse liver in a concentration dependent manner (25 nM to 1000 nM). The TIMPs and TACE were incubated at room temperature for 4 h before 1 $\mu$ M substrate was added to the reaction. After a further 3 hours incubation the fluorescence was measured. The graph shows the mean of three independent measurements with  $\pm$ SD as error bar.

In order to further prove the specificity of inhibition of TACE by TIMP3, which was observed in the whole liver protein extract, inhibition of recombinant TACE catalytic domain (rTACE-CD) was examined. In a concentration dependent inhibition assay the cleavage activity of rTACE-CD was blocked by both WT-TIMP3 and S156C-TIMP3 to the same extent (Fig. 13), as native TACE from liver extracts of WT, KI het and KI hom animals. As a negative control, rTACE-CD was incubated with increasing amounts of: TIMP1, TIMP2 and TIMP4. As expected, hydrolysis of the fluorogenic substrate was not significantly inhibited by these TIMPs.

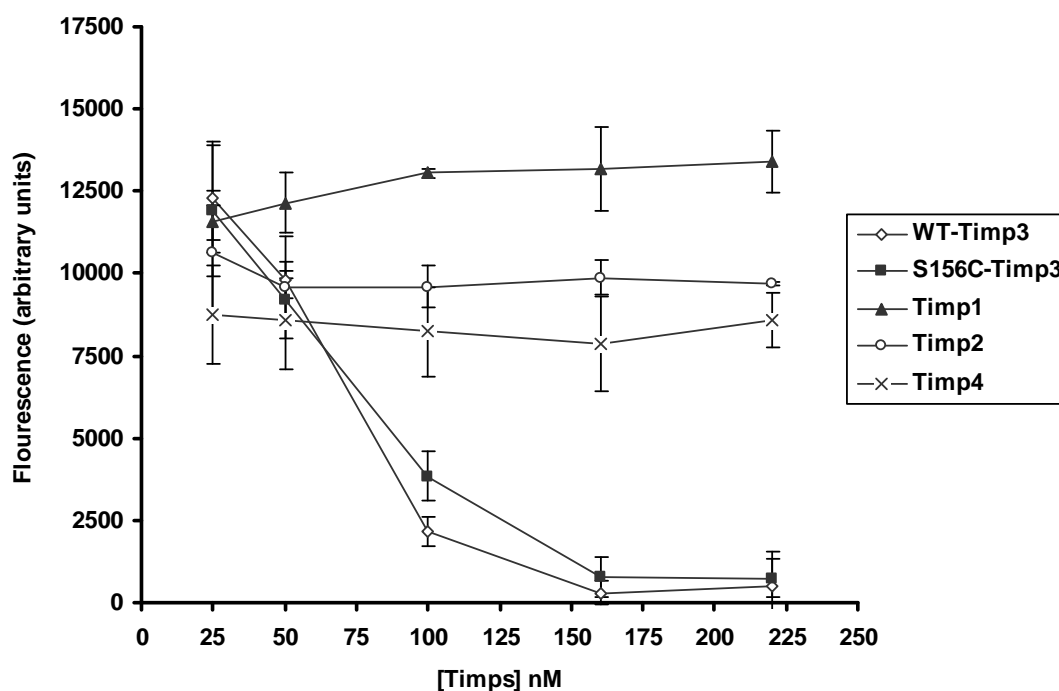


**Figure 13.** Assessment of rTACE-CD inhibition by rTIMPs. Recombinant TACE catalytic domain (100 nM) was incubated with increasing concentrations of TIMPs (6 nM to 220 nM) for 3 h at RT. 1 $\mu$ M of

TACE fluorogenic substrate was added to the reaction and the fluorescence was measured after a further 2 h incubation at 27°C. Graph represents the mean value of 3 independent experiments.

As TIMP3 is capable of inhibiting the cleavage activity of TACE, binding of TIMP3 to rTACE-CD was analysed by ELISA. The experimental data demonstrates that TIMP3 can bind to the TACE catalytic domain in a concentration dependent manner and that the S156C-TIMP3 mutant binds with similar affinity to WT-TIMP3 (Fig. 14) suggesting again that the SFD related mutation does not affect TACE activity both *in vivo* and *in vitro*.

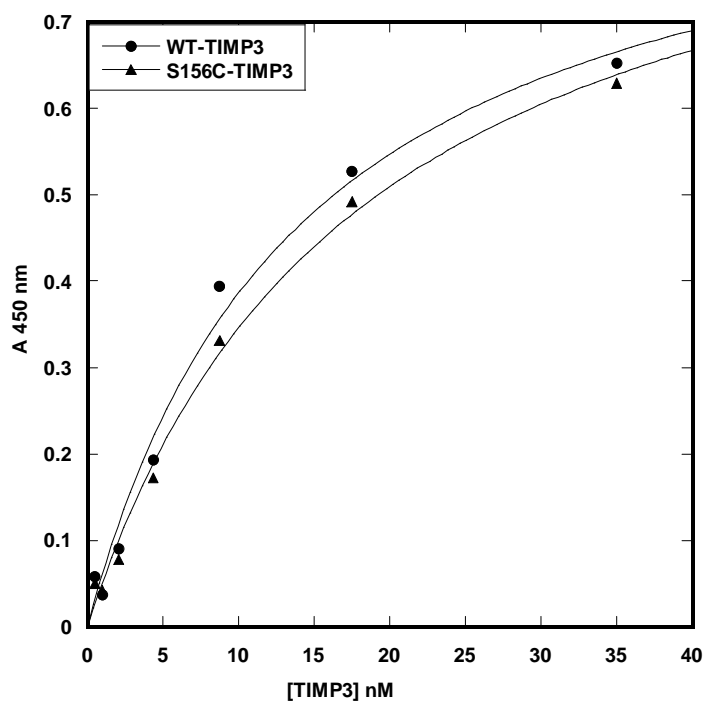


**Figure 14** Analysis of TIMP3 binding to TACE catalytic domain. Wells of a microtiter plate were coated with purified and refolded TACE catalytic domain overnight at 4°C. After blocking with BSA, serial dilutions of TIMP3 were applied and incubated for 1 hour at room temperature. The TIMP3 bound to TACE was detected with an anti-TIMP3 polyclonal antibody followed by incubation with a peroxidase conjugated rabbit secondary antibody. The intensity of the chromogenic reaction generated in the presence of TMB was plotted against the corresponding TIMP3 concentration and the curves were fitted according to equation (8).

### 3.4 Cleavage activity of ADAMTS4/ADAMTS5 and MMPs inhibition by TIMP3

ADAMTS4 (aggrecanase-1) and ADAMTS5 (Aggrecanase-2) are two metalloenzymes which are secreted and bound to the ECM and whose best characterised activity is for cleavage of aggrecan. The proteoglycan aggrecan is the major component of cartilage ECM that gives it the strength to resist to high loads. TIMP3 is able to inhibit the cleavage activity of these two matrix metalloenzymes (Kashiwagi *et al.*, 2001), although they can also be inhibited by other members of the TIMP family, although with lower efficiency (Hashimoto *et al.*, 2001). The aggrecan molecule can also be cleaved by MMPs but the cleavage site is different to that of the ADAMTSs (Fig. 15). The specific cleavage activity of these two types of enzymes can be monitored by so-called neoepitope antibodies which recognise the amino acid sequence exposed after proteolysis of aggrecan. Neoepitope antibodies can react with either the C-terminal or the N-terminal sequence of the epitope generated by the action of a specific matrix metalloenzyme.

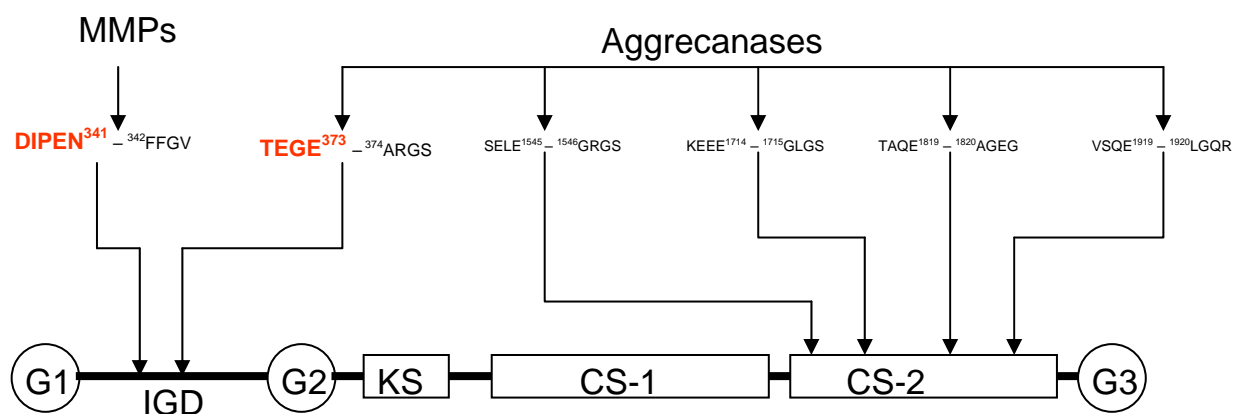


**Figure 15.** Schematic representation of MMPs and ADAMTS cleavage sites in the core Aggrecan molecule. The proteoglycan consists of several regions with high glucosaminoglycan content. G1- first globular domain; IGD-intraglobular domain; G2- second globular domain; KS- aggrecan region rich in keratin sulfate; CS-1 and CS2- regions one and two highly glycosylated with chondroitin sulfate. CS-2 contains gaps in glycosylation where the cleavage site for aggrecanases is located. G3- third globular region, representing the most C-terminal domain of the core proteoglycan. The arrows indicate the cleavage sites for aggrecanases and MMPs. The neoepitope sequences used in the present study and generated by MMPs and ADAMTS4/ADAMTS5 are highlighted in the figure.

In order to investigate TIMP3 function in the context of ADAMTS4/ADAMTS5 mediated aggrecan cleavage, chondrocytes were isolated from the ribs of mice deficient in TIMP3 and with the knock-in mutation (S156C-TIMP3) by treating them with collagenase. To test the identity of the isolated cells, immunocytochemistry was performed for the chondrocyte marker collagen type II. The cells were stained with antibody 5109 (Downs *et al.*, 2001), which recognises collagen type II. The cells showed an intense fluorescence demonstrating that the isolated cells are chondrocytes (Fig. 16A). The cells were further tested for another chondrocyte marker, aggrecan. In immunocytochemistry the anti-aggrecan antibody detected aggrecan localized in the ECM surrounding the cells. In addition the cells were immunostained with antibodies recognising the aggrecan neoepitopes generated by the action of MMP and ADAMTS4/ADAMTS5 (data not shown).

For further characterization of the cells, RT-PCR was performed on RNA isolated from chondrocytes and fibroblasts (Fig. 16B). The primer pairs were chosen in such a way that they anneal to two different exons, to eliminate the possibility of contamination of the RNA preparation with genomic DNA. Another parameter taken into consideration when designing the primers was that they are localized close to the 3' end of the transcripts. The cDNA was synthesized using oligo dT primer which anneals at the polyA signal at the 3' end, using primers designed to bind to the 3' end increases the probability that transcripts with lower expression level are amplified. In the case of very long mRNAs the ability of reverse transcriptase to synthesise the full length cDNA decreases along with the yield of the full length product.

In RT-PCR experiments the GUS ( $\beta$ -glucuronidase) house keeping gene was used as a control for RNA integrity. Experimental data revealed that only the chondrocytes express aggrecan - the substrate of ADAMTS4/ADAMTS5 – whereas fibroblasts do not (Fig. 16B). The other two transcripts analysed by RT-PCR were ADAMTS4/ADAMTS5 and it can be observed that both cell lines express the two matrix metalloenzymes. Supplementary information which can be extracted from the semiquantitative RT-PCR data suggests that at the RNA level the expression profile of the transcripts are not affected by the absence of TIMP3 or by the presence of the TIMP3 mutation in the mutant mice. The data obtained from RT-PCR and immunocytochemistry suggest that the isolated cells are chondrocytes, express the

enzymes and substrate (unlike the fibroblasts) and so provide a suitable system for analysis of the influence of TIMP3 on these proteinases.

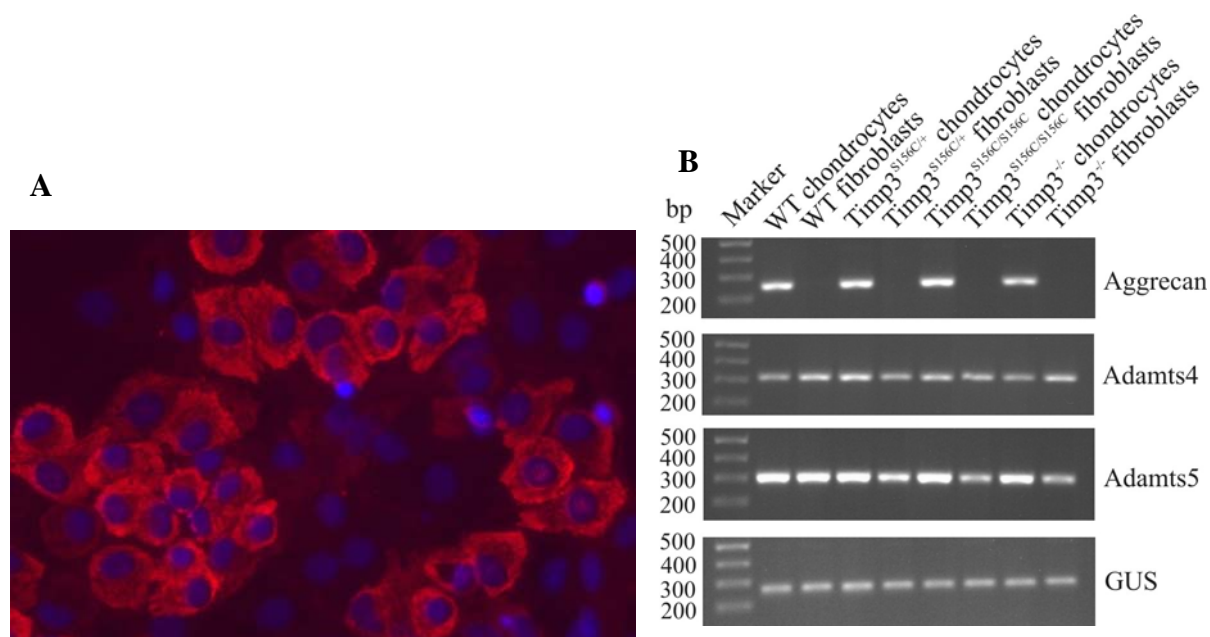
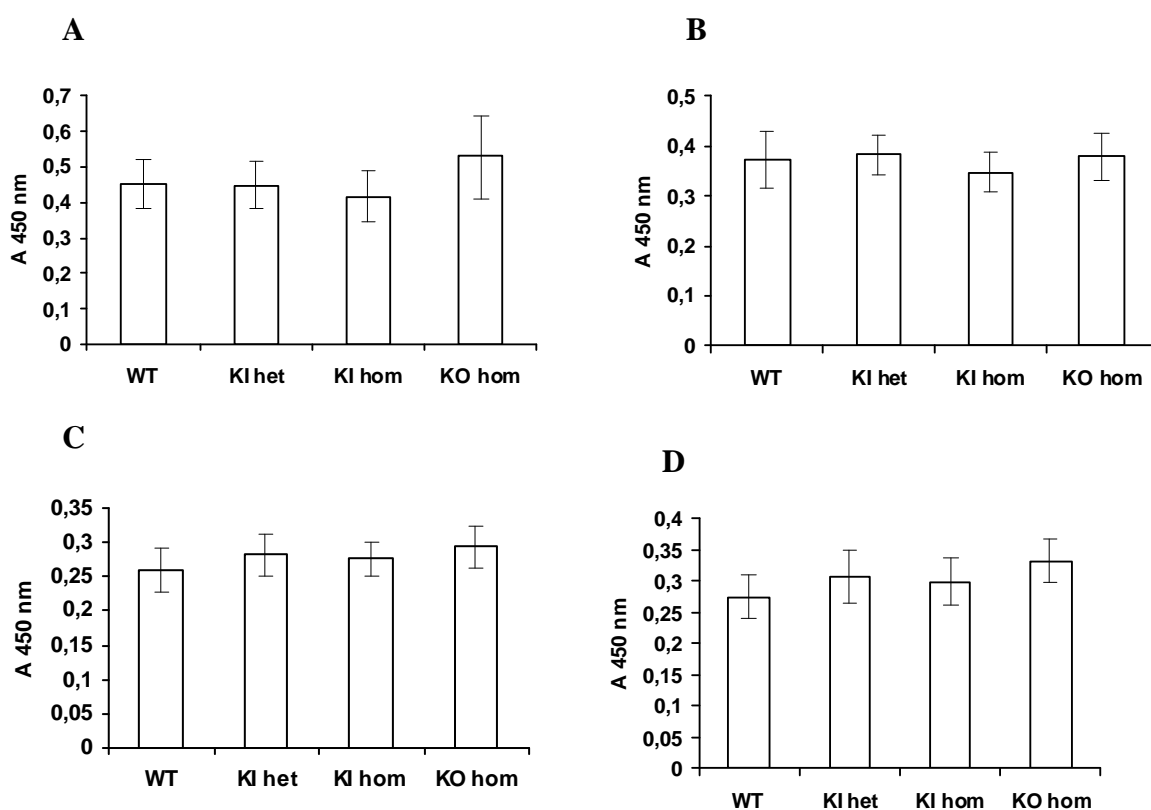


**Figure 16.** Characterization of isolated primary chondrocytes. (A) Representative staining of collagen type II in cultivated chondrocytes by immunocytochemistry. WT chondrocyte cells were grown on cover slips and fixed with 4% paraformaldehyde. After blocking the cells, an antibody specific for collagen type II was added, followed by incubation with an anti-mouse IgG antibody conjugated to Alexa Fluor 594. Collagen type II staining appears in red and the nuclei are stained with DAPI (4',6-Diamidin-2'-phenylindol-dihydrochlorid) in blue. The image was taken with Carl Zeiss Axioscop 2 fluorescence microscope with a magnification of 40x. (B) RT-PCR expression analysis of aggrecan and ADAMTS4/ADAMTS5 in chondrocytes. RNA was isolated from chondrocytes and fibroblasts and first strand cDNA was prepared using 1  $\mu$ g of RNA. The genes were amplified using a touch down PCR program with the primer pairs annealing to two different exons. The fragments amplified have the following sizes; Aggrecan - 250 bp; ADAMTS4 – 306 bp; ADAMTS5 – 302 bp and Gusb - 198 bp. Gus house-keeping gene was used as a control to check for the cDNA quality.

Two neoepitope antibodies were used to analyze the cleavage rate of aggrecan, namely ADAMTS neo (this antibody recognizes the C-terminal amino acid sequence - TEGE<sup>373</sup> - formed after cleavage by ADAMTS4 or ADAMTS5) and MMP neo (the C-terminal of MMP cleaved Aggrecan - DIPEN<sup>341</sup> - is recognized by this antibody). These two aggrecan neoepitope fragments are retained in the ECM bound to hyaluronan (Fosang *et al.*, 2003), making it possible to detect them by immunohistochemistry.

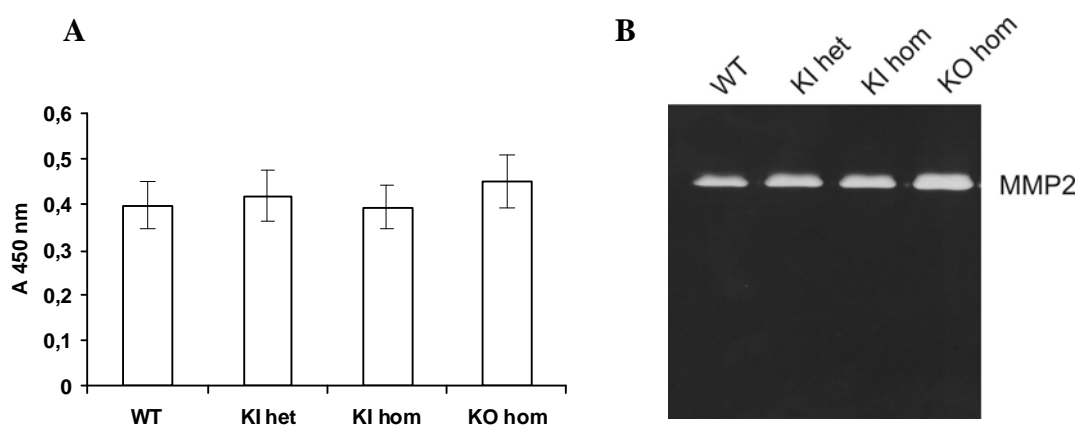
To investigate the cleavage rate of aggrecan due to the matrix metalloenzymes a modified ELISA was employed. In principle, this assay is based on chondrocytes grown in a monolayer in the wells of ELISA plate. The cells were cultured for 7 days, followed by a further 2 days in serum free medium, then fixed with paraformaldehyde and blocked with 3% BSA. The primary antibody was added to the wells and incubated overnight at 4°C followed by incubation with the secondary antibody conjugated with horse radish peroxidise. The end point value was measured after the chromogenic reaction was stopped with 1 N HCl at 450 nm. The native cleavage of aggrecan can be quantified using this assay which provides an approximation of the *in vivo* situation.

Using the neoepitope antibody which recognises the C-terminal sequence generated by ADAMTS4/ADAMTS5 cleavage, ELISA experiments show that there are equal levels of cleavage (neoepitope) in TIMP3 knock-out and S156C-TIMP3 knock-in chondrocytes when they are compared with the WT counterpart (Fig. 17A). Quantification for total aggrecan content by using an antibody which reacts with the uncleaved part of the Aggrecan shows that the levels of Aggrecan amount in the wild-type and mutant chondrocytes are similar (Fig. 17B). The level of the two enzymes responsible for the Aggrecan cleavage –ADAMTS4 and ADAMTS5- are also unchanged in all cell lines analyzed (Fig. 17C and D).



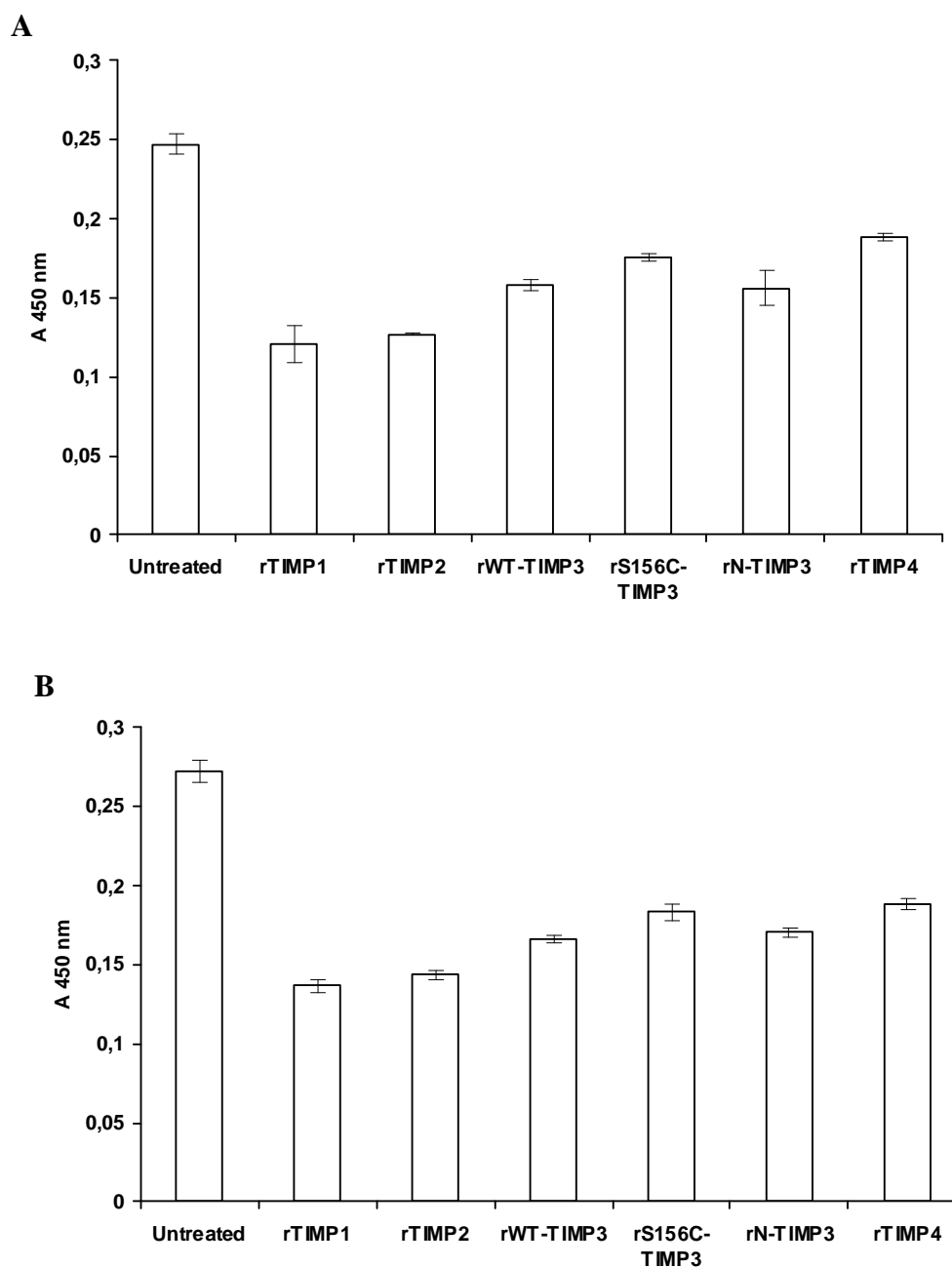
**Figure 17.** Measurement of ADAMTS4/ADAMTS5 generated Aggrecan fragments in chondrocyte-ELISA assay. Detection of the neoepitope generated by ADAMTS4/ADAMTS5 (A), total Aggrecan levels (B), ADAMTS4 levels (C) ADAMTS5 levels (D). Freshly isolated chondrocytes from animals with different genotypes were seeded on an ELISA plate and grown for 7 day and further 2 days in serum free medium. The cells were incubated with the primary antibody and the bound antibody was detected with the secondary antibody conjugated with HRP. After addition of substrate the end point absorbance was measured at 450 nm. The plots represent the mean value of 3 independent experiments with  $\pm$ SD as error bar.

The second group of metalloenzymes which are involved in the catabolism of aggrecan are the MMPs and they cleave aggrecan molecules at a distinct site from that of ADAMTS4/ADAMTS5 (Westling *et al.*, 2002). Using an antibody which detects the neoepitope revealed by MMP cleavage of Aggrecan, the level of Aggrecan proteolysis is unaltered in the mutant cell lines compared to WT (Fig. 18A). MMP activity in conditioned medium from the TIMP3 mutant cell lines was also checked by gelatin zymography. As reported earlier for fibroblasts (Soboleva *et al.*, 2003), MMP2 activity secreted by chondrocytes was unchanged in the cell lines tested (Fig. 18B).



**Figure 18** Detection of MMPs mediated aggrecan cleavage (A) and zymography analysis of MMPs activity (B). Isolated chondrocytes from each genotypes were plated in the wells of an ELISA plate, grown for 7 days followed by two more days in serum free medium. The MMPs cleavage activity was detected in an ELISA using the neoepitope antibody specific for the C-terminal of MMP cleaved aggrecan. The absorbance represents the mean values of 3 independent measurements and  $\pm$ SD as error bar. (B) Serum free conditioned medium from cultured chondrocytes were applied to zymography and analysed for cleavage of the gelatin from the gel.

To analyse if the MMPs mediated cleavage of aggrecan can be blocked *in vitro* by recombinant TIMPs, chondrocytes of all four genotypes were treated with 100 ng/ml inhibitors for two days in medium with serum and two additional days in serum free medium, changing the medium every day. All TIMPs were able to inhibit MMPs mediated cleavage of Aggrecan by decreasing the amount of detected neoepitope (Fig. 19).





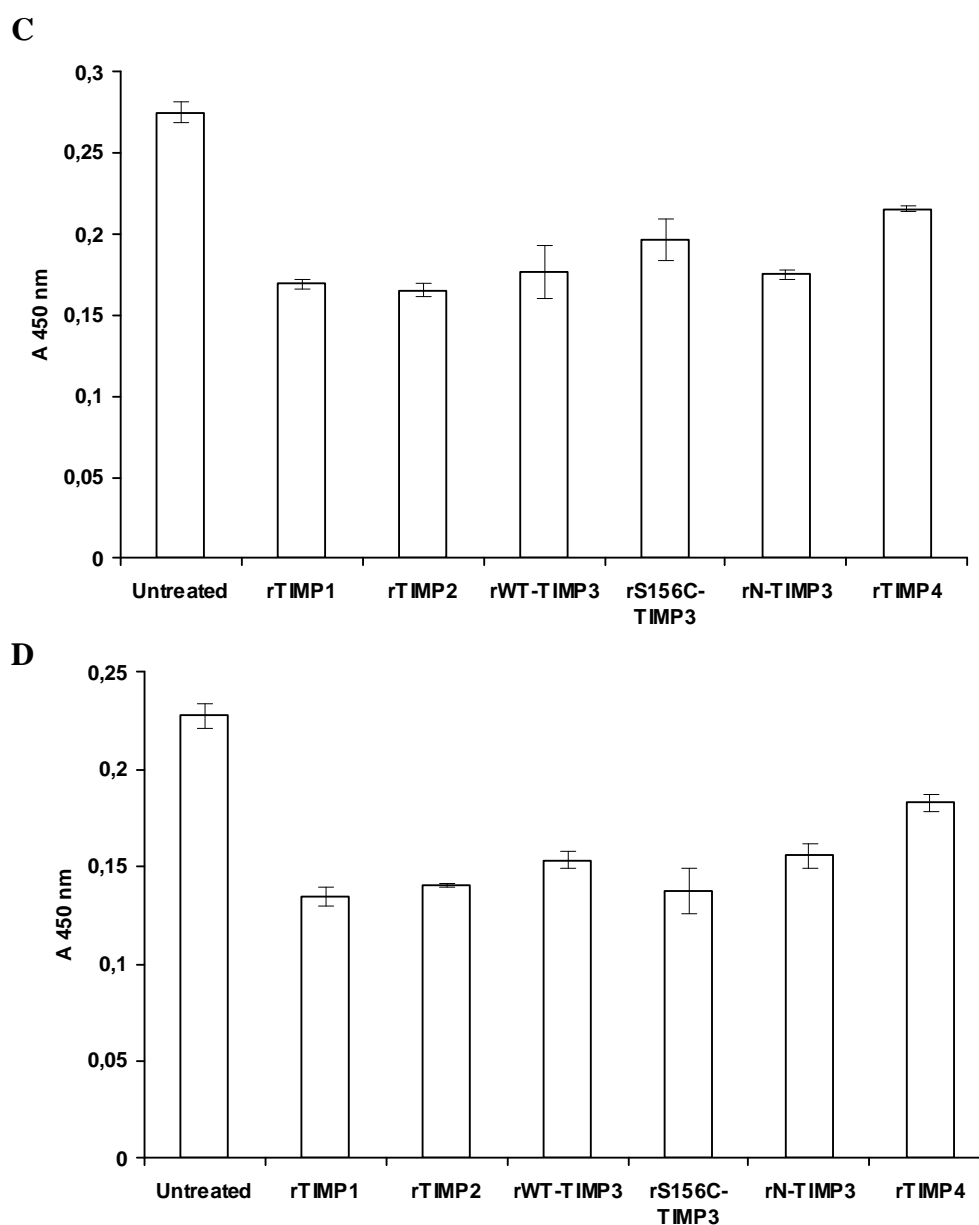


**Figure 19.** *In vivo* inhibition of the MMPs mediated aggrecan cleavage by recombinant TIMPs in cell-based ELISA. Chondrocytes from WT (A), S156C KI het (B), S156C KI hom (C) and TIMP3 KO (D) were grown on ELISA plates for 9 days and treated with 100 ng/ml inhibitors for the last 4 days. After fixing the cells, MMP neoepitope antibody was applied overnight and the bound primary antibody was detected with peroxidase conjugated goat anti-mouse IgG antibody. The end point absorbance was measured at 450 nm and the plots represent the mean value of three point measurements with  $\pm$  SD as error bar.

Collagen type II is the second major cartilage protein and it is catabolised by several known MMPs such as MMP-1, MMP-8, MMP13 and MT1-MMP (Harris and Krane,

1974a, 1974b, 1974c; Hasty *et al.*, 1990, Mitchell *et al.*, 1996; Wernicke *et al.*, 1996; Ohuchi *et al.*, 1997). Catabolism of collagen type II by MMPs can be assessed by using the 9A4 neoepitope antibody that is able to recognize the C-terminal amino acid (GPX<sub>771</sub>GPQG where X is proline or hydroxyproline) of the 3/4 fragment after collagenase cleavage (Otterness *et al.* 1999). In experiments performed on the isolated chondrocytes the levels of collagen type II neopeptide antibody bound suggest that MMP activity is not modified in mice carrying either the TIMP3 deletion or the mutation (Fig. 20A). Quantification of uncleaved collagen type II using the 5109 antibody (Downs *et al.*, 2001), which will measure the total amount of this collagen, in ELISA experiments based on cultivated chondrocytes showed that the amount of this protein is unchanged in any of the cell lines investigated (Fig. 20B).

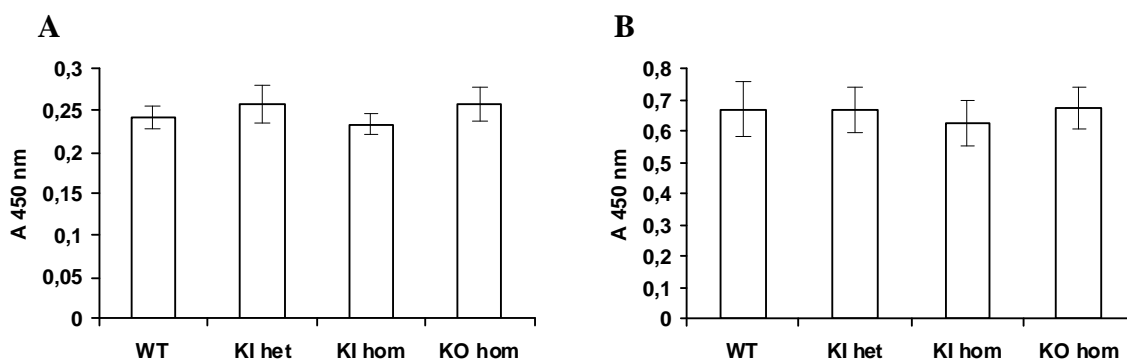


**Figure 20.** Measurement of collagen type II cleavage by MMPs (A) and the total amount of collagen type II (B) in chondrocytes. Chondrocytes isolated from animals with different genotypes were grown in a 96 well microtiter plate for 9 days. 9A4 antibody was used to detect the cleavage activity of MMPs and 5109 (Downs *et al.*, 2001) for the detection of uncleaved collagen type II. Bound primary antibody was detected with HRP conjugated goat anti mouse IgG and the intensity of the chromogenic reaction in the presence of TMB was measured at 450 nm. The plots represent the mean value of three independent measurements with  $\pm$ SD as error bar.

### 3.5 Competitive inhibition of VEGF binding to VEGFR2 by TIMP3

It has been demonstrated that TIMP3 is able to block angiogenesis by competing with VEGF for binding to VEGFR2 (Qi *et al.*, 2003). To investigate the ability of WT-TIMP3 and the S156C-TIMP3 mutant to compete with VEGF for binding to VEGFR2 a competitive ELISA was employed. Incubation of VEGFR2 with increasing concentrations of either recombinant wild-type or S156C-TIMP3 proteins diminished

the binding of VEGFR2 to VEGF immobilized on ELISA plates (Fig. 21). In contrast, TIMP2 was not able to compete with VEGF for its receptor binding and serves as a negative control for the binding test (Fig. 21).

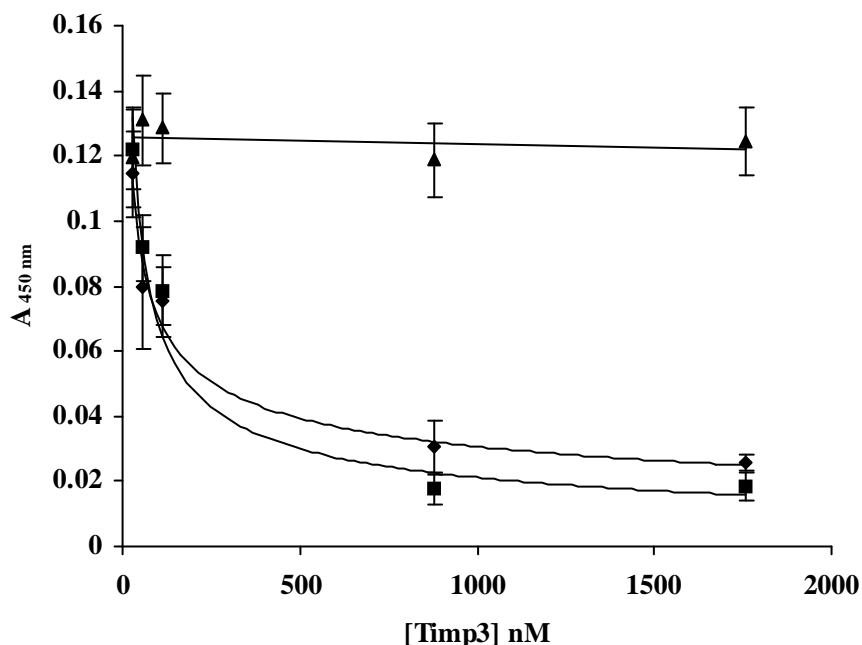


**Figure 21.** Competitive inhibition of VEGF binding to VEGFR2 by WT-TIMP3, S156C-TIMP3. Increasing concentrations of WT-TIMP3 (diamonds), S156C-TIMP3 (squares), TIMP2 (triangles) were added to a constant concentration of VEGFR2 (20 nM) and the complex was incubated overnight at room temperature before being added to wells coated with VEGF. VEGFR2 bound to VEGF was detected with an antibody directed against VEGFR2. After applying the secondary antibody conjugated with HRP the intensity of the chromogenic reaction, was measured at 450 nm. Absorbance values were plotted against the corresponding TIMP concentrations. The data plotted is the mean of 3 independent experiments with  $\pm$ SD as error bar.

### 3.6 Analysis of TIMP3 binding to collagens

In an effort to find new interacting partners of TIMP3 which might help in clarifying the SFD pathomechanism several collagens were analysed for their binding to TIMP3 in an ELISA. Five types of collagen were used to testing for binding of refolded recombinant WT-TIMP3 and the S156C-TIMP3 mutant: collagen type I from rat tail; collagen type II from chicken; collagen type III from calf; collagen type IV from human placenta and collagen type V from human placenta. The ELISA demonstrated that WT-TIMP3 (Fig. 22A) and S156C-TIMP3 (Fig. 22B) bound all collagens tested at approximately similar levels to wells only coated with BSA.

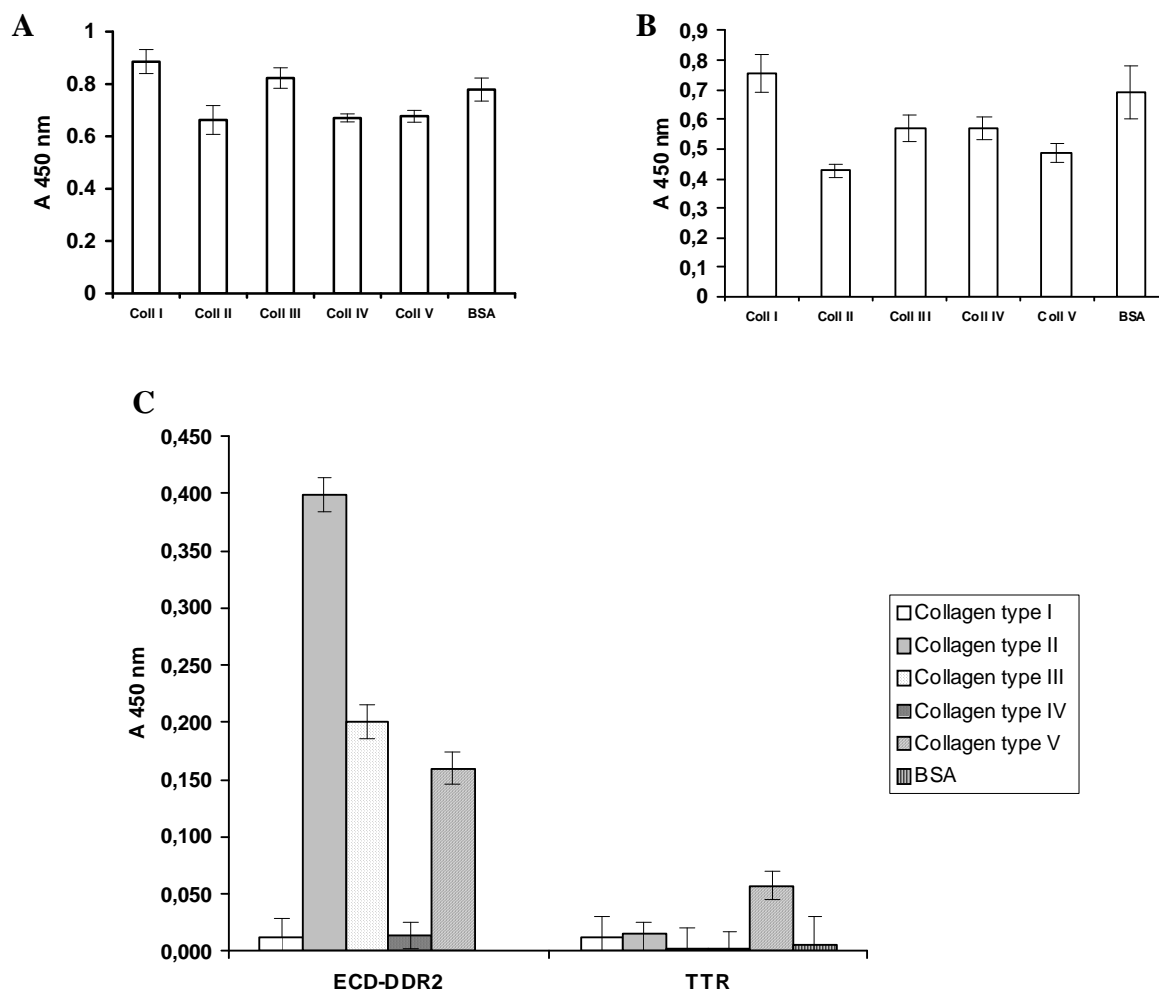


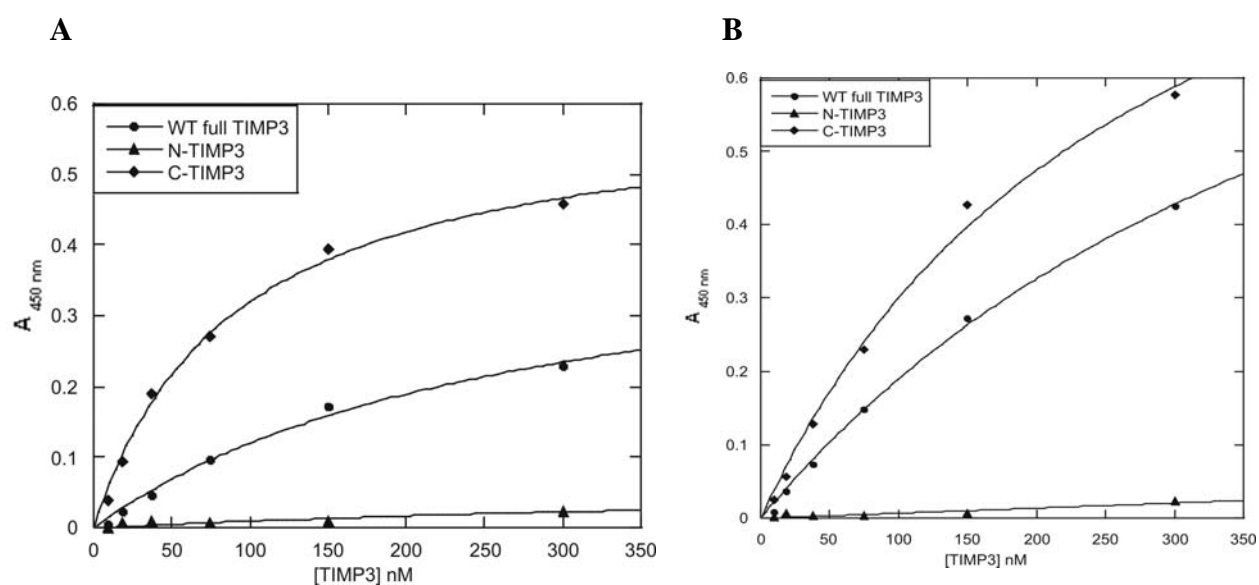
**Figure 22.** TIMP3 binding to various types of collagens in ELISA. The wells of an ELISA plate were coated with 10  $\mu\text{g}/\text{ml}$  solutions of the collagens indicated together with BSA overnight at 4°C followed by blocking with BSA. 1  $\mu\text{M}$  of recombinant WT-TIMP3 (A) or S156C-TIMP3 (B) was added to the collagen coated wells and incubated 1 hour at room temperature. TIMP3 bound to the collagens was detected using a polyclonal anti TIMP3 antibody directed against C-terminal of TIMP3 which was prepared in house. After incubation with the secondary antibody the intensity of the chromogenic reaction was measured at 450 nm. (C) ECD-DDR2 (positive control) and TTR (negative control) binding to collagens was performed exactly as for TIMP3 binding to collagens. The plots represent three point measurements with  $\pm\text{SD}$  as error bar.

To test for the specificity of the entire collagen binding experiment, ECD-DDR2 (Fig. 6A) was used as a positive control for the collagen binding and TTR (Fig. 6A) was used as a negative control. As can be seen from the experimental data TTR does not interact with any of the collagens while ECD-DDR2 binds to collagen types II, III and V (Fig. 22C), as expected, showing that the assay is specific.

In order to further analyze the ability of TIMP3 to bind to collagens and apparently non-specifically to BSA, a concentration dependent ELISA of TIMP3 binding to collagen type V was performed. The results of the assay show that full length WT-TIMP3 binds to collagen type V in a concentration dependent manner (Fig. 23A). Using the individual TIMP3 domains in this ELISA shows that there is no binding of the refolded N-terminal domain of TIMP3 to collagen type V while the C-terminal domain binds collagen type V with similar affinity to full length WT-TIMP3 (Fig. 23A). The same experimental set up was used to test TIMP3 binding to BSA. Application of TIMP3 in a serial dilution gives a similar binding pattern as for binding to collagens: the N-terminal does not bind to BSA while full length TIMP3 and its C-terminal bind unspecifically to the BSA (Fig. 23B). In parallel, the other TIMP family members were analysed for binding to collagens and as can be seen in Fig. 23C TIMP1, TIMP2 and TIMP4 do not interact with collagen type V, this experiment represents a further control for the ELISA.

In an ELISA the antigen is immobilized by adsorption to the surface of the well. This process might cause conformational changes in the immobilized ligand potentially leading to unspecific interactions, therefore the interaction of TIMP3 with a molecule in solution was investigated. A pull down assay of TTR by TIMP3 was performed using Ni-NTA beads which bind to the His tag fused to the C-terminal of TIMP3. Western blot analysis revealed that WT-TIMP3 was able again to bind to an unrelated molecule (TTR) in solution (Fig. 23D).

Taken together, these results suggest that the apparently unspecific interaction of full length WT-TIMP3 and S156C-TIMP3 with the collagens is mediated through the C-terminal domain of TIMP3.



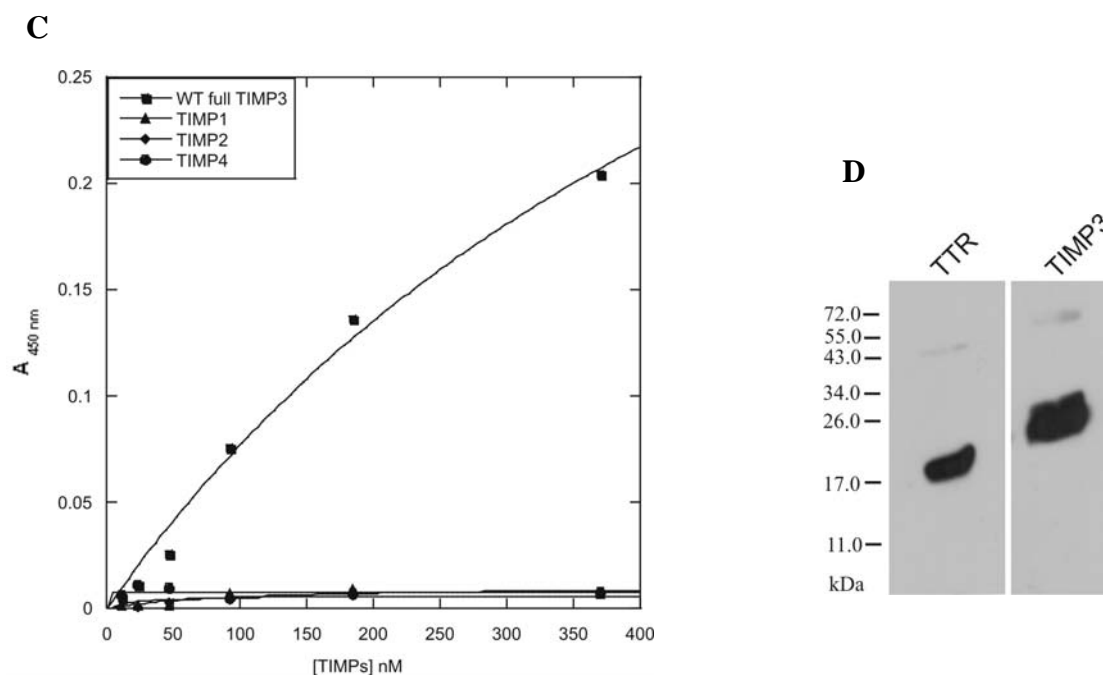


**Figure 23.** ELISA experiments for analysing the binding activity of TIMP3 to collagen type V. 10  $\mu\text{g/ml}$  of human collagen type V (A and C) and BSA (B) was applied to the wells of an ELISA plate and incubated overnight at 4°C. The wells were blocked by adding 3% BSA for 1 hour at room temperature. Purified and refolded TIMP3 and the TIMP3 N-terminal and C-terminal domains (A and B) and TIMP1, TIMP2, TIMP4 (C) were applied in a dilution series and bound TIMP was detected using an anti His tag antibody. The intensity of the chromogenic reaction was measured at 450 nm as end point and plotted against the corresponding TIMP3 concentration. The data were fitted by non-linear least-squares regression according to equation (8). (D) Pull down of TTR by TIMP3. Bacterially expressed TIMP3 was mixed with TTR and incubated overnight at 4°C with gentle rotation. Next day washed Ni-NTA beads were added to the solution and incubated for a further 2 hours. The beads were washed several times with 50 mM  $\text{NaH}_2\text{PO}_4$ , 300 mM NaCl pH 8.0 before the complex was eluted with the above buffer containing 250 mM imidazole. TTR on the blot was detected with anti 1D4 tag antibody and TIMP3 was detected with anti-TIMP3 antibody.

### 3.7 Structural implications of S156C mutation on TIMP3 molecule

The most common mutation in the TIMP3 gene associated with SFD is the introduction of a new free cys residue. Potentially this can mediate the formation of intermolecular disulfide bonds leading to oligomerisation of the mutant TIMP3. To test this possibility, western blotting was employed for the detection of higher molecular weight complexes. For this purpose immortalized fibroblasts cell lines with S156C knock-in mutation were used. ECM proteins secreted by fibroblasts were prepared by

scraping the surface of cell culture dishes with SDS loading buffer and the samples were loaded onto SDS-PAGE in both reducing and oxidizing conditions. Detection of TIMP3 under non-reducing conditions in western blots shows that in samples containing the mutant TIMP3, both from the KI het and the KI hom fibroblasts, a band of approximately 43 kDa (Fig. 24) appears, which could correspond to a dimeric form of the S156C-TIMP3 mutant built up due to intermolecular disulfide bonds. This assumption is supported experimentally by running the same samples under reducing conditions which leads to the dissociation of the 43 kDa complex to the monomeric form (Fig. 24). In addition, the mutant S156C-TIMP3 seems to form even higher molecular weight complexes localized at the top of the gel which might be explained by the formation of aggregates. In contrast, when analysing TIMP3 from the WT fibroblasts, no oligomeric or aggregated forms of the protein are seen.

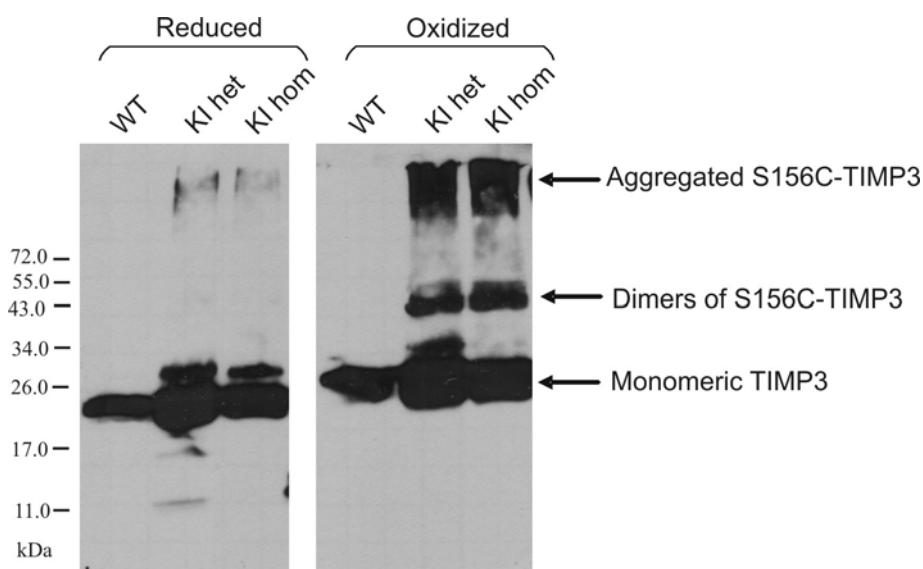


**Figure 24.** Western blot analysis of S156C mutant TIMP3 versus WT-TIMP3. WT fibroblasts and S156C KI fibroblasts were cultured for two days. After removing the cells by trypsinization, ECM bound proteins were solubilised in SDS loading buffer without reducing agent ( $\beta$ -mercaptoethanol). An aliquot from each sample was loaded on a 15% SDS-PAGE under reducing conditions and also under non-reducing conditions. TIMP3 protein on the blot was detected with a polyclonal antibody directed against the C-terminal of TIMP3.

### 3.8 Quantification of the S156C-TIMP3 mutant protein in knock-in fibroblasts

One of the major features found in the eyes of the patients with SFD is the formation of drusens containing, among many other proteins, TIMP3. Therefore, as S156C KI fibroblasts are available, it was decided to measure the amount of mutant TIMP3 protein in these cell lines. The quantity of the TIMP3 was measured in an ELISA using fibroblasts grown in the wells of a microtiter plate. We took advantage of the fact that in the cell culture system TIMP3 is localized bound to the ECM and after cell detachment can be directly detected without further manipulation. This avoids errors occurring during protein handling and in the end gives relatively accurate results. Moreover, the ELISA is also a quantitative assay compared, for example, with western blotting which is more a qualitative method.

Using the method mentioned above, the amount of TIMP3 was measured in different compartments. First an ELISA was performed for TIMP3 bound to ECM. The results show that in fibroblasts carrying the S156C mutant TIMP3, both in homozygotes and heterozygotes, the amount of extracellular TIMP3 is elevated compared to WT counterparts (Fig. 25A). However comparison of KI heterozygous and KI homozygous cell lines showed no significant differences in the levels of mutant protein. Next the TIMP3 cell content was analysed. Equal numbers of cells were allowed to attach for 2 hours in the wells of a microtiter plate and their protein content was quantified as described for the cell based ELISA. The data obtained demonstrates that the amount of TIMP3 is also elevated in fibroblasts cell lines carrying the TIMP3 mutation (Fig. 25B) following the same pattern as for the ECM. The total amount of TIMP3, made up of the cellular protein together with the ECM bound material was also analysed. Again, the amounts of TIMP3 in KI fibroblasts are higher than in wild type cells (Fig. 25C).

A significant parameter which might influence experimental data when comparing different cell lines would be the number of cells (if it is assumed that the cell division rate is higher in one cell line compared to the other and the higher cell number would produce more protein). Therefore,  $\beta$ -actin was used as a normalization factor for the number of the cells. Measurement of the level of this protein suggests that the number of the cells are approximately equal (Fig. 25D), so that the increased TIMP3 concentration in the KI fibroblasts determined by ELISA is due to the mutation in the inhibitor molecule and not of the experimental conditions.



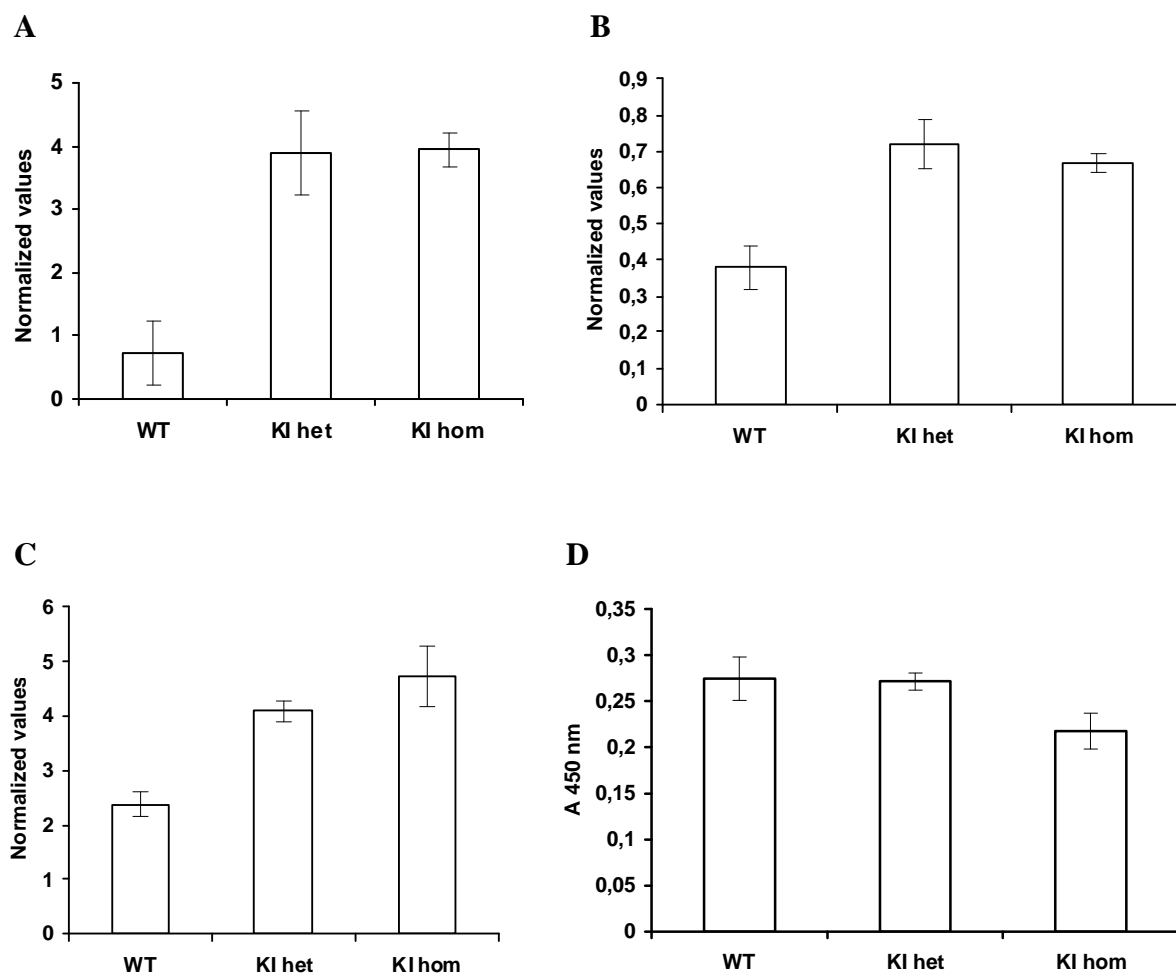


**Figure 25.** Measurement of TIMP3 amount in different compartments in fibroblasts. (A)  $1.5 \times 10^4$  fibroblasts were seeded on an ELISA plate and grown for 2 days. The cells were detached non-enzymatically (cell dissociation buffer enzyme free PBS-based, Gibco) and the ECM bound TIMP3 was detected by ELISA. For cellular TIMP3 (B) and  $\beta$ -actin (D),  $1.5 \times 10^4$  cells were plated and allowed to attach for 2 hours and the amount of TIMP3 and  $\beta$ -actin was measured based on cell ELISA. (C) The same number of fibroblasts were grown for 2 days before being fixed with PFA and TIMP3 was detected as described for cell based ELISA. The plots represent the mean value of three point measurements with  $\pm$ SD as error bar and the data were normalized against  $\beta$ -actin.

### 3.9 TIMP3 turnover in the ECM

Elevated amounts of mutant TIMP3 in the fibroblasts suggests that either the protein is not degraded with the same efficiency as the WT or the mutant transcript is upregulated. Reports in the literature show that the mutant mRNA level is not affected by the mutation (Chong *et al.*, 2003). To analyse the possibility that the mutant TIMP3 is degraded more slowly than the WT and therefore leads to the protein accumulation,

TIMP3 turnover in the ECM was measured. In principle, the method used is based on the following experimental set-up: the KI fibroblasts are grown in the wells of a microtiter plate for a certain time before they are removed and replaced by knock-out fibroblasts. After different time points the knock-out cells are removed and the remaining ECM bound TIMP3 is quantified by ELISA. As the experimental data shows (Fig. 26), the rate of S156C-TIMP3 turnover, both in the knock-in heterozygous and knock-in homozygous cell lines, is significantly lower in the first two days compared to the WT-TIMP3, confirming the hypothesis that the mutant TIMP3 is more resistant to degradation and hence that the protein will accumulate in the ECM.

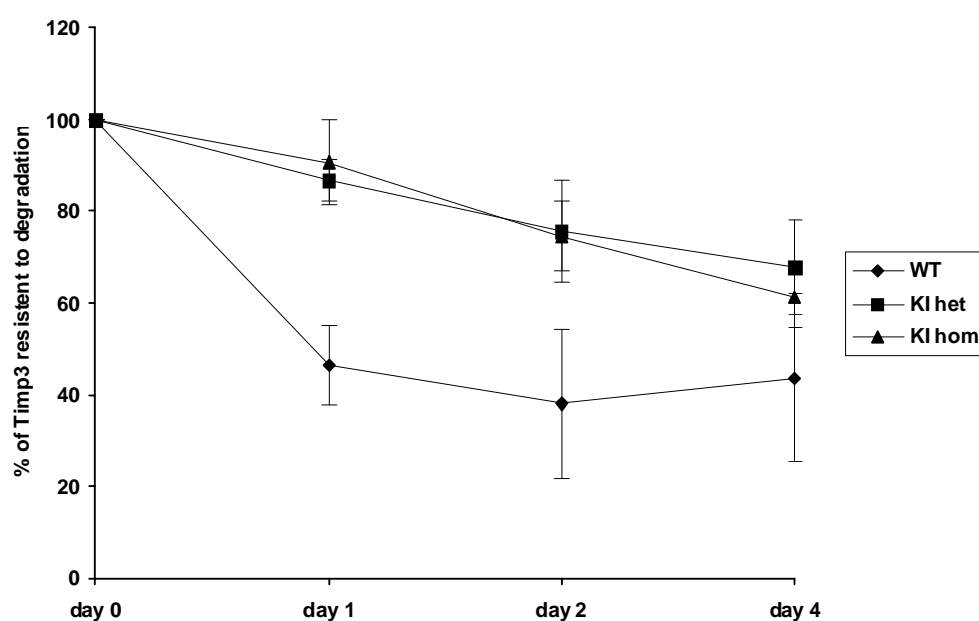


**Figure 26.** Rate of the TIMP3 degradation in the ECM.  $1.5 \times 10^4$  KI heterozygous, KI homozygous or WT fibroblasts were plated and grown for two days on an ELISA plate before the cells were detached non-enzymatically and replaced by  $6 \times 10^3$  TIMP3 knock-out fibroblasts to measure TIMP3 turnover. After the time points indicated in the graph the KO fibroblasts were removed and the remained TIMP3 protein was detected with a polyclonal antibody against TIMP3 based on the principle of a regular ELISA. The error bars  $\pm$ SD represents three point readings.

## 4. Discussion

Although SFD is a rare disorder, a number of phenotypical similarities to age related macular degeneration (AMD) make it an important disease to be elucidated. At present, it is unknown how mutations in TIMP3 initiate the molecular events that lead to disease development and progression and finally to the full known picture of SFD pathology.

TIMP3 is a multifunctional protein involved in many biological processes. Of these, the best characterised activity is the inhibition of metalloenzymes mainly attributed to the N-terminal domain (Lee *et al.*, 2001, Langton *et al.*, 1998, Wei *et al.*, 2005). It plays also a role independent of the enzymatic inhibitory function for which the C-terminus of TIMP3 is responsible, namely binding to VEGFR2, EFEMP1 (Klenotic *et al.*, 2004) and to the ECM (Langton *et al.*, 1998; Yu *et al.*, 2000) although recent evidence suggests that both domains, the N- and the C-terminus, contribute to ECM binding (Lee *et al.*, 2007).

To dissect the pathomechanism of SFD, the present study aimed at deciphering the effects of the pathological mutations on functional aspects of TIMP3 biology both *in vivo* and *in vitro*. We also wanted to investigate whether the known TIMP3 missense mutations result in a dominant negative effect or lead to haploinsufficiency. In order to obtain insight into the pathological characteristics of SFD, two mouse models of TIMP3 mutations were available: the TIMP3 knock-out mouse (Soboleva *et al.*, 2003) and the S156C-TIMP3 knock-in mouse (Weber *et al.*, 2002), both of which should greatly enhance our understanding of the *in vivo* processes involved in this disease. At the same time, recombinant proteins were used to attribute precisely to TIMP3 the effects observed in the mouse models in an attempt to restore the lost TIMP3 protein and its biological function.

### 4.1 TIMP3 involvement in the modulation of sheddase activity of TACE

Many proteins are initially synthesized as membrane-anchored ligands that are subsequently cleaved from the surface of the cells, a process called shedding. It is an important post-translational mechanism for regulating the function of cell surface proteins (Hooper *et al.*, 1997). This diverse group of proteins includes ligands such as cell adhesion molecules, growth factors and cytokines that undergo ectodomain

shedding of the membrane bound precursor to its soluble form. The membrane anchored proteins often have a different qualitative signal from that of the soluble ligand (Brannan *et al.*, 1991; Grell *et al.*, 1995; Suda *et al.*, 1997). The sheddase activity can be provided by both membrane-bound as well as soluble proteases. Members of the zinc dependent membrane type MMPs (MT-MMP) and ADAMs have been identified as being responsible for shedding of the membrane bound proteins identified so far. In addition, soluble proteases such as neutrophil elastase, cathepsin G, and proteinase-3 have been involved in the cleavage of the cell surface proteins (Bank & Ansorge, 2001). Among these proteases, ADAM17 (TACE) has emerged as an important mammalian ectodomain sheddase (Black, 2002; Peschon *et al.*, 1998). The importance of TACE in the shedding process was demonstrated by deleting its catalytic domain in mice (Black *et al.*, 1997). The TACE knock-out mice are not viable and display multiple developmental malformations (Peschon *et al.*, 1998). Moreover, cells derived from TACE deficient mice show lower rates of release of TNF- $\alpha$ , as well as many other cell surface ligands. It has also been reported that the release of TNF- $\alpha$  from the cell surface can be achieved *in vivo* by MMP7 (Haro *et al.*, 2000) and *in vitro* by MT1-MMP, MT2-MMP (d'Ortho *et al.*, 1997) and MT4-MMP (English *et al.*, 2000).

Proteolytic activity of TACE is precisely regulated by different mechanisms. At the transcriptional level, TNF- $\alpha$  stimulates expression of TACE mRNA in a positive feedback manner accompanied by increased TNF-Receptor I (p55) shedding (Bzowska *et al.*, 2004). At the posttranslational level, the enzyme is synthesized as a zymogen with an N-terminal prodomain which confers latency. In order to become catalytically active the prodomain of TACE must be released and cleavage of the propeptide is performed by furin or a furin-like protease (Peiretti *et al.*, 2003; Schlöndorff *et al.*, 2000). The second mechanism by which TACE catalytic activity is controlled is performed by an endogenous inhibitor of many matrix proteinases namely TIMP3. Although TIMP3 belongs to a class of inhibitors with four known members (TIMP1, -2, -3, -4), which have largely overlapping inhibitory activities, only TIMP3 is able to specifically block the cleavage activity of TACE (Amour *et al.*, 1998). *In vivo* the role of TIMP3 in the inhibition of TACE mediated release of TNF- $\alpha$  has been demonstrated by deletion of TIMP3 gene. Mice deficient for TIMP3 show uncontrolled TNF- $\alpha$  shedding leading to chronic hepatic inflammation and failure of liver regeneration (Mohammed *et al.*, 2004). This indicates that TIMP3 is an important endogenous negative regulator for release of the proinflammatory cytokine TNF- $\alpha$  both in health and disease.

TNF- $\alpha$  is a pleiotropic cytokine and it has been implicated in a wide range of human disease including sepsis, diabetes, cancer, osteoporosis, multiple sclerosis, rheumatoid arthritis, and inflammatory bowel disease (Chen and Goeddel, 2002). Proinflammatory TNF- $\alpha$  produced by monocytes positively correlated with the prevalence of choroidal neovascularization in patients suffering from AMD (Cousins *et al.*, 2004). AMD is a principal cause of blindness and has a pathology closely resembling that of SFD. It has also been reported that in a mouse model of AMD macrophages and inflammation play an active role in the development of disease characteristics (Ambati *et al.*, 2003).

Quantification of constitutive TNF- $\alpha$  shedding in the TIMP3 deficient mice demonstrated that the amount of cytokine is elevated in the liver (Mohammed *et al.*, 2004), whereas in several other organs such as spleen, lung, brain or serum the amount of protein shed was not altered compared to the WT counterpart. At the transcriptional level TNF- $\alpha$  mRNA levels were not influenced by TIMP3 deletion, and TACE transcripts in the retina are at the same level in both the knock-out and knock-in animals (Andreas Janssen, personal communication). These experimental data suggest tissue-specific regulation of TACE mediated TNF- $\alpha$  shedding. Based on the available experimental data it was decided to investigate the effect of the S156C-TIMP3 mutant on TACE activity in the livers of gene targeted mice. Results from the present study reproduce the data from another report (Mohammed *et al.*, 2004) showing that TACE activity in the liver of TIMP3 deficient mice is increased. The present study was directed towards understanding what effect the SFD mutation (S156C-TIMP3) has on TACE mediated TNF- $\alpha$  shedding. In this context, the S156C mutation (which is localized to the C-terminal domain of TIMP3) does not lead to significant modification of the inhibitory activity of TIMP3 towards TACE as measured by hydrolysis of the fluorogenic substrate. This is as expected as it is widely accepted that the N-terminal domain of the TIMP3 molecule is mainly involved in matrix metalloproteinases inhibition (Lee *et al.*, 2002a, Langton *et al.*, 1998, Kashiwagi *et al.*, 2001, Lee *et al.*, 2002b). Moreover, a recent report, shows that the full-length and N-terminal domain of TIMP3 display equal inhibitory activities toward TNF- $\alpha$  convertase (Lee *et al.*, 2001). Although, TIMP3 is the only native inhibitor of TACE, transplantation of several critical residues from TIMP3 to TIMP4 led to the conversion of a previously inactive inhibitor of TACE to an active inhibitor of this metalloenzyme (Lee *et al.*, 2002; Lee *et al.*, 2004; Lee *et al.*, 2005). All the SFD related mutations identified are localized to the C-terminal domain of TIMP3, and therefore would not be expected to have any effect

on its inhibitory activity towards TACE (Lee *et al.*, 2001). Furthermore, a nonsense mutation has been identified in a patient which introduces a premature stop codon at amino acid 139 (E139X). This mutation generates a protein corresponding to the N-terminal domain of TIMP3 with the entire C-terminal domain deleted. Reverse zymography using this truncated TIMP3 shows that it retains its inhibitory activity towards the gelatinolytic MMPs (Langton *et al.*, 2000; Langton *et al.*, 2005). Assuming that the mutation causes missfolding of the TIMP3 proteins (see later for discussion), from the results obtained it seems that the oligomeric protein has on its surface the residues important for the inhibition of matrix metalloenzymes. Therefore, these data argue against a loss-of-function mutation in the TIMP3 molecule towards TACE inhibition.

#### **4.2 Regulation of ADAMTS4/ADAMTS5 and MMPs proteolytic activity by TIMP3**

Excessive catabolism of cartilage ECM is a characteristic feature of arthritic diseases and is mediated by two classes of protease: MMPs and ADAMTS. These proteolytic enzymes degrade the two major structural components of cartilage extracellular matrix, namely collagen type II and the proteoglycan aggrecan (Clark *et al.*, 2003) which together represent 90 % of the dry weight of cartilage. The aggrecan molecule can be cleaved at several distinct sites by other members of the ADAMTS family (Arner, 2002), but pathological cleavage by ADAMTS4 and ADAMTS5 takes place at the position G373/A374 (Tortorella *et al.*, 1999; Caterson *et al.*, 2000; Mercuri *et al.*, 1999; Tortorella *et al.*, 2000; Arner *et al.*, 1999) which has been called the aggrecanase site. Another cleavage site which is recognised by the MMPs (e.g. MMP1, 2, 3, 7, 9, and 13) is located in the interglobular region of aggrecan at the position D341/F342 (Flannery *et al.*, 1992; Fosang *et al.*, 1992; Fosang *et al.*, 1993; Fosang *et al.*, 1996; Little *et al.*, 1999; Chambers *et al.*, 2001; van Meurs *et al.*, 1999).

Collagen type II is the second most important structural protein of cartilage and its damage is correlated with chronic arthritic diseases. This type of collagen together with aggrecan gives cartilage the strength to resist to high loads. The collagen matrix can be pathologically degraded by two mechanisms; either mechanical overloading (Radin *et al.*, 1984; Randin and Rose, 1986) or cleavage of the collagen by collagenases-1 (Pelletier *et al.*, 1983; Whitham *et al.*, 1986), collagenase-2 (Hasty *et al.*, 1990; Devarajan *et al.*, 1991) or collagenase-3 (Mitchell *et al.*, 1996; Reboul *et al.*, 1996).

Collagens can also be catabolised by non-collagen proteases such as cathepsins B, K and L (Maciewicz *et al.*, 1990, van Noorden *et al.*, 1991).

Cartilage catabolism due to proteolytic enzymes can be assessed using neoepitope biomarkers. For this purpose specific types of antibodies, called neoepitope antibodies, have been developed which are able to recognise the short amino acid sequence exposed after cleavage by a specific proteinase. Some of these antibodies can be used to monitor the severity and the progression of articular cartilage break-down in a sandwich ELISA (Downs *et al.*, 2001).

MMPs cleavage of the aggrecan molecule at position N341/F342 generates the C-terminal sequence DIPEN and an N-terminal fragment FFGVG. Cleavage by aggrecanases usually generates C-terminal NITEGE and N-terminal ARGSV neoepitopes, although ADAMTS4 and ADAMTS5 can also cleave the aggrecan at other sites as depicted in figure 15. The DIPEN neoepitope generated by MMPs and the NITEGE neoepitope generated by aggrecanases are retained in tissue bound to hyaluronan, whereas the corresponding FFGVG and ARGSVI neoepitopes are released from the articular cartilage (Fosang *et al.*, 2003). MMPs derived FFGVG neoepitope fragments can be detected in human synovial fluids and so represent a candidate biomarker for aggrecan degradation (Fosang *et al.*, 1996). The primary cleavage site for triple helical collagen type II by collagenases is at position G775/L776 giving the characteristic  $\frac{3}{4}$  and  $\frac{1}{4}$  length  $\alpha$  chain fragments which can then be further degraded by different proteases. Therefore, antibodies directed against specific neoepitopes are useful tools for quantification of the cleavage rate of protein substrates by specific proteinase(s).

It has been shown that TIMP3 is a potent inhibitor of ADAMT4/ADAMTS5 mediated aggrecan cleavage (Kashiwagi *et al.*, 2001, Gendron *et al.*, 2003). TIMP1, 2, 4 are also able to inhibit these two enzymes but with much lower efficiency (Hashimoto *et al.*, 2001). In order to systematically analyse the effect of TIMP3 deficiency or the S156 TIMP3 mutation on the activity of ADAMT4/ADAMTS5 and the MMPs a number of experimental approaches were employed to cover both transcriptional and posttranslational effects. At a transcriptional level, according to semiquantitative PCR, none of the transcripts tested were up- or downregulated. In an *in vivo* system based on isolated chondrocytes derived from gene targeted mice the neoepitope antibodies were used to determine the cleavage rate due to the aggrecanases or MMPs. Catabolism of the aggrecan substrate was not significantly affected either in the TIMP3 knock-out or

in the S156C-TIMP3 knock-in chondrocytes when compared to WT counterparts. A possible explanation for these results is that the other three TIMPs are able to compensate for the absence of TIMP3 in inhibition of ADAMTS4. This theory was supported by experiments using recombinant proteins which demonstrate that aggrecan cleavage can be reduced by all TIMPs, emphasising the redundant function of TIMPs. Zymographic analyses demonstrates that various SFD-TIMP mutants, including S156C-TIMP3, retain their ability to inhibit gelatin degradation by MMP2 and MMP9 (Langton *et al.*, 2000, Soboleva *et al.*, 2003). S156C-TIMP3 also blocks aggrecan and collagen type II cleavage by MMPs to a similar extent to wild-type TIMP3, demonstrating that the S156C-TIMP3 protein remains an effective inhibitor of MMPs.

Cultivated chondrocytes from TIMP3-deficient mice displayed similar MMPs-mediated aggrecan cleavage rates to WT chondrocytes. Immunohistochemical localization of aggrecan degradation products revealed no major difference in aggrecan cleavage neoepitopes in knee joints of mice lacking TIMP3 when compared to wild-type mice under induced acute conditions of inflammatory arthritis (Mahmoodi *et al.*, 2005). However, in articular cartilage from TIMP3 knock-out mice 6 months or older, increased labelling for the MMP cleavage product was observed (Sahebjam *et al.*, 2007) suggesting that an imbalance between TIMP3 and MMP activities in these mice develops over time *in vivo*. On the other hand, the aggrecan region cleaved by MMPs is not essential for the catabolism of proteoglycan during development (Little *et al.*, 2005). The results from the present study suggest that TIMP3 is not crucial for the maintenance of cartilage integrity and SFD TIMP-3 mutant blocks the catalytic activities of these enzymes with the same efficiency as the WT-TIMP-3. These data suggest that either the mutation in TIMP-3 molecule is far from the interaction site between TIMP-3 and the inhibited enzymes or the inhibitory function is taken over by the other TIMP family members.

### **4.3 TIMP3 and angiogenesis**

The growth of blood vessels is an essential process for organ growth and repair and deregulation of angiogenesis contributes to many pathological condition including tumour spreading, inflammation, ischemic, infectious and immune disorders (Carmeliet, 2003). Pathological angiogenesis of the retina is a serious condition which leads to irreversible loss of vision and is associated with a number of different retinal degenerative conditions.



The SFD mutation S156C was originally identified in a family with relatively early onset of symptoms in the third decade of life with choroidal neovascularisation as an important feature (Felbor *et al.*, 1995). Relative recently, a direct association between TIMP3 and neovascularisation has been shown. Qi *et al.*, 2003 demonstrated that TIMP3 is able to block angiogenesis by competing with VEGF for binding to VEGFR2, inhibiting downstream signalling which otherwise would lead to the initiation of new blood vessel formation.

Results from the present study show that the S156C mutation does not have a significant effect on the capacity of TIMP3 to bind to VEGFR2 compared to WT recombinant protein, suggesting that the mutant protein retains its antiangiogenic property. Although one of the characteristics of SFD is neovascularization, the unaffected ability of the mutant TIMP3 to compete for VEGFR2 binding suggests that this angiogenic feature is not the primary cause which triggers the onset of the disease phenotype, but it may contribute at a later stage to aggravate the disorder.

#### **4.4 TIMP3 interaction with ECM components**

The extracellular matrix is a highly organized structure consisting of a complex mixture of proteins and polysaccharides which has not only a structural scaffolding role but also biochemical signalling properties. All of the biochemical components of the ECM are secreted locally by resident cells and there is a reciprocal influence. The interplay of cells with the surrounding matrix is mediated by cell surface receptors and coreceptors which modulate cell behaviour. Thus, upon receiving a specific signal, the cell can proliferate, migrate, differentiate, enter apoptosis or undergo morphogenesis.

One of the major protein components of extracellular matrix are members of the large collagen family, originally thought to be only involved in the maintenance of the structural integrity of tissues and organs. Recently, it has become apparent that different types of collagens have a more complex function than simply scaffolding. Non-collagenous fragments of collagens IV, XV and XVIII can influence angiogenesis, tumourigenesis, proliferation, apoptosis or survival and suppresses various morphogenetic pathways (Ortega & Werb, 2002; Davis *et al.*, 2000; O'Reilly *et al.*, 1997).

As the prime molecular mechanism which gives rise to the characteristics of SFD is still not fully understood, a search for new interacting partners for TIMP3 was undertaken in an attempt to gain insight into the pathomechanism of SFD. As the collagens are the

major insoluble fibrous protein component of the extracellular matrix and TIMP3 is the only family member which tightly binds to the ECM it seemed reasonable to analyse the interaction of TIMP3 with different collagens. The binding of TIMP3 to collagens was performed both in solution and with the collagens immobilized by adsorption to a solid surface. Using both procedures TIMP3 showed binding to five different types of collagen. Unexpectedly, when performing the same experiment using negative controls for TIMP3 binding (BSA and TTR), TIMP3 also bound to the negative control proteins as well. In an effort to dissect the molecular basis for this apparent unspecific binding of TIMP3 to the BSA, the two domains of TIMP3 (C-terminal and N-terminal) were expressed separately, purified and refolded. Analysis of the binding of TIMP3 domains to collagens and BSA revealed that the C-terminal domain was responsible for this apparent unspecific binding, while the N-terminal did not contribute significantly to the interaction. Interestingly, the C-terminal domain of TIMP3 bound to collagen with higher affinity than the full length protein. Therefore, the binding of TIMP3 to different ECM molecules is mediated by the C-terminal domain of the inhibitor. In this context, in the literature it has been described that TIMP3 heterologously expressed in mammalian cells was able to bind to elastin, laminin, fibronectin, collagen type I and IV, but the negative control represented by an unrelated protein was omitted (Majid *et al.*, 2006). Recently, a yeast two hybrid screen has identified TIMP3 as a strong binding partner for EFEMP1 (Klenotic *et al.*, 2004) and the binding between the two proteins was confirmed in solution by coimmunoprecipitation. This interaction is also mediated by the C-terminal domain of TIMP3. The authors of this report found the interaction between TIMP3 and EFEMP1 interesting because the EFEMP1 is mutated in another retinal degenerative disease (Malattia Leventinese or Doyne honeycomb retinal dystrophy) which shares a common pathological phenotype with SFD despite differing underlying molecular defects. However, in the absence of a negative control to which TIMP3 does not bind it is difficult to interpret the significance of these interactions.

#### **4.5 S156C-TIMP3 mutant oligomerization and aggregation**

Most of the SFD causing mutations in the TIMP3 molecule generate free cys residues, and all are localized to the C-terminal region of the inhibitor. For secreted proteins in the extracellular space formation of disulfide bonds between cysteine residues are important to stabilize the correctly folded conformation of proteins (Raina & Missiakas, 1997). Therefore, a free cysteine residue in the TIMP3 molecule could

potentially disturb folding of the protein either by intrachain non-native disulfide bond formation or by building up oligomeric structures via intermolecular disulfide bonds. Several independent TIMP3 mutant molecules have been expressed in a variety of cells for analyzing disulfide linked oligomerization. Thus, S156C, G166C, G167C, Y168C and S181C mutant TIMP3 have been expressed in COS-7 cells (Langton *et al.*, 1998; Langton *et al.*, 2000) or baby hamster kidney (BHK) cells (Yeow *et al.*, 2002). Using this mammalian overexpression system it has been shown that these TIMP3 mutants are able to form dimers and oligomers. In contrast, expression of the S156C-TIMP3 mutant in ARPE-19 cells failed to demonstrate higher molecular weight complexes (Qi *et al.*, 2002) however, analysis of endogenous mutant TIMP3 under control of the natural promoter revealed that mutant TIMP3 forms high molecular weight complexes both in the patients fibroblasts (Arris *et al.*, 2003; Weber *et al.*, 2002) and fibroblasts derived from mice carrying S156C mutation (Weber *et al.*, 2002; Soboleva *et al.*, 2003). In this study further evidence is presented for the existence of disulfide bond mediated dimers in fibroblasts from the mutant mouse. As well as TIMP3 dimers aggregates of mutant TIMP3 can be observed at the top of the gel and which can be converted to the monomeric form by adding a reducing agent. This proves that the formation of aggregated protein is mediated by interchain disulfide bonds. This implies that the high molecular weight complexes are a common feature of the SFD associated TIMP3 mutants, which is a widely accepted pathological characteristic of the SFD.

As it has been shown so far that the mutant TIMP3 retains its normal biological functions, it was reasonable to analyze the functional consequences of the oligomeric structure of the mutant TIMP3. Quantification of mutant TIMP3 protein both in ECM and in cells revealed that a possible consequence of oligomerization is accumulation of the mutant TIMP3 in higher amounts than in WT-TIMP3 fibroblasts. The amount of mutant TIMP3 was elevated in both KI heterozygous and KI heterozygous animals, but there was no significant difference in levels between the two S156C knock-in cell lines. Furthermore, determination of TIMP3 turnover in the ECM showed that in the two KI cell lines the mutant TIMP3 is degraded at a slower rate than the wild-type protein, a result that is supported by another report (Langton *et al.*, 2005) although in these experiments heterologously expressed mutant TIMP3 was used. The present data suggest that the mutation in the TIMP3 molecule causes an impairment of turnover of TIMP3 in the ECM and leads to its accumulation. This conclusion is supported by the fact that at transcriptional level the mutation in the TIMP3 gene does not have any

effect on the transcript production (Chong *et al.*, 2003) so that the probable explanation for the higher amounts of mutant TIMP3 found in the two compartments is that the protein is aggregated and is resistant to proteolytic degradation.

The accumulation of protein aggregates intracellularly and in the extracellular matrix is a predominant feature of many age related neurodegenerative diseases including Alzheimer's, Parkinson's, Huntington's, Prion (Haass & Solkoe, 2007) and amyotrophic lateral sclerosis (Bruns & Kopito, 2007). Protein aggregates are oligomeric complexes of non-native conformers that arise from non-native homomeric or heteromeric interactions (Wetzel, 1994; Haase-Pettingell & King, 1998; Kopito, 2000). The aggregated proteins can further organise in higher order structures which are microscopically distinct cellular regions into which aggregated proteins are sequestered (inclusion bodies) (Kopito, 2000) which are sometimes called aggresomes (Johnston *et al.*, 1998). Besides the major aggregated protein species the aggresome contains other molecules including the chaperone Hsc70, the Hsp40 proteins Hdj1 and Hdj2, the chaperonin TriC/TCP (García-Mata *et al.*, 1999; Wigley *et al.*, 1999) and proteasome subunits 19S and 26S (Wójcik *et al.*, 1996; Wójcik 1997; Fabunmi *et al.*, 2000; Antón *et al.*, 1999). Microscopically, aggresomes are usually localized in a pericentriolar structure, in close proximity to the nucleus (Johnston *et al.*, 1998, Laszlo *et al.*, 1991; Vidair *et al.*, 1996; Brown *et al.*, 1994). Protein aggregates associated with neurodegenerative diseases and deposited in the form of inclusion bodies can lead to impairment of the Ubiquitin-Proteasome System (UPS) (Bence *et al.*, 2001). The UPS plays an important role in the maintenance of cellular quality control by degrading missfolded, unassembled or damaged proteins (Ciechanover *et al.*, 2000). Impairment of UPS function by aggregation-prone proteins has been observed in a number of neurodegenerative diseases including a huntingtin fragment containing a pathogenic polyglutamine repeat and a folding mutant of cystic fibrosis transmembrane conductance regulator (Bence *et al.*, 2001; Bennett *et al.*, 2005; Bennett *et al.*, 2007). Mutations linked to autosomal dominant retinitis pigmentosa results in the production of a missfolded and highly aggregation-prone form of rhodopsin that can inhibit UPS function (Saliba *et al.*, 2002; Illing *et al.*, 2002; Rajan & Kopito, 2005). This would suggest that retinal degeneration may share common pathogenic features with other adult onset degenerative diseases of the central nervous system.

The results from the present study demonstrate that the biological functions of TIMP3 are not affected by S156C mutation in TIMP3 molecules associated with SFD. On the other hand, the consequence of the mutation can be observed in protein missfolding which leads to aggregation of mutant TIMP3 and finally to accumulation in the cell and in the extracellular matrix. Taken together, it seems plausible to suggest that the pathomechanism is not due to a loss-of-function, but rather a toxic gain-of-function and it can be supposed that TIMP3 might be missfolded and accumulate in the ECM. Therefore, it is reasonable to propose that the missfolded form of mutant TIMP3 is the initial major cause of the SFD disorder. This possibility would classify SFD in the category of conformational diseases (Kopito & Ron, 2000) specific for neurodegenerative disorders.

In summary, this work addresses the question of whether the effect of the Ser156Cys-TIMP3 mutant in SFD is due to haploinsufficiency or a dominant negative effect. Examination of the inhibitory activity of TIMP3 mutant towards the MMPs, ADAMTS4/ADAMTS5 and TACE indicates that the pathogenic mutation has no effect on the enzymatic activities, implying that the mutation has a dominant negative effect. This assumption is supported experimentally when the turnover of mutant TIMP3 vs. WT TIMP3 is compared; the mutated TIMP3 tends to form higher molecular weight oligomers, accumulates in the cell and ECM and appears to be significantly more resistant to ECM turnover.

Further studies are required to completely elucidate the SFD pathomechanism and the primary molecular events which trigger initiation of the disease. Identifying the initial molecular processes involved in SFD pathology could potentially indicate therapeutic target(s) and facilitate the development of an effective therapeutic agent which could slow down or stop disease progression. One molecular mechanism which needs further investigation is the protein accumulation/aggregation of mutant TIMP3 and its consequences on SFD pathology. If the protein aggregation plays a role in the pathomechanism of SFD that would not be surprising as a number of neurodegenerative diseases have this molecular cause.

## 5. Summary

Sorsby fundus dystrophy (SFD) is an autosomal dominant disorder of the central retina (Sorsby *et al.*, 1949). It is characterized by subretinal neovascularization, atrophy of the retinal pigment epithelium and the choriocapillaris. It is a progressive disorder leading ultimately to blindness. Mutations in the TIMP3 molecule have been linked to SFD (Weber *et al.*, 1994). So far, several point mutations have been identified in the TIMP3 molecule, all localized at the C-terminal domain of the inhibitor, the majority of which result in a single unpaired cysteine residue in the mature protein. TIMP3 belongs to a family of secreted proteins comprising four members (TIMP1, -2, -3, -4). TIMP3 is ECM (extracellular matrix) bound inhibitor with a molecular mass of 24 kDa having 12 conserved Cys residues consisting of two domains which fold independently with 3 disulfide bonds in each domain.

TIMP3 is a multifunctional protein involved in the inhibition of matrix metalloproteinases (MMPs) (Murphy *et al.*, 1994). It can block the TACE (tumour necrosis factor (TNF)- $\alpha$  converting enzyme) (or ADAM17 - a disintegrin and metalloproteinase) mediated ectodomain shedding of pro-TNF- $\alpha$  (Amour *et al.*, 1998), Syndecan-1 and Syndecan-4 (Fitzgerald *et al.*, 2000), L-selectin (Borland *et al.*, 1999), and interleukin-6 receptor (Hargreaves *et al.*, 1998). TIMP3 is also involved in the inhibition of the ADAMTSs (a disintegrin-like and metalloproteinase with thrombospondin type 1 motif) especially ADAMTS4, ADAMTS5 (Kashiwagi *et al.*, 2001) and ADAMTS2 (Wang *et al.*, 2006). TIMP3 also blocks angiogenesis by binding to VEGFR2 (vascular endothelial growth factor receptor 2) (Qi *et al.*, 2003) and also interacts with EFEMP1 (epithelial growth factor-containing fibulin-like extracellular matrix protein 1) (Klenotic *et al.*, 2004).

TIMP3 is unique among the TIMPs in that it can inhibit TACE mediated TNF- $\alpha$  shedding. We have measured TACE activity in liver extracts from mice deficient for the TIMP3 gene using cleavage of a fluorogenic substrate and found increased TACE activity. We were also interested to analyse the influence of the SFD mutation on the inhibition of TACE activity. The S156C mutation in the C-terminal domain of TIMP3 does not lead to significant modification of the inhibitory activity towards TACE as measured in this assay.

Another biological function of TIMP3 is its ability to block ADAMTS4/ADAMTS5 (aggrecanase-1, aggrecanase-2) and MMPs mediated cleavage of aggrecan (Kashiwagi *et al.*, 2001). TIMP3 influence on Aggrecan cleavage can be monitored by so-called

neopeptide antibodies – which recognize the newly created epitope after cleavage of the aggrecan by ADAMTS4/ADAMTS5 or MMPs. In a cell-based ELISA using chondrocytes it was found that cleavage activity of ADAMTS4/ADAMTS5 and MMPs towards aggrecan are not affected either in TIMP3 knock-out (KO) chondrocytes or S156C-TIMP3 knock-in (KI) chondrocytes compared to WT counterparts.

It has been also demonstrated that TIMP3 is able to block angiogenesis by competing with VEGF for binding to VEGFR2 (Qi *et al.*, 2003). We have also used recombinant proteins to analyse the antiangiogenic property of TIMP3 via its known function of competing with VEGF ligand for its receptor (VEGFR2). The results demonstrate that the S156C mutation in the TIMP3 molecule does not have a significant effect on its capacity to bind VEGFR2 compared to WT recombinant protein.

As the pathomechanism of SFD is still unknown it seemed reasonable to search for new interacting partners which might help gain insight into the molecular basis of the disease. In this context, the ability of TIMP3 to bind several different types of collagens was tested. In an ELISA, recombinant TIMP3 was able to bind to five different types of collagens in a concentration dependence manner. In parallel, TIMP3 interacted with BSA and another unrelated protein (TTR), indicating that the interactions are apparently unspecific. These interactions are mediated by the C-terminal domain of TIMP3.

Cysteine residues are required for the formation of disulfide bonds which stabilize the folded conformation of proteins (Raina *et al.*, 1997). Therefore, a free cysteine residue in the TIMP3 molecule could potentially disturb folding of the protein. To analyse this hypothesis we have performed western blotting and detected higher molecular weight complexes caused by intermolecular disulfide bonds. As fibroblasts from the S156C KI mouse were available we quantified the amount of mutant TIMP3 in heterozygous and homozygous immortalized cell lines. ELISA results showed increased amounts of the mutant protein compared to the WT in both the ECM and cells. We next tested if the accumulation of mutant protein is due to increased resistance of the misfolded protein to proteolytic degradation. TIMP3 turnover in the ECM, determined by ELISA, revealed that S156C-TIMP3 mutant does indeed have a slower turnover compared to the WT.

These results indicate that the pathomechanism of SFD is not due to a loss-of-function, but rather a toxic gain-of-function caused by accumulation of misfolded mutant TIMP3 in the ECM. Therefore, it is reasonable to conclude that the oligomeric form of TIMP3 is the major cause of the SFD disorder. This would classify SFD in the category of conformational diseases specific for the neurodegenerative disorders.

## 6. Appendix

### Abbreviations

ADAM	A disintegrin and metalloproteinase
ADAM-TS	ADAM with thrombospondin motifs
AMD	Age-related macular degeneration
Amp	Ampicillin
APS	Ammonium persulfate
A <sub>x</sub>	Absorption at x nm
bp	Base pairs
BSA	Bovine serum albumin
CD	Catalytic domain
cDNA	Complementary DNA
DAPI	4',6-Diamidin-2'-phenylindol-dihydrochloride
DMSO	Dimethylsulfoxide
DNA	Deoxyribonucleic acid
dNTPs	Deoxynucleotide triphosphates
ECM	Extracellular matrix
EDTA	Ethylenediaminetetraacetic acid
ELISA	Enzyme-linked immunosorbent assay
FRET	Fluorescence resonance energy transfer
GFP	Green fluorescent protein
GST	Glutathione S-transferase
GusB	β-glucuronidase
Het	Heterozygous
Hom	Homozygous
IMAC	Immobilized metal affinity chromatography
IPTG	Isopropyl-β-D-thiogalactopyranoside
K <sub>D</sub>	Dissociation constant
kDa	Kilo Dalton
KI	Knock-in
KO	Knock-out
LB	Luria Bertani



MMP	Matrix metalloproteinase
MOPS	Morpholinepropanesulfonic acid
Ni-NTA	Nickel-nitrilo triacetic acid
OD <sub>x</sub>	Optical density at x nm
PBS	Phosphate buffered saline
PCR	Polymerase chain reaction
PVDF	Polyvinylidene difluoride
RNA	Ribonucleic acid
RPE	Retinal pigment epithelium
rpm	Revolutions per minute
SDS-PAGE	Sodium dodecylsulfate polyacrylamide gel electrophoresis
TACE	TNF- $\alpha$ converting enzyme
TEMED	N,N,N',N'-tetramethylene diamine
TIMPs	Tissue inhibitor of matrix-metalloproteinases
TNF- $\alpha$	Tumour necrosis factor alpha
Tris	Tris-(hydroxymethyl)-aminomethane
U	Unit (measure of enzyme activity)
v/v	Volume per volume
VEGF	Vascular endothelial growth factor
VEGFR2	Vascular endothelial growth factor receptor II
w/v	Weight per volume
WT	Wildtype
$\beta$ -ME	$\beta$ -mercaptoethanol

### List of oligodeoxynucleotides used in the present study

#### Sequencing primers

pCEP4_new-F	5'-GGACTTTCCAAAATGTCGTAATAA-3'
pCEP4_new-R	5'-CAAATAAAGCAATAGCATCACAAAT-3'
pET_F	5'-ATACGACTCACTATAGGGG-3'
pET_R	5'-TAGTTATTGCTCAGCGGTG-3'
M13-F	5'-CGCCAGGGTTTTCCCAGTCACGAC-3'
M13-R	5'-AGCGGATAACAATTTTCACACAGGA-3'

Seq_p_pEGFP-C1_F	5'-AATGTCGTAACAACACTCCGCC-3'
Seq_p_pEGFP-C1_R	5'-TATGTTTCAGGTTTCAGGGGG-3'
pcDNA3-R	5'-TAGGGCCCTCTAGATGCATG-3'
pcDNA3-F2	5'-CACTGCTTACTGGCTTATCG-3'
pGEX_F	5'-GGGCTGGCAAGCCACGTTTG-3'
pGEX-R	5'-CCGGGAGCTGCATGTGTCAGAGG-3'
pFLAG-F	5'-CGTGTACGGTGGGAGGTCTA-3'
pFLAG-R	5'-TTATTAGGACAAGGCTGGTG-3'
RT-PCR primers	
Sq_Agc_F	5'-GTCCCCTGCAATTACCAGC-3'
RT_Agc_R	5'-GCCTGTGCTTGTAGGTGTTG-3'
Sq_Adamts4_F	5'-GCACTGGGCTACTACTACG-3'
RT_Adamts4_R	5'-GGCCAGGTAGATGCTCTTGA-3'
Sq_Adamts5_F	5'-GAGAACTGGATGTGACGGC-3'
Sq_Adamts5_R	5'-CGGTACCATTGATGTGCGATG-3'
GUSB3	5'-ACTATCGCCATCAACAACACTGACC-3'
GUSB5R	5'-GTGACGGTGATGTCATCGAT-3'
Cloning primers	
Timp1_N_F	5'-GCTAGCCATATGTGTAGCTGTGCCCCACCC-3'
Timp1_C_R	5'-GCTAGCCTCGAGTCGGGCCCAAGGGATCTC-3'
Timp2_N_F	5'-GCTAGCCATATGTGCAGCTGCTCCCCGGTG-3'
Timp2_C_R	5'-GCTAGCCTCGAGCGGGTCCTCGATGTCAAG-3'
Timp3_N_F	5'-GCTAGCCATATGTGCACATGCTCTCCCAGCC-3'
Timp3_N_R	5'-GCTAGCCTCGAGATTGCAACCCAGGTGGTAGC-3'
Timp3_C_F	5'-GCTAGCCATATGTGCAAGATCAAGTCCTGC-3'
Timp3_C_R	5'-GCTAGCCTCGAGGGGATCTGTGGCGTTGCTG-3'
Timp4_N_F	5'-GCTAGCCATATGTGCAGCTGTGCGCCTGCG-3'
Timp4_C_R	5'-GCTAGCCTCGAGGGGCTGGATGATGTCAACG-3'
TACE_CD_pET_F	5'-GACGCTCATATGCGAGCTGAACCTAACCCCTTG-3'
TACE_CD_pET_R	5'-GGCAGCCTCGAGCACCTTGTTGCTGCGCTCC-3'
Pept_GA_F	5'-CCGCGTGGATCCGGGGTGGGTGGTGAAGACG-3'

Pept\_GA\_R            5'-  
 CACGATGCGGCCGCTCAAGGGGCAAGTGTGAGGGCC-3'  
 Pept\_Gm\_F            5'-CCGCGTGGATCCGGGGTGGGTGGTGAAGACG-3'  
 Pept\_Gm\_R            5'-  
 CACGATGCGGCCGCTCACTCTCCCTCTGTGACATTAC-3'  
 Pept\_Gh\_F            5'-CCGCGTGGATCCCATCACCGTCCAGACAGTG-3'  
 Pept\_Gh\_R            5'-  
 CACGATGCGGCCGCTCATTACCCTCAGTGATGTTTCG-3'  
 MMP13\_F            5'-GTAGCTAGCTATGGTGATGATGATGATGATGACC-3'  
 MMP13\_R            5'-CTACTCGAGACACCACAATATGGAATTTGTTGGC-3'  
 Agc\_E\_F            5'-CCGCGTGGATCCTCTGTTTCTGGGGTAGGTG-3'  
 Agc\_E\_R            5'-  
 CACGATGCGGCCGCTCAACTAATGTCCGCACTACTGTC-3'  
 Adamts4\_E\_F        5'-CCGCGTGGATCCGCTGCCTACAACCACCGAAC-3'  
 Adamts4\_E\_R        5'-CACGATGCGGCCGCTCATTGGTCTCGAGGGGCC-3'

#### List of plasmids employed in the study

pET-21a(+)	Novagen; Studier <i>et al.</i> , 1990
pLysS	Novagen, Studier <i>et al.</i> , 1990
pGEX-4T3	Amersham Biosciences
pGEM	Promega
pcDNA3	Invitrogen
pCEP4	Invitrogen
pEGFP-C1	Clontech
pFLAG-CMV	Sigma

## 7. References

- Alberts B, Johnson A, Lewis J, Raff M, Watson J.** 1994. Molecular Biology of the Cell. 3<sup>rd</sup> edition
- Ahonen M, Baker AH, Kähäri VM.** 1998. Adenovirus-mediated gene delivery of tissue inhibitor of metalloproteinases-3 inhibits invasion and induces apoptosis in melanoma cells. *Cancer Res.* **58**, 2310-2315

- Ahonen M, Poukkula M, Baker AH, Kashiwagi M, Nagase H, Eriksson JE, Kahari VM.** 2003. Tissue inhibitor of metalloproteinases-3 induces apoptosis in melanoma cells by stabilization of death receptors. *Oncogene*. **22**, 2121-2134.
- Ambati J, Anand A, Fernandez S, Sakurai E, Lynn BC, Kuziel WA, Rollins BJ, Ambati BK.** 2003. An animal model of age-related macular degeneration in senescent Ccl-2- or Ccr-2-deficient mice. *Nat Med*. **9**, 1390-1397
- Amour A, Knight CG, Webster A, Slocombe PM, Stephens PE, Knäuper V, Docherty AJ, Murphy G.** 2000. The *in vitro* activity of ADAM-10 is inhibited by TIMP-1 and TIMP-3. *FEBS Lett*. **473**, 275-279.
- Amour A, Slocombe PM, Webster A, Butler M, Knight CG, Smith BJ, Stephens PE, Shelley C, Hutton M, Knäuper V, Docherty AJ, Murphy G.** 1998. TNF-alpha converting enzyme (TACE) is inhibited by TIMP-3. *FEBS Lett*. **435**, 39-44.
- Anand-Apte B, Pepper MS, Voest E, Montesano R, Olsen B, Murphy G, Apte SS, Zetter B.** 1997. Inhibition of angiogenesis by tissue inhibitor of metalloproteinase-3. *Invest Ophthalmol Vis Sci*. **38**, 817-823.
- Antón LC, Schubert U, Bacík I, Princiotta MF, Wearsch PA, Gibbs J, Day PM, Realini C, Rechsteiner MC, Bennink JR, Yewdell JW.** 1999. Intracellular localization of proteasomal degradation of a viral antigen. *J Cell Biol*. **146**, 113-124.
- Apte SS.** 2004. A disintegrin-like and metalloprotease (reprolysin type) with thrombospondin type 1 motifs: the ADAMTS family. *Int J Biochem Cell Biol*. **36**, 981-985.
- Apte SS, Hayashi K, Seldin MF, Mattei MG, Hayashi M, Olsen BR.** 1994a. Gene encoding a novel murine tissue inhibitor of metalloproteinases (TIMP), TIMP-3, is expressed in developing mouse epithelia, cartilage, and muscle, and is located on mouse chromosome 10. *Dev Dyn*. **200**, 177-197.
- Apte SS, Mattei MG, Olsen BR.** 1994b. Cloning of the cDNA encoding human tissue inhibitor of metalloproteinases-3 (TIMP-3) and mapping of the TIMP3 gene to chromosome 22. *Genomics*. **19**, 86-90.

- Arner CE.** 2002. Aggrecanase-mediated cartilage degradation. *Curr Opin Pharmacol.* 2002 **2**, 322-329.
- Arner EC, Pratta MA, Trzaskos JM, Decicco CP, Tortorella MD.** 1999. Generation and characterization of aggrecanase. A soluble, cartilage-derived aggrecan-degrading activity. *J Biol Chem.* **274**, 6594-6601.
- Arris CE, Bevitt DJ, Mohamed J, Li Z, Langton KP, Barker MD, Clarke MP, McKie N.** 2003. Expression of mutant and wild-type TIMP3 in primary gingival fibroblasts from Sorsby's fundus dystrophy patients. *Biochim Biophys Acta.* **1638**, 20-28.
- Bachman KE, Herman JG, Corn PG, Merlo A, Costello JF, Cavenee WK, Baylin SB, Graff JR.** 1999. Methylation-associated silencing of the tissue inhibitor of metalloproteinase-3 gene suggest a suppressor role in kidney, brain, and other human cancers. *Cancer Res.* **59**, 798-802.
- Baker AH, George SJ, Zaltsman AB, Murphy G, Newby AC.** 1999. Inhibition of invasion and induction of apoptotic cell death of cancer cell lines by overexpression of TIMP-3. *Br J Cancer.* **79**, 1347-55
- Baker AH, Zaltsman AB, George SJ, Newby AC.** 1998. Divergent effects of tissue inhibitor of metalloproteinase-1, -2, or -3 overexpression on rat vascular smooth muscle cell invasion, proliferation, and death *in vitro*. TIMP-3 promotes apoptosis. *J Clin Invest.* **101**, 1478-1487
- Bank U, Ansoorge S.** 2001. More than destructive: neutrophil-derived serine proteases in cytokine bioactivity control. *J Leukoc Biol.* **69**, 197-206.
- Barbazetto IA, Hayashi M, Klais CM, Yannuzzi LA, Allikmets R.** 2005. A novel TIMP3 mutation associated with Sorsby fundus dystrophy. *Arch Ophthalmol.* **123**, 542-543.
- Bauer EA, Stricklin GP, Jeffrey JJ, Eisen AZ.** 1975. Collagenase production by human skin fibroblasts. *Biochem Biophys Res Commun.* **64**, 232-240
- Bence NF, Sampat RM, Kopito RR.** 2001. Impairment of the ubiquitin-proteasome system by protein aggregation. *Science.* **292**, 1552-1555.

- Bennett EJ, Bence NF, Jayakumar R, Kopito RR.** 2005. Global impairment of the ubiquitin-proteasome system by nuclear or cytoplasmic protein aggregates precedes inclusion body formation. *Mol Cell.* **17**, 351-365.
- Bennett EJ, Shaler TA, Woodman B, Ryu KY, Zaitseva TS, Becker CH, Bates GP, Schulman H, Kopito RR.** 2007. Global changes to the ubiquitin system in Huntington's disease. *Nature.* **448**, 704-708.
- Bernfield M, Götte M, Park PW, Reizes O, Fitzgerald ML, Lincecum J, Zako M.** 1999. Functions of cell surface heparan sulfate proteoglycans. *Annu Rev Biochem.* **68**, 729-777.
- Black RA, Rauch CT, Kozlosky CJ, Peschon JJ, Slack JL, Wolfson MF, Castner BJ, Stocking KL, Reddy P, Srinivasan S, Nelson N, Boiani N, Schooley KA, Gerhart M, Davis R, Fitzner JN, Johnson RS, Paxton RJ, March CJ, Cerretti DP.** 1997. A metalloproteinase disintegrin that releases tumour-necrosis factor-alpha from cells. *Nature.* **385**, 729-733.
- Black RA.** 2002. Tumor necrosis factor-alpha converting enzyme. *Int J Biochem Cell Biol.* **34**, 1-5.
- Blenis J, Hawkes SP.** 1983. Transformation-sensitive protein associated with the cell substratum of chicken embryo fibroblasts. *Proc Natl Acad Sci U S A.* **80**, 770-774
- Bond M, Murphy G, Bennett MR, Amour A, Knauper V, Newby AC, Baker AH.** 2000. Localization of the death domain of tissue inhibitor of metalloproteinase-3 to the N terminal. Metalloproteinase inhibition is associated with proapoptotic activity. *J Biol Chem.* **275**, 41358-41363.
- Borland G, Murphy G, Ager A.** 1999. Tissue inhibitor of metalloproteinases-3 inhibits shedding of L-selectin from leukocytes. *J Biol Chem.* **274**, 2810-2815
- Bourguignon LY, Zhu H, Shao L, Chen YW.** 2000. CD44 interaction with tiam1 promotes Rac1 signaling and hyaluronic acid-mediated breast tumor cell migration. *J Biol Chem.* **275**, 1829-1838.
- Brannan CI, Lyman SD, Williams DE, Eisenman J, Anderson DM, Cosman D, Bedell MA, Jenkins NA, Copeland NG.** 1991. Steel-Dickie mutation encodes a

- c-kit ligand lacking transmembrane and cytoplasmic domains. *Proc Natl Acad Sci U S A.* **88**, 4671-4674.
- Brown CR, Doxsey SJ, White E, Welch WJ.** 1994. Both viral (adenovirus E1B) and cellular (hsp 70, p53) components interact with centrosomes. *J Cell Physiol.* **160**, 47-60.
- Bruns CK, Kopito RR.** 2007. Impaired post-translational folding of familial ALS-linked Cu, Zn superoxide dismutase mutants. *EMBO J.* **26**, 855-866
- Buschmann I, Schaper W.** 1999. Arteriogenesis Versus Angiogenesis: Two Mechanisms of Vessel Growth. *News Physiol Sci.* **14**, 121-125.
- Bussolino F, Mantovani A, Persico G.** 1997. Molecular mechanisms of blood vessel formation. *Trends Biochem Sci.* **22**, 251-256
- Bzowska M, Jura N, Lassak A, Black RA, Bereta J.** 2004. Tumour necrosis factor-alpha stimulates expression of TNF-alpha converting enzyme in endothelial cells. *Eur J Biochem.* **271**, 2808-2820.
- Cao J, Sato H, Takino T, Seiki M.** 1995. The C-terminal region of membrane type matrix metalloproteinase is a functional transmembrane domain required for pro-gelatinase A activation. *J Biol Chem.* **270**, 801-805.
- Carmeliet P.** 2005. Angiogenesis in life, disease and medicine. *Nature.* **438**, 932-936.
- Caterson B, Flannery CR, Hughes CE, Little CB.** 2000. Mechanisms involved in cartilage proteoglycan catabolism. *Matrix Biol.* **19**, 333-344.
- Chambers MG, Cox L, Chong L, Suri N, Cover P, Bayliss MT, Mason RM.** 2001. Matrix metalloproteinases and aggrecanases cleave aggrecan in different zones of normal cartilage but colocalize in the development of osteoarthritic lesions in STR/ort mice. *Arthritis Rheum.* **44**, 1455-1465.
- Chen C, Okayama H.** 1987. High-efficiency transformation of mammalian cells by plasmid DNA. *Mol Cell Biol.* **7**, 2745-2752.
- Chen G, Goeddel DV.** 2002. TNF-R1 signaling: a beautiful pathway. *Science.* **296**, 1634-1635.

- Ciechanover A, Orian A, Schwartz AL.** 2000. Ubiquitin-mediated proteolysis: biological regulation via destruction. *Bioessays*. **22**, 442-451.
- Clark IM, Parker AE.** 2003. Metalloproteinases: their role in arthritis and potential as therapeutic targets. *Expert Opin Ther Targets*. **7**, 19-34.
- Clarke M, Mitchell KW, Goodship J, McDonnell S, Barker MD, Griffiths ID, McKie N.** 2001. Clinical features of a novel TIMP-3 mutation causing Sorsby's fundus dystrophy: implications for disease mechanism. *Br J Ophthalmol*. **85**, 1429-1431.
- Colognato H, Yurchenco PD.** 2000. Form and function: the laminin family of heterotrimers. *Dev Dyn*. **218**, 213-234.
- Contin C, Pitard V, Itai T, Nagata S, Moreau JF, Dechanet-Merville J.** 2003. Membrane-anchored CD40 is processed by the tumor necrosis factor-alpha-converting enzyme. Implications for CD40 signaling. *J Biol Chem*. **278**, 32801-32809.
- Cousins SW, Espinosa-Heidmann DG, Csaky KG.** 2004. Monocyte activation in patients with age-related macular degeneration: a biomarker of risk for choroidal neovascularization? *Arch Ophthalmol*. **122**, 1013-1018.
- Cruz AC, Frank BT, Edwards ST, Dazin PF, Peschon JJ, Fang KC.** 2004. Tumor necrosis factor-alpha-converting enzyme controls surface expression of c-Kit and survival of embryonic stem cell-derived mast cells. *J Biol Chem*. **279**, 5612-5620
- Davis GE, Bayless KJ, Davis MJ, Meininger GA.** 2000. Regulation of tissue injury responses by the exposure of matricryptic sites within extracellular matrix molecules. *Am J Pathol*. **156**, 1489-1498.
- Debelle L, Tamburro AM.** 1999. Elastin: molecular description and function. *Int J Biochem Cell Biol*. **31**, 261-272.
- Devarajan, P., Mookhtiar, K., Van Wart, H. and Berliner, N.** 1991. Structure and expression of the cDNA encoding human neutrophil collagenase. *Blood* **77**, 2731-2738.



- Docherty AJ, Lyons A, Smith BJ, Wright EM, Stephens PE, Harris TJ, Murphy G, Reynolds JJ.** 1985. Sequence of human tissue inhibitor of metalloproteinases and its identity to erythroid-potentiating activity. *Nature*. **318**, 66-69.
- d'Ortho MP, Will H, Atkinson S, Butler G, Messent A, Gavrilovic J, Smith B, Timpl R, Zardi L, Murphy G.** 1997. Membrane-type matrix metalloproteinases 1 and 2 exhibit broad-spectrum proteolytic capacities comparable to many matrix metalloproteinases. *Eur J Biochem*. **250**, 751-757.
- Downs JT, Lane CL, Nestor NB, McLellan TJ, Kelly MA, Karam GA, Mezes PS, Pelletier JP, Otterness IG.** 2001. Analysis of collagenase-cleavage of type II collagen using a neoepitope ELISA. *J Immunol Methods*. **247**, 25-34.
- English WR, Puente XS, Freije JM, Knauper V, Amour A, Merryweather A, Lopez-Otin C, Murphy G.** 2000. Membrane type 4 matrix metalloproteinase (MMP17) has tumor necrosis factor-alpha convertase activity but does not activate pro-MMP2. *J Biol Chem*. **275**, 14046-14055.
- Evanko SP, Angello JC, Wight TN.** 1999. Formation of hyaluronan- and versican-rich pericellular matrix is required for proliferation and migration of vascular smooth muscle cells. *Arterioscler Thromb Vasc Biol*. **19**, 1004-1013.
- Fabunmi RP, Wigley WC, Thomas PJ, DeMartino GN.** 2000. Activity and regulation of the centrosome-associated proteasome. *J Biol Chem*. **275**, 409-413.
- Fadeel B, Orrenius S, Zhivotovsky B.** 1999. Apoptosis in human disease: a new skin for the old ceremony? *Biochem Biophys Res Commun*. **266**, 699-717.
- Fan H, Derynck R.** 1999. Ectodomain shedding of TGF-alpha and other transmembrane proteins is induced by receptor tyrosine kinase activation and MAP kinase signaling cascades. *EMBO J*. **18**, 6962-6972.
- Fata JE, Leco KJ, Voura EB, Yu HY, Waterhouse P, Murphy G, Moorehead RA, Khokha R.** 2001. Accelerated apoptosis in the Timp-3-deficient mammary gland. *J Clin Invest*. **108**, 831-841.

- Fedak PW, Smookler DS, Kassiri Z, Ohno N, Leco KJ, Verma S, Mickle DA, Watson KL, Hojilla CV, Cruz W, Weisel RD, Li RK, Khokha R.** 2004. TIMP-3 deficiency leads to dilated cardiomyopathy. *Circulation*. **110**, 2401-2409.
- Felbor U, Stohr H, Amann T, Schonherr U, Weber BH.** 1995. A novel Ser156Cys mutation in the tissue inhibitor of metalloproteinases-3 (TIMP3) in Sorsby's fundus dystrophy with unusual clinical features. *Hum Mol Genet*. **4**, 2415-2416
- Felbor U, Suvanto EA, Forsius HR, Eriksson AW, Weber BH.** 1997. Autosomal recessive Sorsby fundus dystrophy revisited: molecular evidence for dominant inheritance. *Am J Hum Genet*. **1** 57-62.
- Ferrara F.** 1995. The role of vascular endothelial growth factor in pathological angiogenesis. *Breast Cancer Research and Treatment* **36**, 127-137
- Ferrara N.** 2002. VEGF and the quest for tumour angiogenesis factors. *Nat Rev Cancer*. **2**, 795-803
- Ferrara N, Gerber HP, LeCouter J.** 2003. The biology of VEGF and its receptors. *Nat Med*. **9**, 669-676.
- Fitzgerald ML, Wang Z, Park PW, Murphy G, Bernfield M.** 2000. Shedding of syndecan-1 and -4 ectodomains is regulated by multiple signaling pathways and mediated by a TIMP3-sensitive metalloproteinase. *J Cell Biol*. **148**, 811-824
- Flannery CR, Lark MW, Sandy JD.** 1992. Identification of a stromelysin cleavage site within the interglobular domain of human aggrecan: evidence for proteolysis at this site *in vivo* in human articular cartilage. *J Biol Chem* **267**, 1008-1014.
- Fosang AJ, Last K, Knauper V, Murphy G, Hardingham TE, Tschesche H.** 1993. Fibroblast and neutrophil collagenases cleave at two sites in the cartilage aggrecan interglobular domain. *Biochem J* **295**, 273-6.
- Fosang AJ, Last K, Knauper V, Murphy G, Neame PJ.** 1996. Degradation of cartilage aggrecan by collagenase-3 (MMP13). *FEBS Lett* **380**, 17-20.

- Fosang AJ, Last K, Maciewicz RA.** 1996. Aggrecan is degraded by matrix metalloproteinases in human arthritis. Evidence that matrix metalloproteinase and aggrecanase activities can be independent. *J Clin Invest.* **98**, 2292-2299.
- Fosang AJ, Neame PJ, Last K, Hardingham TE, Murphy G, Hamilton JA.** 1992. The interglobular domain of cartilage aggrecan is cleaved by PUMP, gelatinases, and cathepsin B. *J Biol Chem* **267**, 19470-19474.
- Fosang AJ, Stanton H, Little CB, Atley LM.** 2003. Neopeptides as biomarkers of cartilage catabolism. *Inflamm Res.* **52**, 277-282.
- Franzke CW, Tasanen K, Schacke H, Zhou Z, Tryggvason K, Mauch C, Zigrino P, Sunnarborg S, Lee DC, Fahrenholz F, Bruckner-Tuderman L.** 2002. Transmembrane collagen XVII, an epithelial adhesion protein, is shed from the cell surface by ADAMs. *EMBO J.* **21**, 5026-5035.
- Garcia-Mata R., Bebok Z., Sorscher E.J., Sztul E.S.** 1999. Characterization and dynamics of aggresome formation by a cytosolic GFP- chimera. *Journal of Cell Biology*, 146, 1239-1254.
- Gariano RF and Gardner TW.** 2004. Retinal angiogenesis in development and disease. *Nature* **438**, 960-966
- Garton KJ, Gough PJ, Blobel CP, Murphy G, Greaves DR, Dempsey PJ, Raines EW.** 2001. Tumor necrosis factor-alpha-converting enzyme (ADAM17) mediates the cleavage and shedding of fractalkine (CX3CL1). *J Biol Chem.* **276**, 37993-38001
- Garton KJ, Gough PJ, Philalay J, Wille PT, Blobel CP, Whitehead RH, Dempsey PJ, Raines EW.** 2003. Stimulated shedding of vascular cell adhesion molecule 1 (VCAM-1) is mediated by tumor necrosis factor-alpha-converting enzyme (ADAM 17). *J Biol Chem.* **278**, 37459-37464
- Gendron C, Kashiwagi M, Hughes C, Caterson B, Nagase H.** 2003. TIMP-3 inhibits aggrecanase-mediated glycosaminoglycan release from cartilage explants stimulated by catabolic factors. *FEBS Lett.* **555**, 431-436.

- Greene J, Wang M, Liu YE, Raymond LA, Rosen C, Shi YE.** 1996. Molecular cloning and characterization of human tissue inhibitor of metalloproteinase 4. *J Biol Chem.* 271, 30375-30380.
- Grell M, Douni E, Wajant H, Löhden M, Clauss M, Maxeiner B, Georgopoulos S, Lesslauer W, Kollias G, Pfizenmaier K, Scheurich P.** 1995. The transmembrane form of tumor necrosis factor is the prime activating ligand of the 80 kDa tumor necrosis factor receptor. *Cell.* **83**, 793-802.
- Gu H, Marth JD, Orban PC, Mossmann H, Rajewsky K.** 1994. Deletion of a DNA polymerase beta gene segment in T cells using cell type-specific gene targeting. *Science.* **265**, 103-106.
- Gu H, Zou YR, Rajewsky K.** 1993. Independent control of immunoglobulin switch recombination at individual switch regions evidenced through Cre-loxP-mediated gene targeting. *Cell.* **73**, 1155-1164.
- Haass C, Selkoe DJ.** 2007. Soluble protein oligomers in neurodegeneration: lessons from the Alzheimer's amyloid beta-peptide. *Nat Rev Mol Cell Biol.* **8**, 101-112.
- Haase-Pettingell CA and King J.** 1998. Formation of aggregates from a thermolabile *in vivo* folding intermediate in P22 tailspike maturation. A model for inclusion body formation. *J. Biol. Chem.* **263**, 4977-4983.
- Hansen HP, Dietrich S, Kisseleva T, Mokros T, Mentlein R, Lange HH, Murphy G, Lemke H.** 2000. CD30 shedding from Karpas 299 lymphoma cells is mediated by TNF-alpha-converting enzyme. *J Immunol.* **165**, 6703-6709
- Hargreaves PG, Wang F, Antcliff J, Murphy G, Lawry J, Russell RG, Croucher PI.** 1998. Human myeloma cells shed the interleukin-6 receptor: inhibition by tissue inhibitor of metalloproteinase-3 and a hydroxamate-based metalloproteinase inhibitor. *Br J Haematol.* **101**, 694-702
- Haro H, Crawford HC, Fingleton B, Shinomiya K, Spengler DM, Matrisian LM.** 2000. Matrix metalloproteinase-7-dependent release of tumor necrosis factor-alpha in a model of herniated disc resorption. *J Clin Invest.* **105**, 143-150.
- Harris, Jr. E.D., Krane, S.** 1974a. Collagenases. *N. Engl. J. Med.* **291**, 557-563.

- Harris, Jr. E.D., Krane, S.** 1974b. Collagenases. *N. Engl. J. Med.* **291**, 605–609.
- Harris, Jr. E.D., Krane, S.** 1974c. Collagenases. *N. Engl. J. Med.* **291**, 652–661.
- Hashimoto G, Aoki T, Nakamura H, Tanzawa K, Okada Y.** 2001. Inhibition of ADAMTS4 (aggrecanase-1) by tissue inhibitors of metalloproteinases (TIMP-1, 2, 3 and 4). *FEBS Lett.* **494**, 192-195.
- Hasty KA, Pourmotabbed TF, Goldberg GI, Thompson JP, Spinella DG, Stevens RM, Mainardi CL.** 1990. Human neutrophil collagenase. A distinct gene product with homology to other matrix metalloproteinases. *J Biol Chem.* **265**, 11421-11424
- Herron GS, Banda MJ, Clark EJ, Gavrilovic J, Werb Z.** 1986. Secretion of metalloproteinases by stimulated capillary endothelial cells. II. Expression of collagenase and stromelysin activities is regulated by endogenous inhibitors. *J Biol Chem.* **261**, 2814-2818.
- Hooper NM, Karran EH, Turner AJ.** 1997. Membrane protein secretases. *Biochem J.* **321**, 265-279.
- Illing ME, Rajan RS, Bence NF, Kopito RR.** 2002. A rhodopsin mutant linked to autosomal dominant retinitis pigmentosa is prone to aggregate and interacts with the ubiquitin proteasome system. *J Biol Chem.* **277**, 34150-34160.
- Iozzo RV.** 1998. Matrix proteoglycans: from molecular design to cellular function. *Annu Rev Biochem.* **67**, 609-652.
- Jacobson SG, Cideciyan AV, Bennett J, Kingsley RM, Sheffield VC, Stone EM.** 2002. Novel mutation in the TIMP3 gene causes Sorsby fundus dystrophy. *Arch Ophthalmol.* **120**, 376-379.
- Jacobson SG, Cideciyan AV, Regunath G, Rodriguez FJ, Vandenberg K, Sheffield VC, Stone EM.** 1995. Night blindness in Sorsby's fundus dystrophy reversed by vitamin A. *Nat Genet.* **11**, 27-32.
- Jennifer A. Johnston, Cristina L. Ward, and Ron R. Kopito.** 1998. Aggresomes: A Cellular Response to Misfolded Proteins. *J. Cell Biol.* **143**, 1883-1898

- Kang SH, Choi HH, Kim SG, Jong HS, Kim NK, Kim SJ, Bang YJ.** 2000. Transcriptional inactivation of the tissue inhibitor of metalloproteinase-3 gene by DNA hypermethylation of the 5'-CpG island in human gastric cancer cell lines. *Int J Cancer.* **86**, 632-635.
- Kashiwagi M, Tortorella M, Nagase H, Brew K.** 2001. TIMP-3 is a potent inhibitor of aggrecanase 1 (ADAM-TS4) and aggrecanase 2 (ADAM-TS5). *J Biol Chem.* **276**, 12501-12504
- Klein R, Klein BE, Linton KL.** 1992. Prevalence of age-related maculopathy: The Beaver Dam Eye Study. *Ophthalmology.* **99**, 933-943.
- Klenotic PA, Munier FL, Marmorstein LY, Anand-Apte B.** 2004. Tissue inhibitor of metalloproteinases-3 (TIMP-3) is a binding partner of epithelial growth factor-containing fibulin-like extracellular matrix protein 1 (EFEMP1). Implications for macular degenerations. *J Biol Chem.* **279**, 30469-30473.
- Knäuper V, López-Otin C, Smith B, Knight G, Murphy G.** 1996. Biochemical characterization of human collagenase-3. *J Biol Chem.* **271**, 1544-1550.
- Knight CG, Willenbrock F, Murphy G.** 1992. A novel coumarin-labelled peptide for sensitive continuous assays of the matrix metalloproteinases. *FEBS Lett.* **296**, 263-266.
- Kopito RR, Ron D.** 2000. Conformational disease. *Nat Cell Biol.* **2**, 207-209.
- Kopito RR.** 2000. Aggresomes, inclusion bodies and protein aggregation. *Trends Cell Biol.* **10**, 524-530.
- Kuettner KE, Hiti J, Eisenstein R, Harper E.** 1976. Collagenase inhibition by cationic proteins derived from cartilage and aorta. *Biochem Biophys Res Commun.* **72**, 40-46.
- Langton KP, Barker MD, McKie N.** Localization of the functional domains of human tissue inhibitor of metalloproteinases-3 and the effects of a Sorsby's fundus dystrophy mutation. *J Biol Chem.* **273**, 16778-16781.
- Langton KP, McKie N, Curtis A, Goodship JA, Bond PM, Barker MD, Clarke M.** 2000. A novel tissue inhibitor of metalloproteinases-3 mutation reveals a common

- molecular phenotype in Sorsby's fundus dystrophy. *J Biol Chem.* **275**, 27027-27031.
- Langton KP, McKie N, Smith BM, Brown NJ, Barker MD.** 2005. Sorsby's fundus dystrophy mutations impair turnover of TIMP-3 by retinal pigment epithelial cells. *Hum Mol Genet.* **14**, 3579-3586.
- László L, Tuckwell J, Self T, Lowe J, Landon M, Smith S, Hawthorne JN, Mayer RJ.** 1991. The latent membrane protein-1 in Epstein-Barr virus-transformed lymphoblastoid cells is found with ubiquitin-protein conjugates and heat-shock protein 70 in lysosomes oriented around the microtubule organizing centre. *J Pathol.* **164**, 203-214.
- Leco KJ, Waterhouse P, Sanchez OH, Gowing KL, Poole AR, Wakeham A, Mak TW, Khokha R.** 2001. Spontaneous air space enlargement in the lungs of mice lacking tissue inhibitor of metalloproteinases-3 (TIMP-3). *J Clin Invest.* **108**, 817-829.
- Lee MH, Atkinson S, Murphy G.** 2007. Identification of the extracellular matrix (ECM) binding motifs of tissue inhibitor of metalloproteinases (TIMP)-3 and effective transfer to TIMP-1. *J Biol Chem.* **282**, 6887-6898.
- Lee MH, Knauper V, Becherer JD, Murphy G.** 2001. Full-length and N-TIMP-3 display equal inhibitory activities toward TNF-alpha convertase. *Biochem Biophys Res Commun.* **280**, 945-950.
- Lee MH, Maskos K, Knäuper V, Dodds P, Murphy G.** 2002. Mapping and characterization of the functional epitopes of tissue inhibitor of metalloproteinases (TIMP)-3 using TIMP-1 as the scaffold: a new frontier in TIMP engineering. *Protein Sci.* **11**, 2493-2503.
- Lee MH, Rapti M, Murphy G.** 2004. Delineating the molecular basis of the inactivity of tissue inhibitor of metalloproteinase-2 against tumor necrosis factor-alpha-converting enzyme. *J Biol Chem.* **279**, 45121-45129.
- Lee MH, Rapti M, Murphy G.** 2005. Total conversion of tissue inhibitor of metalloproteinase (TIMP) for specific metalloproteinase targeting: fine-tuning

- TIMP-4 for optimal inhibition of tumor necrosis factor- $\alpha$ -converting enzyme. *J Biol Chem.* **280**, 15967-15975.
- Lee MH, Verma V, Maskos K, Becherer JD, Knauper V, Dodds P, Amour A, Murphy G.** 2002b. The C-terminal domains of TACE weaken the inhibitory action of N-TIMP-3. *FEBS Lett.* **520**, 102-106.
- Lee MH, Verma V, Maskos K, Nath D, Knauper V, Dodds P, Amour A, Murphy G.** 2002a. Engineering N-terminal domain of tissue inhibitor of metalloproteinase (TIMP)-3 to be a better inhibitor against tumour necrosis factor- $\alpha$ -converting enzyme. *Biochem J.* **364**, 227-234.
- Lin RJ, Blumenkranz MS, Binkley J, Wu K, Vollrath D.** 2006. A Novel His158Arg Mutation in TIMP3 Causes a Late-Onset Form of Sorsby Fundus Dystrophy. *Am J Ophthalmol.* **142**, 839-848.
- Little CB, Flannery CR, Hughes CE, Mort JS, Roughley PJ, Dent C, Caterson B.** 1999. Aggrecanase versus matrix metalloproteinases in the catabolism of the interglobular domain of aggrecan *in vitro*. *Biochem J.* **344**, 61-68.
- Little CB, Meeker CT, Hembry RM, Sims NA, Lawlor KE, Golub SB, Last K, Fosang AJ.** 2005. Matrix metalloproteinases are not essential for aggrecan turnover during normal skeletal growth and development. *Mol Cell Biol.* **25**, 3388-3399.
- Loechel F, Fox JW, Murphy G, Albrechtsen R, Wewer UM.** 2000. ADAM 12-S cleaves IGFBP-3 and IGFBP-5 and is inhibited by TIMP-3. *Biochem Biophys Res Commun.* **278**, 511-515.
- Lowry OH, Rosebrough NJ, Farr AL, and Randall RJ.** 1951. Protein measurement with the folin phenol reagent. *J Biol Chem.* **193**, 265-275.
- Lum L, Wong BR, Josien R, Becherer JD, Erdjument-Bromage H, Schlondorff J, Tempst P, Choi Y, Blobel CP.** 1999. Evidence for a role of a tumor necrosis factor- $\alpha$  (TNF- $\alpha$ )-converting enzyme-like protease in shedding of TRANCE, a TNF family member involved in osteoclastogenesis and dendritic cell survival. *J Biol Chem.* **274**, 13613-13618



- Lundberg KS, Shoemaker DD, Adams MW, Short JM, Sorge JA, Mathur EJ.** 1991. High-fidelity amplification using a thermostable DNA polymerase isolated from *Pyrococcus furiosus*. *Gene*. **108**, 1-6.
- Maciewicz, R.A., Wotton, S.F., Etherington, D.J. and Duance, V.C.** 1990. Susceptibility of the cartilage collagens type II, IX and XI to degradation by the cysteine proteinases, cathepsins B and L. *FEBS Lett*. **269**, 189–193.
- Mahmoodi M, Sahebjam S, Smookler D, Khokha R, Mort JS.** 2005. Lack of tissue inhibitor of metalloproteinases-3 results in an enhanced inflammatory response in antigen-induced arthritis. *Am J Pathol*. **166**, 1733-1740.
- Majid MA, Smith VA, Matthews FJ, Newby AC, Dick AD.** 2006. Tissue inhibitor of metalloproteinase-3 differentially binds to components of Bruch's membrane. *Br J Ophthalmol*. **90**, 1310-1315.
- Malfait AM, Liu RQ, Ijiri K, Komiya S, Tortorella MD.** 2002. Inhibition of ADAM-TS4 and ADAM-TS5 prevents aggrecan degradation in osteoarthritic cartilage. *J Biol Chem*. **277**, 22201-22208.
- Matthews RT, Gary SC, Zerillo C, Pratta M, Solomon K, Arner EC, Hockfield S.** 2000. Brain-enriched hyaluronan binding (BEHAB)/brevican cleavage in a glioma cell line is mediated by a disintegrin and metalloproteinase with thrombospondin motifs (ADAMTS) family member. *J Biol Chem*. **275**, 22695-22703.
- Mercuri FA, Doege KJ, Arner EC, Pratta MA, Last K, Fosang AJ.** 1999. Recombinant human aggrecan G1-G2 exhibits native binding properties and substrate specificity for matrix metalloproteinases and aggrecanase. *J Biol Chem*. **274**, 32387-32395.
- Mitchell PG, Magna HA, Reeves LM, Lopresti-Morrow LL, Yocum SA, Rosner PJ, Geoghegan KF, Hambor JE.** 1996. Cloning, expression, and type II collagenolytic activity of matrix metalloproteinase-13 from human osteoarthritic cartilage. *J Clin Invest*. **97**, 761-768.
- Mochizuki S, Okada Y.** 2007. ADAMs in cancer cell proliferation and progression. *Cancer Sci*. **98**, 621-628.

- Mochizuki S, Shimoda M, Shiomi T, Fujii Y, Okada Y.** 2004. ADAM28 is activated by MMP-7 (matrilysin-1) and cleaves insulin-like growth factor binding protein-3. *Biochem Biophys Res Commun.* **315**, 79-84.
- Mohammed FF, Smookler DS, Taylor SE, Fingleton B, Kassiri Z, Sanchez OH, English JL, Matrisian LM, Au B, Yeh WC, Khokha R.** 2004. Abnormal TNF activity in Timp3<sup>-/-</sup> mice leads to chronic hepatic inflammation and failure of liver regeneration. *Nat Genet.* **36**, 969-977.
- Montero JC, Yuste L, Diaz-Rodriguez E, Esparis-Ogando A, Pandiella A.** 2000. Differential shedding of transmembrane neuregulin isoforms by the tumor necrosis factor-alpha-converting enzyme. *Mol Cell Neurosci.* **16**, 631-648.
- Murphy G, Willenbrock F.** 1995. Tissue inhibitors of matrix metalloendopeptidases. *Methods Enzymol.* **248**, 496-510
- Nakamura H, Fujii Y, Inoki I, Sugimoto K, Tanzawa K, Matsuki H, Miura R, Yamaguchi Y, Okada Y.** 2000. Brevican is degraded by matrix metalloproteinases and aggrecanase-1 (ADAMTS4) at different sites. *J Biol Chem.* **275**, 38885-38890.
- Nakamura M, Ishida E, Shimada K, Kishi M, Nakase H, Sakaki T, Konishi N.** 2005. Frequent LOH on 22q12.3 and TIMP-3 inactivation occur in the progression to secondary glioblastomas. *Lab Invest.* **85**, 165-175.
- Nath D, Williamson NJ, Jarvis R, Murphy G.** 2001. Shedding of c-Met is regulated by crosstalk between a G-protein coupled receptor and the EGF receptor and is mediated by a TIMP-3 sensitive metalloproteinase. *J Cell Sci.* **114**, 1213-1220.
- Nutt CL, Zerillo CA, Kelly GM, Hockfield S.** 2001. Brain enriched hyaluronan binding (BEHAB)/brevican increases aggressiveness of CNS-1 gliomas in Lewis rats. *Cancer Res.* **61**, 7056-7059.
- Ohuchi E, Imai K, Fujii Y, Sato H, Seiki M, Okada Y.** 1997. Membrane type 1 matrix metalloproteinase digests interstitial collagens and other extracellular matrix macromolecules. *J Biol Chem.* **272**, 2446-2451.

- Oliferenko S, Kaverina I, Small JV, Huber LA.** 2000. Hyaluronic acid (HA) binding to CD44 activates Rac1 and induces lamellipodia outgrowth. *J Cell Biol.* **148**, 1159-1164.
- O'Reilly MS, Boehm T, Shing Y, Fukai N, Vasios G, Lane WS, Flynn E, Birkhead JR, Olsen BR, Folkman J.** 1997. Endostatin: an endogenous inhibitor of angiogenesis and tumor growth. *Cell.* **88**, 277-285.
- Ortega N, Werb Z.** 2002. New functional roles for non-collagenous domains of basement membrane collagens. *J Cell Sci.* **115**, 4201-4214.
- Otterness IG, Downs JT, Lane C, Bliven ML, Stukenbrok H, Scampoli DN, Milici AJ, Mézes PS.** 1999. Detection of collagenase-induced damage of collagen by 9A4, a monoclonal C-terminal neopeptide antibody. *Matrix Biol.* **18**, 331-341.
- Peiretti F, Canault M, Deprez-Beauclair P, Berthet V, Bonardo B, Juhan-Vague I, Nalbone G.** 2003. Intracellular maturation and transport of tumor necrosis factor alpha converting enzyme. *Exp Cell Res.* **285**, 278-285.
- Pelletier, J.-P, Martel-Pelletier, J, Althman, RD, Ghandur-Mnaymneh, L, Enis, JE, and Woessner Jr., J.F.** 1983. Collagenase and collagenolytic activity in human osteoarthritic cartilage. *Arthritis Rheum.* **26**, 63-68.
- Peschon JJ, Slack JL, Reddy P, Stocking KL, Sunnarborg SW, Lee DC, Russell WE, Castner BJ, Johnson RS, Fitzner JN, Boyce RW, Nelson N, Kozlosky CJ, Wolfson MF, Rauch CT, Cerretti DP, Paxton RJ, March CJ, Black RA.** 1998. An essential role for ectodomain shedding in mammalian development. *Science* **282**, 1281-1284.
- Porter S, Clark IM, Kevorkian L, Edwards DR.** 2005. The ADAMTS metalloproteinases. *Biochem J.* **386**, 15-27.
- Prockop DJ, Kivirikko KI.** 1995. Collagens: molecular biology, diseases, and potentials for therapy. *Annu Rev Biochem.* **64**, 403-434.
- Qi JH, Ebrahem Q, Moore N, Murphy G, Claesson-Welsh L, Bond M, Baker A, Anand-Apte B.** 2003. A novel function for tissue inhibitor of metalloproteinases-

- 3 (TIMP3): inhibition of angiogenesis by blockage of VEGF binding to VEGF receptor-2. *Nat Med.* **9**, 407-415.
- Qi JH, Ebrahem Q, Yeow K, Edwards DR, Fox PL, Anand-Apte B.** 2002. Expression of Sorsby's fundus dystrophy mutations in human retinal pigment epithelial cells reduces matrix metalloproteinase inhibition and may promote angiogenesis. *J Biol Chem.* **277**, 13394-13400.
- Radin EL, Martin RB, Burr DB, Caterson B, Boyd RD, Goodwin C.** 1984. Effects of mechanical loading on the tissues of the rabbit knee. *J Orthop Res.* **2**, 221-234.
- Radin EL, Rose RM.** 1986. Role of subchondral bone in the initiation and progression of cartilage damage. *Clin Orthop Relat Res.* **213**, 34-40.
- Raina S, Missiakas D.** 1997. Making and breaking disulfide bonds. *Annu Rev Microbiol.* **51**, 179-202.
- Rajewsky K, Gu H, Kühn R, Betz UA, Müller W, Roes J, Schwenk F.** 1996. Conditional gene targeting. *J Clin Invest.* **98**, 600-603.
- Reboul, P., Pelletier, J.P., Tardif, G., Cloutier, J.M. and Martel-Pelletier, J.** 1996. The new collagenase, collagenase-3, is expressed and synthesized by human chondrocytes but not by synoviocytes. A role in osteoarthritis. *J. Clin. Invest.* **97**, 2011–2019.
- Rio C, Buxbaum JD, Peschon JJ, Corfas G.** 2000. Tumor necrosis factor-alpha-converting enzyme is required for cleavage of erbB4/HER4. *J Biol Chem.* **275**, 10379-10387.
- Rizzolo LJ.** 1997. Polarity and the development of the outer blood-retinal barrier. *Histol Histopathol.* **12**, 1057-1067.
- Robertson KD, Wolffe AP.** 2000. DNA methylation in health and disease. *Nat Rev Genet.* **1**, 11-19
- Rosenblum BB, Lee LG, Spurgeon SL, Khan SH, Menchen SM, Heiner CR, Chen SM.** 1997. New dye-labeled terminators for improved DNA sequencing patterns. *Nucleic Acids Res.* **25**, 4500-4504.

- Rovida E, Paccagnini A, Del Rosso M, Peschon J, Dello Sbarba P.** 2001. TNF-alpha-converting enzyme cleaves the macrophage colony-stimulating factor receptor in macrophages undergoing activation. *J Immunol.* **166**, 1583-1589.
- Sahebjam S, Khokha R, Mort JS.** 2007. Increased collagen and aggrecan degradation with age in the joints of Timp3(-/-) mice. *Arthritis Rheum.* **56**, 905-909.
- Saiki, R. K., Gelfand, D. H., Stoffel, S., Scharf, S. J., Higuchi, R., Horn, G. T. Mullis, K.B. & Ehrlich, H. A.** (1988) Primer-directed enzymatic amplification of DNA with athermostable DNA polymerase. *Science.* **239**, 487-491.
- Saikumar P, Dong Z, Mikhailov V, Denton M, Weinberg JM, Venkatachalam MA.** 1999. Apoptosis: definition, mechanisms, and relevance to disease. *Am J Med.* **107**, 489-506.
- Saliba RS, Munro PM, Luthert PJ, Cheetham ME.** 2002. The cellular fate of mutant rhodopsin: quality control, degradation and aggresome formation. *J Cell Sci.* **115**, 2907-2918.
- Sandy JD, Westling J, Kenagy RD, Iruela-Arispe ML, Verscharen C, Rodriguez-Mazaneque JC, Zimmermann DR, Lemire JM, Fischer JW, Wight TN, Clowes AW.** 2001. Versican V1 proteolysis in human aorta *in vivo* occurs at the Glu441-Ala442 bond, a site that is cleaved by recombinant ADAMTS-1 and ADAMTS-4. *J Biol Chem.* **276**, 13372-13378.
- Sato H, Takino T, Okada Y, Cao J, Shinagawa A, Yamamoto E, Seiki M.** 1994. A matrix metalloproteinase expressed on the surface of invasive tumour cells. *Nature.* **370**, 61-65.
- Schlöndorff J, Becherer JD, Blobel CP.** 2000. Intracellular maturation and localization of the tumour necrosis factor alpha convertase (TACE). *Biochem J.* **347**, 131-138.
- Schwarzbauer JE, Sechler JL.** 1999. Fibronectin fibrillogenesis: a paradigm for extracellular matrix assembly. *Curr Opin Cell Biol.* **11**, 622-627.

- Smith MR, Kung H, Durum SK, Colburn NH, Sun Y.** 1997. TIMP-3 induces cell death by stabilizing TNF-alpha receptors on the surface of human colon carcinoma cells. *Cytokine*. **9**, 770-780.
- Sorsby A, Mason MEJ, Gardner N.** 1949. A fundus dystrophy with unusual features. *Br J Ophthalmol* **33**, 67-97
- Sousa MM, Saraiva MJ.** 2001. Internalization of transthyretin. Evidence of a novel yet unidentified receptor-associated protein (RAP)-sensitive receptor. *J Biol Chem*. **276**, 14420-14425
- Stetler-Stevenson WG, Brown PD, Onisto M, Levy AT, Liotta LA.** 1990. Tissue inhibitor of metalloproteinases-2 (TIMP-2) mRNA expression in tumor cell lines and human tumor tissues. *J Biol Chem*. **265**, 13933-13938.
- Stetler-Stevenson WG, Krutzsch HC, Liotta LA.** 1989. Tissue inhibitor of metalloproteinase (TIMP-2). A new member of the metalloproteinase inhibitor family. *J Biol Chem*. **264**, 17374-17378
- Stryer L.** 1978. Fluorescence energy transfer as a spectroscopic ruler. *Annu Rev Biochem*. **47**, 819-846.
- Studier FW, Rosenberg AH, Dunn JJ, Dubendorff JW.** 1990. Use of T7 RNA polymerase to direct expression of cloned genes. *Methods Enzymol*. **185**, 60-89.
- Suda T, Hashimoto H, Tanaka M, Ochi T, Nagata S.** 1997. Membrane Fas ligand kills human peripheral blood T lymphocytes, and soluble Fas ligand blocks the killing. *J Exp Med*. **186**, 2045-2050.
- Sun Y, Hegamyer G, Kim H, Sithanandam K, Li H, Watts R, Colburn NH.** 1995. Molecular cloning of mouse tissue inhibitor of metalloproteinases-3 and its promoter. Specific lack of expression in neoplastic JB6 cells may reflect altered gene methylation. *J Biol Chem*. **270**, 19312-19319.
- Sunnarborg SW, Hinkle CL, Stevenson M, Russell WE, Raska CS, Peschon JJ, Castner BJ, Gerhart MJ, Paxton RJ, Black RA, Lee DC.** 2002. Tumor necrosis factor-alpha converting enzyme (TACE) regulates epidermal growth factor receptor ligand availability. *J Biol Chem*. **277**, 12838-12845

- Tabata Y, Isashiki Y, Kamimura K, Nakao K, Ohba N.** 1998. A novel splice site mutation in the tissue inhibitor of the metalloproteinases-3 gene in Sorsby's fundus dystrophy with unusual clinical features. *Hum Genet.* **103**, 179-182.
- Tabor S, Richardson CC.** 1995. A single residue in DNA polymerases of the Escherichia coli DNA polymerase I family is critical for distinguishing between deoxy- and dideoxyribonucleotides. *Proc Natl Acad Sci U S A.* **92**, 6339-6343.
- Thathiah A, Blobel CP, Carson DD.** 2003. Tumor necrosis factor-alpha converting enzyme/ADAM 17 mediates MUC1 shedding. *J Biol Chem.* **278**, 3386-3394.
- Thomas KR, and Capecchi MR.** 1987. Site-directed mutagenesis by gene targeting in mouse embryo-derived stem cells. *Cell.* **51**, 503-512.
- Toole BP.** 2000. Hyaluronan is not just a goo! *J Clin Invest.* **106**, 335-336.
- Tortorella MD, Burn TC, Pratta MA, Abbaszade I, Hollis JM, Liu R, Rosenfeld SA, Copeland RA, Decicco CP, Wynn R, Rockwell A, Yang F, Duke JL, Solomon K, George H, Bruckner R, Nagase H, Itoh Y, Ellis DM, Ross H, Wiswall BH, Murphy K, Hillman MC Jr, Hollis GF, Newton RC, Magolda RL, Trzaskos JM, Arner EC.** 1999. Purification and cloning of aggrecanase-1: a member of the ADAMTS family of proteins. *Science.* **284**, 1664-1666.
- Tortorella MD, Pratta M, Liu RQ, Austin J, Ross OH, Abbaszade I, Burn T, Arner E.** 2000. Sites of aggrecan cleavage by recombinant human aggrecanase-1 (ADAMTS-4). *J Biol Chem.* **275**, 18566-18573.
- Uhlmann D.** 2006. Vascular endothelial growth factor: the good, the bad, and the ugly. *Transplantation.* **82**, 450-451.
- van Meurs JB, van Lent PL, Holthuysen AE, Singer II, Bayne EK, van den Berg WB.** 1999. Kinetics of aggrecanase- and metalloproteinase-induced neoepitopes in various stages of cartilage destruction in murine arthritis. *Arthritis Rheum.* **42**, 1128-1139.
- van Noorden CJF, and Everts V.** 1991. Selective inhibition of cysteine proteinases by z-phe-alaCH<sub>2</sub>F suppresses digestion of collagen by fibroblasts and osteoclasts. *Biochem. Biophys. Res. Commun.* **178**, 178-184.

- Vázquez F, Hastings G, Ortega MA, Lane TF, Oikemus S, Lombardo M, Iruela-Arispe, ML.** (1999) METH-1, a human ortholog of ADAMTS-1, and METH-2 are members of a new family of proteins with angio-inhibitory activity. *J. Biol. Chem.* **274**, 23349–23357
- Vidair CA, Huang RN, Doxsey SJ.** 1996. Heat shock causes protein aggregation and reduced protein solubility at the centrosome and other cytoplasmic locations. *Int J Hyperthermia.* **12**, 681-695.
- Vogel W.** 1999. Discoidin domain receptors: structural relations and functional implications. *FASEB J.* **13**, 77-82.
- Voss S, Skerra A.** 1997. Mutagenesis of a flexible loop in streptavidin leads to higher affinity for the Strep-tag II peptide and improved performance in recombinant protein purification. *Protein Eng.* **10**, 975-982.
- Wajih N, Walter J, Sane DC.** 2002. Vascular origin of a soluble truncated form of the hepatocyte growth factor receptor (c-met). *Circ Res.* **90**, 46-52.
- Wang WM, Ge G, Lim NH, Nagase H, Greenspan DS.** 2006. TIMP-3 inhibits the procollagen N-proteinase ADAMTS-2. *Biochem J.* **398**, 515-519
- Weber BH, Vogt G, Pruett RC, Stohr H, Felbor U.** 1994. Mutations in the tissue inhibitor of metalloproteinases-3 (TIMP3) in patients with Sorsby's fundus dystrophy. *Nat Genet* **8**, 352-356.
- Weber BH, Lin B, White K, Kohler K, Soboleva G, Herterich S, Seeliger MW, Jaissle GB, Grimm C, Reme C, Wenzel A, Asan E, Schrewe H.** 2002. A mouse model for Sorsby fundus dystrophy. *Invest Ophthalmol Vis Sci.* **43**, 2732-2740.
- Wernicke D, Seyfert C, Hinzmann B, Gromnica-Ihle E.** 1996. Cloning of collagenase 3 from the synovial membrane and its expression in rheumatoid arthritis and osteoarthritis. *J Rheumatol.* **23**, 590-595.
- Weskamp G, Schlondorff J, Lum L, Becherer JD, Kim TW, Saftig P, Hartmann D, Murphy G, Blobel CP.** 2004. Evidence for a critical role of the tumor necrosis factor alpha convertase (TACE) in ectodomain shedding of the p75 neurotrophin receptor (p75NTR). *J Biol Chem.* **279**, 4241-4249.



- Westling J, Gottschall PE, Thompson VP, Cockburn A, Perides G, Zimmermann DR, Sandy JD.** 2004. ADAMTS4 (aggrecanase-1) cleaves human brain versican V2 at Glu405-Gln406 to generate glial hyaluronate binding protein. *Biochem J.* **377**, 787-795.
- Wetzel R.** 1994. Mutations and off-pathway aggregation of proteins. *Trends Biotechnol.* **12**, 193–198.
- Whitham SE, Murphy G, Angel P, Rahmsdorf HJ, Smith BJ, Lyons A, Harris TJ, Reynolds JJ, Herrlich P, Docherty AJ.** 1986. Comparison of human stromelysin and collagenase by cloning and sequence analysis. *Biochem J.* **240**, 913-916.
- Wigley WC, Fabunmi RP, Lee MG, Marino CR, Muallem S, DeMartino GN, Thomas PJ.** 1999. Dynamic association of proteasomal machinery with the centrosome. *J Cell Biol.* **145**, 481-490.
- Wild A, Ramaswamy A, Langer P, Celik I, Fendrich V, Chaloupka B, Simon B, Bartsch DK.** 2003. Frequent methylation-associated silencing of the tissue inhibitor of metalloproteinase-3 gene in pancreatic endocrine tumors. *J Clin Endocrinol Metab.* **88**, 1367-1373.
- Wojcik C.** 1997. An inhibitor of the chymotrypsin-like activity of the proteasome (PSI) induces similar morphological changes in various cell lines. *Folia Histochemica et Cytobiologica*, **35**, 211-214.
- Wojcik C, Schroeter D, Wilk S, Lamprecht J, Paweletz N.** 1996. Ubiquitin-mediated proteolysis centers in HeLa cells: Indication from studies of an inhibitor of the chymotrypsin-like activity of the proteasome. *Eur J Cell Biol.* **71**, 311-318.
- Woolley DE, Roberts DR, Evanson JM.** 1975. Inhibition of human collagenase activity by a small molecular weight serum protein. *Biochem Biophys Res Commun.* **66**, 747-754.
- Yeow KM, Kishnani NS, Hutton M, Hawkes SP, Murphy G, Edwards DR.** 2002. Sorsby's fundus dystrophy tissue inhibitor of metalloproteinases-3 (TIMP-3) mutants have unimpaired matrix metalloproteinase inhibitory activities, but affect cell adhesion to the extracellular matrix. *Matrix Biol.* **21**, 75-88.

- Yu WH, Yu S, Meng Q, Brew K, Woessner JF Jr.** 2000. TIMP-3 binds to sulfated glycosaminoglycans of the extracellular matrix. *J Biol Chem.* **275**, 31226-31232.
- Zhang H, Kelly G, Zerillo C, Jaworski DM, Hockfield S.** 1998. Expression of a cleaved brain-specific extracellular matrix protein mediates glioma cell invasion *In vivo*. *J Neurosci.* **18**, 2370-2376.
- Zatterstrom UK, Felbor U, Fukai N, Olsen BR.** 2000. Collagen XVIII/endostatin structure and functional role in angiogenesis. *Cell Struct Funct.* **25**. 97-101.
- Zou J, Zhu F, Liu J, Wang W, Zhang R, Garlisi CG, Liu YH, Wang S, Shah H, Wan Y, Umland SP.** 2004. Catalytic activity of human ADAM33. *J Biol Chem.* **279**, 9818-9830.

## Acknowledgments

I would like to take this opportunity to express my sincere gratitude to **Professor Dr. Bernhard H.F. Weber** for the very interesting project offered to me and for his continuous support during my Ph.D. studies.

I am very grateful to **Professor Dr. Rainer Deutzman** for accepting to be a member of the present thesis committee and for reviewing this work.

Special thanks to **PD Dr. Heidi Stöhr** for her help in preparing the paper manuscript and very nice and interesting discussions.

Many thanks to **Dr. Neil Taylor** for proof-reading the present thesis.

Big thanks to **Jürgen Kaschkötö** for his patience and invaluable competence in helping me with all computer stuff anytime I have asked him.

Thanks to **Dr. Bernd Becker** for his enthusiastic discussions.

I would like also to thank to all present and former members of the Institute of Human Genetics from Regensburg and Würzburg for their collegiality. Many thanks to **Mrs. Ilse Neuman** and **Mrs. Sabine Fürst** for their competent and kind administrative help during my stay in Würzburg and Regensburg.

Thanks to the internship students I have worked with and who have contributed to the progress of the present work: **Anna Pilsel, Carola Stribl, and Kathrin Bauer**.

## Curriculum vitae

### Personal data

Name: Marton Fogarasi  
Date of birth: 28 December 1974  
Place of birth: Targu Secuiesc, Romania  
Citizenship: Romanian

### Education:

1981-1989 **Primary School**, Targu Secuiesc, Romania  
1989-1993 **High School**, Targu Secuiesc, Romania  
1994-1998 **B.Sc.**, Biochemistry, Al.I.Cuza University of Jassy, Romania  
1998-2000 **M.Sc.**, Molecular Genetics, Al.I.Cuza University of Jassy, Romania  
2001-2003 **Graduate Research Training** at the Institute of Biological Chemistry, Freising, Germany  
2004-2007 **PhD thesis** at the Institute of Human Genetics, Regensburg, Germany. Title: Mouse models targeted for the tissue inhibitor of metalloproteinases-3 (TIMP3) - molecular and functional dissection of Sorsby fundus dystrophy (SFD)  
2008- Present **Postdoctoral Scientist** at Cambridge Research Institute, University of Cambridge, Cambridge, UK

### Publications:

Martin Schlapschy, **Marton Fogarasi**, Helga Gruber, Oliver Gresch, Claudia Schäfer, Yasmine Aguib, Arne Skerra. 2009. Functional humanization of an anti-CD16 Fab fragment: obstacles of switching from murine  $\lambda$  to human  $\lambda$  or  $\kappa$  light chains. *Protein Eng Des Sel.* **22**, 175-188

**Marton Fogarasi**, Andreas Janßen, Bernhard H. F. Weber, Heidi Stöhr. 2008. Molecular dissection of TIMP3 mutation S156C associated with Sorsby fundus dystrophy. *Matrix Biol.* **27**, 381-392

Andreas Janssen, **Marton Fogarasi**, Heinrich Schrewe, Matthias Seeliger, Ernst Tamm, Albrecht May, Bernhard H.F. Weber, Heidi Stöhr. 2008. Abnormal vessel formation in the choroid of TIMP3-deficient mice indicates an unbalanced VEGF-mediated angiogenesis in the retina. *Invest Ophthalmol Vis Sci.* **49**, 2812-2822.

Martin Schlapschy, Monica K. Dommel, Kamyar Hadian, **Marton Fogarasi**, Ingo P. Korndörfer, Arne Skerra. 2004. The periplasmic *E. coli* chaperone Skp is a trimer in solution: biophysical and preliminary crystallographic characterization. *Biol. Chem.* **385**, 137-143.

#### **Poster presentation**

**Marton Fogarasi**, Bernhard H. F. Weber. 2005. Functional implications of the Sorsby fundus dystrophy mutation TIMP3 (Ser156Cys) in the inhibition of matrix metalloproteinases. Proretina. Potsdam, Germany